Lead isotopes as a palaeodietary tracer in southwestern South Africa

Mari Scott

Supervisor: Dr Petrus le Roux

Co-supervisors: Prof Judith Sealy and Dr Robyn Pickering

Dissertation presented for the degree of Master of Science

Department of Geological Sciences

University of Cape Town

February 2018

DECLARATION

I know the meaning of plagiarism and declare that all the work in the document, save for that which is properly acknowledged, is my own. This dissertation has been submitted to the Turnitin module and I confirm that my supervisors have seen my report and any concerns revealed by such have been resolved with my supervisors.

Signed: Signed by candidate

ACKNOWLEDGMENTS

My sincere thanks go to my supervisor Dr Petrus le Roux and co-supervisors Prof Judith Sealy and Dr Robyn Pickering, who made this master's thesis possible.

My thanks extend to the South African Research Chairs Initiative of the Department of Science and Technology and the National Research Foundation of South Africa (grant number 84407) for generous bursary support, without which I could not have completed my master's degree.

I also thank Fayrooza Rawoot and Christel Tinguely, of the Department of Geological Sciences at UCT, for their assistance in preparing and analysing my samples.

Lastly, I thank Mr Danie Kotzé from Rooiheuwel farm, who allowed me to collect necessary samples on his farm, as well as Frans Radloff for providing me with essential samples from his previous studies.

ABSTRACT

This thesis evaluates the utility of lead (Pb) isotopes, in combination with strontium (Sr) isotopes, as a geochemical tracer for studying the palaeodiets and palaeo-landscape usage in southwestern South Africa. Isotopes of light elements, carbon (C), nitrogen (N), oxygen (O), and sulphur (S), are widely used as (palaeo) environmental tracers, but do not yield information on the geological substrates on which individuals have lived. Sr isotopes in bones and teeth are useful in distinguishing between areas of distinct bedrock geology, however, the efficiency of Sr is limited at near-coastal areas, which forms a major part of this study area. This is because Sr has a relatively high concentration and long residence time in seawater. In addition, coastal soils contain not only aerosol-derived marine Sr, but frequently also include fragments of shells and other marine carbonates, so their $^{87}Sr/^{86}Sr$ is like the ocean. This study analysed Pb and Sr concentrations and isotopic compositions of animals and plants derived from the various geological substrates of southwestern South Africa. In order to do this, a detailed Sr-Pb separation scheme was developed, involving the separation and pre-concentration of Sr and Pb from a single digested sample by means of ion-exchange chromatography. Elemental concentrations were measured with a Thermo X-series II quadrupole ICP-MS instrument. Sr concentrations ranged between 111 ppm and 1862 ppm, while Pb concentrations were lower, ranging between 0.012 ppm and 2.30 ppm. Isotopic ratios were determined by means of a Nu Instruments high resolution multi-collector inductively-coupled-plasma mass spectrometry (HR-MC-ICP-MS). Samples were introduced into the system as solutions, producing an order of magnitude more precise results than laser ablation analysis on the same material. Sr isotopes are useful for distinguishing between individuals living in near-coastal environments and those living further inland, while Pb isotopes could differentiate between granites and shales/sandstones. Pb isotopes proved to be a valuable palaeodietary tracer and can be used in combination with Sr isotopes to extent our knowledge of palaeo-landscape usage at coastal-marine environments.

TABLE OF CONTENTS

DECLARATION i

ACKNOWLEDGMENTS ii

ABSTRACT iii

TABLE OF CONTENTS iv

Chapter 1: Introduction 1

1.1 Project Overview 1

1.2 Aims of the study 2

Chapter 2: Background 3

2.1 Isotopes overview 3

2.2 Sr isotopes in the geosphere and biosphere 4

2.3 Pb isotopes in the geosphere and biosphere 5

2.4 The geological substrates of southwestern South Africa 10

2.5 Individuals' tissues for reconstructing paleo-diets 12

2.5.1 Bone structure 12

2.5.2 Tooth structure 13

2.5.3 Pb and Sr in bones and teeth 13

2.6 Previous archaeological studies using Sr and Pb isotopes 14

2.6.1 Pb and Sr isotopes as palaeodietary tracers 15

2.6.2 Pb and Sr isotopes as palaeodietary tracers in southwestern South Africa 18

2.7 Measuring Sr and Pb isotopes 22

2.8 Potential limitations of Sr and Pb isotopes as palaeodietary indicators 24

2.8.1 Diagenesis 24

2.8.2 Anthropogenic Pb pollution 25

Chapter 3: Materials and Methodology 26

3.1 Bone and tooth samples 31

3.2 Plant samples 32

3.3 Measurement of Sr and Pb concentrations by ICP-MS 33
3.4 Combined Sr-Pb separation scheme 34
3.5 Measurement of Sr and Pb isotope composition using high resolution multi-collector inductively-coupled-plasma mass spectrometry (HR-MC-ICP-MS) 36
Chapter 4: Results 37
4.1 Method evaluation 37
4.2 Concentration data 41
4.3 Isotopic composition data 45
4.3.1 Sr isotopic ratios 45
4.3.2 Pb isotopic ratios 48
Chapter 5: Discussion and Conclusions 58
5.1 Utility of Sr and Pb isotopes at coastal marine environments 61
5.2 Utility of samples derived from leaded-petrol era 65
5.3 Conclusion 67
References 68

Chapter 1: Introduction

1.1 Project Overview

Understanding both palaeo-landscape usage and palaeo-diets are significant for the archaeological study of evolution and migration of humans and animals. Stable isotope techniques are widely used in reconstructing palaeo-diets, and are based on the principle that individuals' body tissues will reflect the isotopic composition of the food and water ingested during their lifetimes, in other words: "You are what you eat" (Ambrose & Norr, 1993; Parkington, 1991). DeNiro and Epstein (1978) investigated the influence of animals' diets on the distribution of carbon isotopes and subsequently nitrogen isotopes (DeNiro & Epstein, 1981) in their bodies. Since then, there has been a great deal of work on dietary and environmental tracing based on isotopes of light elements (C, N, O, H and to a lesser extent, S). These traditional isotope systems essentially track flows of nutrients and water through foodwebs, however, they do not yield information on the geological substrates on which the organisms have lived. Sr isotopic analysis of bones and teeth is commonly used to reconstruct diets and is a valuable tracer in distinguishing between areas of distinct bedrock geology. However, constraints with this isotope system occur in situations where different parts of the landscape have similar $^{87}Sr/^{86}Sr$, e.g. marine compared with coastal terrestrial environments where the Sr isotope ratios are like those of seawater. Therefore, any additional isotopic system that can further assist in discriminating palaeo-landscape usage will be of great value in archaeological and palaeontological studies.

This master's thesis will focus on Pb isotopes as an additional geochemical tracer for studying palaeo-landscape usage of individuals. Some of the basic principles of using geochemical tracers are that the preferred isotope system should vary in predictable ways across the study region, and these isotopes should be incorporated into the material of interest during life. This study will analyse Pb as well as Sr isotopic compositions of contemporary animals' bones and teeth by means of high resolution multi-collector inductively-coupled-plasma mass spectrometry (HR-MC-ICP-MS). Samples can be introduced into the system as solids (for laser ablation) or as solutions. In the case of solution analysis, it is necessary to separate the Sr and Pb isotope fractions for each sample, prior to introduction into MC-ICP-MS system. This study will assess the precision of measuring Pb and Sr isotopic ratios by means of solution-MC-ICP-MS, and ultimately the integrity of the data.

1.2 Aims of the study

The primary aim of this master's thesis is to investigate whether Pb isotopes will enable us to discriminate between the distinct geological substrates of southwestern South Africa. To achieve this aim, both Pb and Sr isotope systems will be studied, to assess whether Pb isotopic data enables better discrimination between different geological substrates compared with Sr isotopes. This is important in archaeological and palaeontological studies, because Sr isotopes are of limited value in distinguishing near-coastal from marine environments. It is of interest to ascertain whether the sea influences the Pb isotopic ratios of samples at near-coastal localities. Another aim of this study is to determine the utility of Pb isotope measurements on archival samples that were collected during the time when leaded petrol was in use in South Africa. This is important because there is a large body of materials in museum and other collections that can be drawn on in future studies.

To answer these questions, Sr and Pb isotopic compositions and concentrations were measured on plants and animals collected from the major geological substrates of southwestern South Africa. These include shales, sandstones, granites and recent marine-derived sands, ranging in age from pre-Cambrian to Quaternary. This allows for the characterisation of the range of bioavailable Sr and Pb isotope ratios for each substrate, and to assess similarities and differences. Some previous work on Sr isotopes as palaeodietary indicators has been done in this region (Sealy, et al., 1991; Copeland, et al., 2016; Lehmann, et al., 2018) but this is the first study to include Pb isotopes.

Chapter 2: Background

2.1 Isotopes overview

All matter, which is everything that has mass and takes up space, is made up of particles called atoms. An atom consists of a central nucleus, which is composed of protons (positively charged) and neutrons (uncharged), surrounded by electrons (negatively charged) revolving in orbits about the nucleus (Rutherford, 1913). The number of protons in the nucleus is known as the atomic number of an atom, whereas the sum of the protons and neutrons is known as the atomic mass number (Khan, 2010). The concept of isotopes was introduced by Frederick Soddy in 1913, for atoms whose nucleus contains the same number of protons (same atomic number), but a different number of neutrons (different atomic mass number). There are two basic types of isotopes: (1) stable isotopes, which do not change over time, and (2) unstable (radioactive) isotopes, which decay over predictable periods.

Radioactive decay is the process by which an unstable nucleus emits particles (alpha, beta or gamma) and energy to reach a more stable nucleus (Malainey, 2010). During alpha (α) decay the unstable nucleus emits an α-particle, which is identical to the nucleus of a helium-4 atom (two protons and two neutrons); consequently, the atomic mass number decreases by 4 and the atomic number decreases by 2 (Malainey, 2010). This type of decay occurs in heavy radioactive isotopes, with atomic numbers greater than 82 and masses greater than 209 (Malainey, 2010). Beta (β) decay occurs when an unstable nucleus emits a β-particle, which is a high-energy, high-speed electron / positron (electron with positive electric charge) (Martin, et al., 2012), depending on the type of β-decay. There are two types: negative beta (β-) decay occurs when a neutron decays into a proton, which stays in the nucleus, and creates an electron (the beta particle), which is emitted from the nucleus with high speed (Martin, et al., 2012). The new nucleus will have one more proton and one less neutron, thus the mass number remains unchanged and the atomic number increases by one. Positive beta (β+) decay occurs when a proton is converted into a neutron and creates a positive beta particle (also known as a positron), which is emitted from the nucleus. The new nucleus will have one less proton and one more neutron, thus the mass number remains the same, but the atomic number reduces by one.

The rate at which radioactive isotopes are expected to decay is expressed as the half-life. Each isotope has its own half-life, defined as the length of time it takes for half of the amount of a radioactive isotope, known as the parent isotope, to decay into an isotope of a new element, known as the daughter isotope (Edwards & Pojeta, 1993). Half-lives can range from less than a second to more than a million years (Porcelli & Baskaran, 2011). By measuring the ratio of the amount of the

parent to daughter isotope, scientists can determine how many half-lives the element has undergone and estimate an absolute age of a sample (Edwards & Pojeta, 1993). Half-lives of radioactive isotopes are useful for understanding geological timescales and have been used extensively in dating of materials, especially rocks (Edwards & Pojeta, 1993). The focus of this study is on Sr and Pb isotopes.

2.2 Sr isotopes in the geosphere and biosphere

Strontium (Sr) has an atomic number of 38 and belongs to group 2 (valence: +2) of the periodic table, which also includes beryllium (Be), magnesium (Mg), calcium (Ca), barium (Ba), and radium (Ra). Sr is classified as a lithophile element, meaning it bonds readily with silicate. Since its ionic radius is only slightly larger than that of calcium, Sr^{2+} substitutes for Ca^{2+} in minerals including plagioclase feldspar, calcite, dolomite, aragonite, gypsum and, most importantly regarding archaeological materials, apatite in bones and teeth (Bentley, 2006). Sr has four naturally occurring isotopes; ^{84}Sr (0.58% abundance), ^{86}Sr (9.87%), ^{87}Sr (7.03%) and ^{88}Sr (82.52%) (Rankama, 1954), of which ^{87}Sr is the only radiogenic isotope. The abundances of ^{88}Sr, ^{86}Sr and ^{84}Sr are constant through time, while the amount of ^{87}Sr is continually increasing (Montgomery, 2002). ^{87}Sr is formed over time through negative beta-decay (Capo, et al., 1998) of rubidium-87 (^{87}Rb), with a half-life of 4.88×10^{10} years (Faure, 1986). The Sr isotopic ratio is generally measured as ^{87}Sr relative to ^{86}Sr ($^{87}Sr/^{86}Sr$), due to these two isotopes having similar abundances and being only one atomic mass unit apart (Montgomery, 2002). Sr isotopes have been used extensively in geological studies for dating rocks (Pollard, et al., 2007), given that $^{87}Sr/^{86}Sr$ increases through geological time and will be higher in older rocks and/or those with higher rubidium contents (Faure, 1986).

Sr isotopes are valuable in archaeology and palaeontology as a means of reconstructing past movements of people and animals across geological boundaries. Sr is released from rocks through chemical weathering and moves (without alteration of $^{87}Sr/^{86}Sr$) from the source rock into the soils and groundwater (Montgomery, 2002). Different components of rocks with different $^{87}Sr/^{86}Sr$ may weather at different rates, so that the bioavailable $^{87}Sr/^{86}Sr$ values may differ from that of the underlying bedrock (Sillen, et al., 1998). Rb-bearing minerals (micas and K-feldspar) are usually more resistant to weathering than the Sr-bearing minerals (plagioclase and calcite), resulting in lower $^{87}Sr/^{86}Sr$ values for the Sr released through chemical weathering than that of the bedrock (Montgomery, 2002). As with bedrock, the Sr isotope ratios of whole soil samples are not necessarily indicative of the bioavailable Sr that enters the food chain (Sillen, et al., 1998). Studies should use

the bioavailable $^{87}Sr/^{86}Sr$ values from local animals and plants to discriminate among the various substrates over which individuals might have moved (Sillen, et al., 1998; Price, et al., 2002). Plants and animals are appropriate sample materials for evaluating bioavailable $^{87}Sr/^{86}Sr$ because Sr passes through the food chain from plants to animals and humans without significant fractionation of its isotopes (Ericson, 1985).

$^{87}Sr/^{86}Sr$ values of the Sr released from local bedrocks into soil and water may be altered by mixing of non-local Sr from other rock types. This could be due to rivers flowing through different geologies, precipitation and wind-blown dust (Montgomery, 2002; Whipkey, et al., 2000). Near-coastal terrestrial environments tend to have some contribution of Sr from sea spray, due to the aerosols derived from sea water being transported inland by wind, where they are deposited (Whipkey, et al., 2000). In the ocean, Sr has a relatively high concentration of 7.62 ppm (Capo et al., 1998). $^{87}Sr/^{86}Sr$ is homogeneously distributed in the ocean, due to the long residence time (2×10^7 years), with a well-recognised $^{87}Sr/^{86}Sr$ value of 0.709241 ± 32 for present-day seawater (Veizer, 1989).

2.3 Pb isotopes in the geosphere and biosphere

Lead (Pb) has an atomic number of 82 and belongs to group 14 of the periodic table, which also includes C, Si, Ge and Sn, of which Pb has the most metallic characteristics. Pb can exist in two valence states: Pb^{2+} which is the most common state, and Pb^{4+} which is rare and restricted to highly alkaline or oxidizing solutions (Dickin, 1995). In silicates, Pb^{2+} can substitute for potassium (K^+) in K-feldspar and for Ca^{2+} in plagioclase (Dickin, 1995). Pb has four naturally occurring isotopes: ^{204}Pb (1.4% abundance), ^{206}Pb (24%), ^{207}Pb (22.6%), and ^{208}Pb (52%) (Rankama, 1954). The abundance of ^{204}Pb has been constant since the Earth was formed, while ^{206}Pb, ^{207}Pb and ^{208}Pb have increased in nature from slow radioactive decay of uranium (U) and thorium (Th) (Rankama, 1954). Uranium-lead (U-Pb) dating depends on two separate decay chains: ^{238}U, with a half-life of 4.467×10^9 years (Faure, 1986), undergoes radio-active decay through the "uranium series" to form ^{206}Pb; whereas ^{235}U, with a half-life of 0.7038×10^9 years (Faure, 1986), decays through the "actinium series" to produce ^{207}Pb as the final stable element in this decay chain (Snelling, 2017). Thorium-lead (Th-Pb) dating depends on one decay chain: ^{232}Th, with a long half-life of 14.010×10^9 years (Faure, 1986), decays very slowly through the "thorium series" to form stable ^{208}Pb. All three of these radiogenic isotopes of Pb are formed through alpha-decay of their respective parent isotopes.

Table 1: Summary of the Sr and Pb isotopes of interest, with their respective parent isotopes and their half-lives

Parent isotope	Half-life (years)	Daughter isotope	Type of Decay
^{87}Rb	4.75×10^{10}	^{87}Sr	β-
^{238}U	4.47×10^{9}	^{206}Pb	α
^{235}U	7.04×10^{8}	^{207}Pb	α
^{232}Th	1.4×10^{10}	^{208}Pb	α

Pb is a chalcophile element, meaning it bonds readily with sulphur (S) to form several important sulphide minerals, of which galena (PbS) is the most common (Dickin, 1995). Other minerals such as anglesite ($PbSO_4$), cerrusite ($PbCO_3$) and minim (Pb_3O_4) are also Pb-bearing (Ghazi & Millette, 2006). Pb can be found in many types of rocks and the isotopic composition of Pb can vary significantly. The $^{206}Pb/^{204}Pb$, $^{207}Pb/^{204}Pb$ and $^{208}Pb/^{204}Pb$ isotopic ratios (where ^{204}Pb is used as the reference isotope), will increase with geological time and with increasing levels of U and Th in a studied system (Bilström, 2008). Radiogenic Pb, with high U/Pb and Th/Pb ratios, is found mainly in accessory minerals such as zircon and apatite (Erel, et al., 1994). On the other hand, minerals like galena, plagioclase and K-feldspar are characterized by U/Th free systems which suggest that their post-crystalline Pb isotope ratios remains the same once Pb has been incorporated into its mineral lattice (Bilström, 2008). Therefore, these minerals that were formed at different times and in different geological environments will have different sets of Pb isotope ratios (Bilström, 2008).

Pb in surface water run-off originates from chemical weathering of rocks, industrial discharges and atmospheric deposition (Ghazi & Millette, 2006). Atmospheric transport and deposition of airborne Pb increases the Pb levels in soils, surface waters and the food chain (Ghazi & Millette, 2006). Pb in modern rainwater seems to be mainly evaporated particles derived from petrol or industrial aerosols, most of which appears to be taken up by surface soils (Bacon & Bain, 1995). Like Sr, bioavailable Pb is transferred through the food chain without significant fractionation of its isotopes (Montgomery, 2002), from the source bedrock by chemical weathering to soils and groundwater, then taken up by plants through their roots (Adriano, 1986). Modern plants exhibit similar Pb isotope ratios to the soils in which they grow (Montgomery, 2002).

Pb has a much shorter residence time in oceans (80-100 years) than Sr (2×10^7 years), resulting in fluctuating Pb compositions in the ocean (Montgomery, 2002). Schaule and Patterson (1981) was one of the first studies to measure Pb concentrations in seawater. Since then increasingly more studies have measured Pb concentration and isotope ratios of seawater from the North and South

Atlantic, North and South Pacific, Indian Ocean, and the Southern Ocean (Boyle, et al., 2014). Extensive research is available on the spatial and temporal variability of Pb in the North Atlantic Ocean (Boyle, et al., 1986; Shen & Boyle, 1987; Shen & Boyle, 1988; Helmers, et al., 1990; Helmers, et al., 1991; Helmers & van der Loeff, 1993; Veron, et al., 1993; Veron, et al., 1994; Veron, et al., 1999; Hamelin, et al., 1997). However, research on the fluctuating Pb compositions in the South Atlantic Ocean is limited (Helmers & van der Loeff, 1993; Alleman, et al., 2001). Helmers & van der Loeff (1993) measured the Pb concentrations of the South Atlantic surface waters, sampled in 1990. A Pb concentration of 29 pmol/kg was measured at 32.195° S and 13.52° E (south-west coast of South Africa) (Helmers & van der Loeff, 1993). Alleman et al. (2001) measured the Pb isotopic ratios of the Equatorial and South Atlantic surface waters, sampled during May – June 1996. The cruise track of this study was along the east coast of South America (western South Atlantic) from 10°N to 33°S. Sample station "Fish 1" (33.82° S and 46.28° W) is positioned on a similar latitude as Cape Town (33.92° S and 18.42° E) and the following Pb isotopic ratios were measured at this station: $^{206}Pb/^{204}Pb$ = 18.3800, $^{208}Pb/^{206}Pb$ = 2.0900, $^{206}Pb/^{207}Pb$ = 1.1650 (Table 3) (Alleman, et al., 2001).

A more recent study by Paul et al. (2015) analysed the Pb isotopic compositions and concentrations for seawater, sampled during October 2010, from different depths in the south-eastern Atlantic Ocean (latitude: 36.46° S, longitude 13.39° E). Table 2 illustrates their results for the Pb concentration profile of the south-eastern Atlantic Ocean, showing surface enrichment with depletion at depth (Paul, et al., 2015). These results shows that Pb has a much lower concentration in seawater than Sr. The highest Pb concentration was measured at 25.2 pmol/kg at a depth of 49 m below sea-level. From there, the Pb concentration showed a constant decrease down the seawater depth profile. This enrichment of Pb in the ocean's surface, is due to increased anthropogenic Pb pollution and terrestrial run-off over the past century (Libes, 1992; Montgomery, 2002; Paul, et al., 2015). When comparing the Pb concentration and isotopic data of current surface waters in the South Atlantic Ocean to that measured in the 1990s, a decrease in the Pb concentration can be observed from 29 pmol/kg in 1990 (Helmers & van der Loeff, 1993) to 17.7 pmol/kg in 2010 (Paul, et al., 2015). Also, the $^{206}Pb/^{204}Pb$ ratios have decreased from 18.3800 in May/June 1996 (Alleman, et al., 2001) to 18.0730 in October 2010 (Paul, et al., 2015). Conversely, the $^{208}Pb/^{206}Pb$ ratios have increased from 2.0900 in May/June 1996 (Alleman, et al., 2001) to 2.1040 in October 2010 (Paul, et al., 2015).

Table 2: Pb isotope and concentration data for a seawater depth profile from the south-eastern Atlantic Ocean (D357 stations 3, GEOTRACES transect GA10; latitude: 36.46° S, longitude 13.39° E; sampled in October 2010). The commonly measured ratios of $^{207}Pb/^{206}Pb$ and $^{208}Pb/^{206}Pb$ were analysed to high precision, while $^{206}Pb/^{204}Pb$, $^{207}Pb/^{204}Pb$ and $^{208}Pb/^{204}Pb$ were determined to an uncertainty of better than ±3‰ (Paul, et al., 2015).

Sample	Depth (m)	[Pb] pmol/kg[a]	±1sd[b]	$206_{Pb}/204_{Pb}$[c]	$207_{Pb}/204_{Pb}$[c]	$208_{Pb}/204_{Pb}$[c]	$207_{Pb}/206_{Pb}$[c]	$208_{Pb}/206_{Pb}$[c]
Fish 113	2–3	17.7	0.9	18.073	15.620	38.030	0.86428	2.1040
183	25	20.5	0.4	18.111	15.624	38.017	0.86266	2.0991
180	49	25.2	0.5	18.013	15.618	37.922	0.86707	2.1053
177	99	22.4	0.8	18.044	15.614	37.941	0.86533	2.1027
174	198	17.3	0.6	18.125	15.627	38.015	0.86221	2.0975
171	397	22.3	0.6	18.087	15.618	37.970	0.86350	2.0993
170	594	15.7	0.5	18.031	15.600	37.885	0.86518	2.1011
169	989	11.5	0.5	18.007	15.604	37.911	0.86655	2.1052
167	1975	9.6	0.4	18.234	15.623	38.159	0.85677	2.0927
166	2955	5.3	0.4	18.418	15.717	38.452	0.85331	2.0879
164	3931	6.1	0.4	18.370	15.625	38.266	0.85050	2.0830
163	4724	7.1	0.4	18.540	15.664	38.537	0.84492	2.0785

[a] Pb concentrations are corrected for a mean total blank of 11.7 ± 4.3 pg.

[b] The uncertainties of the concentration data propagate both the (within-run) precision of the isotopic analyses and the uncertainty of the blank correction (see text).

[c] For the Pb isotopes, assumed external 2sd reproducibilities of ±1250 ppm for $^{20x}Pb/^{204}Pb$ and of ±800 ppm for $^{207}Pb/^{206}Pb$, $^{208}Pb/^{206}Pb$ are larger than the ±2se internal uncertainties in all cases. Based on this, appropriate 2sd uncertainties are ±0.023 for $^{206}Pb/^{204}Pb$, ±0.020 for $^{207}Pb/^{204}Pb$, ±0.047 to 0.048 for $^{208}Pb/^{204}Pb$, ±0.00068 to 0.00069 for $^{207}Pb/^{206}Pb$ and ±0.0017 for $^{208}Pb/^{206}Pb$.

Table 3: Pb isotopic compositions of the Equatorial and South Atlantic surface seawater, sampled during the third Intergovernmental Oceanographic Commission (IOC-III) Baseline Contaminant cruise (May– June 1996) from 33°S to 10°N (Alleman, et al., 2001).

Samples (Location)	Date	Distance (Km)	$\frac{^{206}Pb}{^{204}Pb}$	St. Dev.	$\frac{^{208}Pb}{^{206}Pb}$	St. Dev.	$\frac{^{206}Pb}{^{207}Pb}$	St. Dev.
Fish 1 (33°49′S 46°17′W)	5/20/96	1000	18.38	0.71	2.090	0.006	1.165	0.003
Fish 4 Station 10 (33°04′S 40°27′W)	5/21/96	1520	18.21	0.12	2.086	0.001	1.165	0.001
Fish 6 (28°54′S 36°57′W)	5/24/96	1920	18.19	0.09	2.083	0.001	1.165	0.001
Fish 9 (25°23′S 33°20′W)	5/25/96	2700	18.17	0.05	2.087	0.001	1.164	0.000
Fish 10 (23°39′S 31°34′W)	5/26/96	2960	18.04	0.06	2.098	0.001	1.158	0.000
Fish 11 Station 8 (17°15′S 25°15′W)	5/28/96	3910	18.10	0.16	2.102	0.001	1.155	0.001
Fish 12 (14°07′S 24°06′W)	5/30/96	3980	18.05	0.05	2.103	0.001	1.156	0.000
Fish 14 (11°06′S 23°11′W)	5/31/96	4400	18.02	0.12	2.010	0.001	1.158	0.001
Fish 15 (10°24′S 23°01′W)	5/31/96	4680	18.02	0.07	2.103	0.001	1.156	0.000
Fish 18 (6°12′S 21°44′W)	6/1/96	5240	18.03	0.05	2.104	0.001	1.155	0.000
Fish 21 (2°23′S 20°33′W)	6/1/96	5700	18.16	0.18	2.098	0.001	1.161	0.001
Fish 22 Romanche (0°53′S 20°07′W)	6/2/96	5900	18.05	0.03	2.102	0.001	1.157	0.000
Fish 24 (2°42′N 21°36′W)	6/5/96	6420	18.19	0.30	2.105	0.003	1.158	0.002
Fish 26 (4°34′N 22°48′W)	6/6/96	7050	18.13	0.04	2.103	0.001	1.159	0.000
Fish 27 (5°09′N 26°50′W)	6/7/96	7150	18.16	0.03	2.101	0.001	1.161	0.000
Fish 29 (5°49′N 30°54′W)	6/8/96	7620	18.13	0.36	2.010	0.003	1.162	0.002
Fish 31 (6°28′N 35°06′W)	6/9/96	8100	18.15	0.13	2.096	0.001	1.163	0.001
Fish 34 (7°17′N 40°09′W)	6/10/96	8600	18.14	0.05	2.099	0.001	1.162	0.000
Fish 37 Station 6 (7°55′N 44°39′W)	6/11/96	9060	18.06	0.12	2.095	0.002	1.164	0.001
Fish 39 (6°07′N 46°21′W)	6/13/96	9350	18.11	0.04	2.103	0.001	1.159	0.000
Fish 40 Amazon 1 (5°28′N 48°01′W)	6/15/96	9560	18.53	0.21	2.084	0.002	1.177	0.001
RM Fish 1 (6°56′N 49°04′W)	6/17/96	9750	18.18	0.14	2.092	0.001	1.165	0.001
RM Fish 2 (7°44′N 50°10′W)	6/17/96	9900	18.12	0.04	2.096	0.000	1.163	0.000
RM Fish 3 (8°54′N 52°03′W)	6/18/96	10140	18.28	0.09	2.082	0.001	1.171	0.001

2.4 The geological substrates of southwestern South Africa

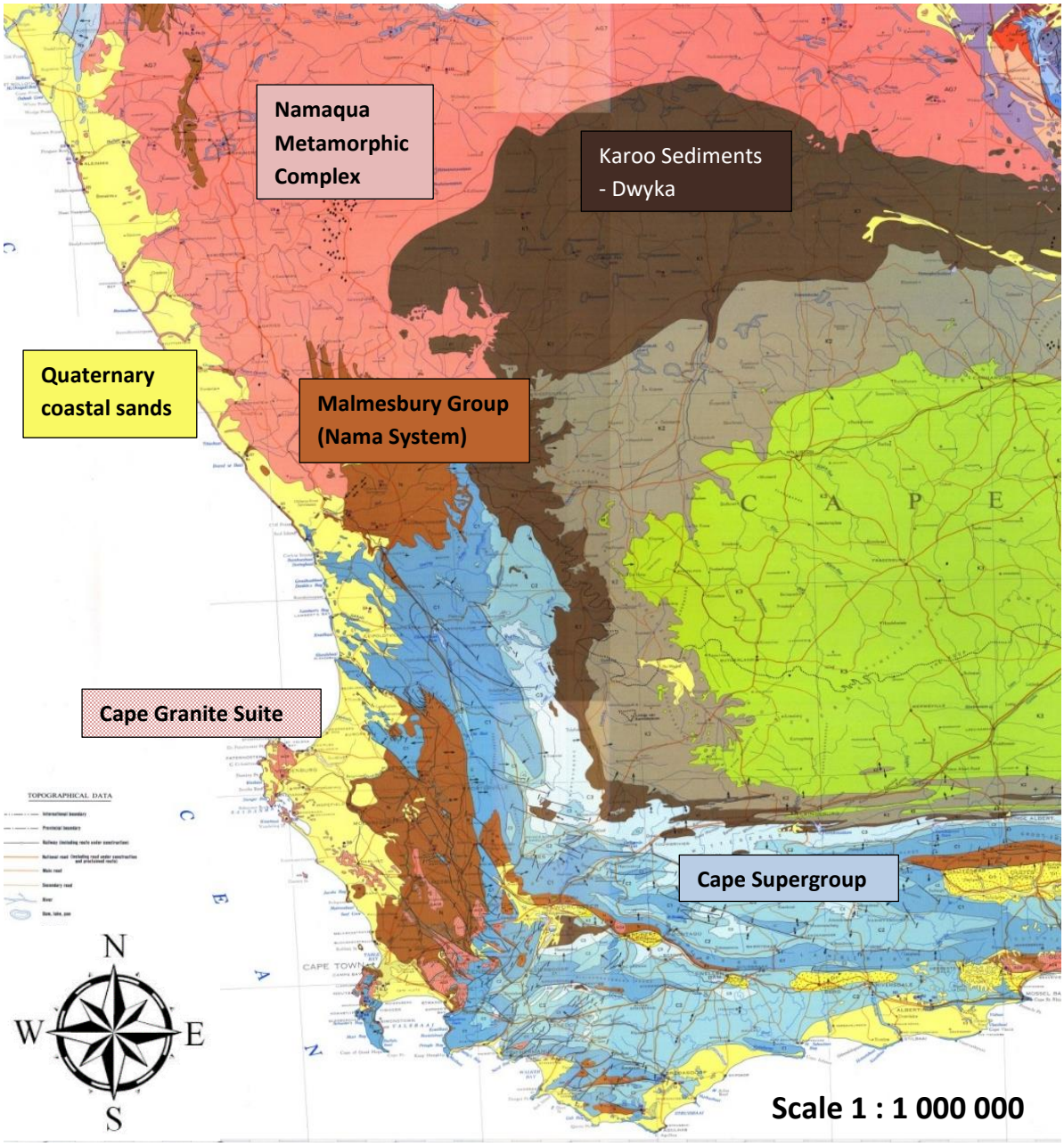

Figure 1: Geological map of southwestern South Africa, illustrating the different geological formations. Adapted from Schifano et al. (1970).

The late-Precambrian Malmesbury Group is the oldest rock formation (560 Ma) in the southwestern Cape of South Africa, consisting of alternating layers of dark grey fine-grained greywacke, sandstone and shale. Outcrops of the Malmesbury Group sediments can be seen near Vanrhynsdorp as well as in Moorreesburg and Malmesbury (Figure 1). Late Precambrian to Early Cambrian granitoids of the Cape Granite Suite intruded the Malmesbury Group about 540 million years ago. These granite plutons are exposed along the southwestern coast of South Africa near Vredenburg Peninsula extending towards the Cape Peninsula. The Malmesbury Group and granite basement rock is largely covered by Ordovician sandstones of the Table Mountain Group and Devonian shales of the Bokkeveld and Witteberg Groups of the Cape Supergroup (Thamn & Johnson, 2006).

During the Late Carboniferous Period (about 330 Ma ago), climatic changes resulted in a rapid growth of continental ice sheets and a drop in sea level, which exposed the upper Witteberg Group sediments of the Cape Supergroup. Erosion took place, followed by large continental glaciers moving over these exposed layers and deposition of a very thick succession of Karoo Supergroup sediments. The Main Karoo Basin is the most extensive, occupying the southern half of the Northern Cape, north of the Cederberg Mountain range. The earliest Karoo sediments comprise massive glacial tillites of the Upper Carboniferous Dwyka Group (Johnson, et al., 2006), followed by dark shales, some sandstones and coal seams of the Ecca Group and grey-green to reddish mudstones of the Early Triassic Beaufort group.

The youngest geological substrate is the Quaternary limestones and Holocene coastal sands (Roberts, et al., 2006) along the coastal areas of the Western Cape. During sea-level fluctuations of the Late Cenozoic, a series of coastal limestones, calcarenites, conglomerates and calcareous sandstones of the Bredasdorp Group was deposited between Plettenberg Bay and Hermanus. The limestones of the Bredasdorp Group can be sub-divided into the Wankoe, Waenhuiskrans and Strandveld Formations (Roberts, et al., 2006). The younger marine carbonate rocks have high Sr concentrations and low $^{87}Sr/^{86}Sr$, while the older shales and granite substrates tend to have lower Sr concentrations with higher $^{87}Sr/^{86}Sr$ values (Faure, 1986). This topic will be discussed in more detail later.

The geology of the Northern Cape Province is very different from that of south-western South Africa. The Northern Cape Province consists of even older Mesoproterozoic rocks of the Namaqua Metamorphic Complex, which form the western end of the Namaqua-Natal orogenic belt of metamorphism and granitization. The bedrock of the Namaqua Metamorphic Complex largely comprises highly deformed ultrametamorphic rocks, gneisses and migmatites (Cornell, et al., 2006).

2.5 Individuals' tissues for reconstructing paleo-diets

The most frequently analysed materials in archaeological studies are the hard tissues of individuals, which are their bones and teeth (Montgomery, 2002). This is because bones and teeth tend to preserve best and teeth (especially enamel) preserve even better than bones (Aberg, et al., 1998). The chemical and molecular composition of teeth and bones is under strong biological control, but the isotopic composition tracks that of food and drink ingested at the time of tissue formation. Comparisons of different tissues in a single individual can be used to identify if an individual has moved geographic locations since childhood, if those locations are isotopically distinct. In humans (and other species with teeth that form in early life) teeth show the dietary/geochemical signature of where they lived when young, while bones will show where they lived the years prior to their death (Ericson, 1985; Sealy, et al., 1995). Hair and fingernails, if preserved, may also be useful for determining short-term dietary changes of individuals (Tykot, 2004; O'Connell & Hedges, 1999). Hair and fingernails grow at a rate of about 1 cm/month and reflect an individual's more recent diet (O'Connell & Hedges, 1999). Increasingly more studies are using differences in tissue turnover rates to determine changes in a specific individual's diet and landscape usage over time (Schroeder, et al., 2009; Lamb, et al., 2014; Kootker, et al., 2016).

2.5.1 Bone structure

Bone consists of two major components: (1) an organic matrix composed mostly of a fibrous protein known as collagen and (2) an inorganic mineral, apatite, made largely of calcium phosphate (LeGeros, 1981; LeGeros, 1991). Collagen makes up about 20 – 25% of the weight of fresh bone. Since it is frequently well preserved, it is the most widely analysed component of archaeological bone (Sealy, et al., 2014). Sr and Pb are, however, located mainly in bone apatite, so studies of these elements necessarily focus on the inorganic component of calcified tissues. Living bone tissue constantly remodels (or renews) throughout an individual's lifetime, with old bone tissue replaced by new tissue as an individual grows and gets older (Mitton, et al., 2010). In this process, cells called osteoclasts break down old bone, and osteoblasts deposit new tissue (Mitton, et al., 2010). Therefore, bone reflects the isotopic composition of food sources over many years of an individual's lifetime (Tykot, 2004). The rate at which bones remodel depends on the skeletal element and the type of bone analysed. Remodelling in the mid-femoral shaft of long-bones, such as the tibia and femur, is between 1.5 and 4% per year in adults aged between 20 and 80 years (Hedges, et al., 2007), while ribs replace their chemical constituents after only a few years (Jowsey, et al., 1965).

2.5.2 Tooth structure

Teeth also consist of organic and inorganic materials, and are made up of four major tissues; enamel, dentin, cementum and dental pulp (root canal). Tooth enamel, which forms the outer layer of each tooth crown, is the hardest and most mineralized tissue in the body (Gutiérrez-Salazar & Reyes-Gasga, 2003). It is mainly inorganic, consisting primarily of highly crystalline hydroxyapatite (Gutiérrez-Salazar & Reyes-Gasga, 2003). Tooth enamel forms early in life. Unlike bone, enamel does not remodel once formed, and therefore retains its original isotopic composition, which reflects the environment and diet during dental formation (i.e. during childhood). Consequently, isotope data determined from tooth enamel can be compared to the local environment and geology of an area (Gage, et al., 1989), thus distinguishing indigenous individuals who grew up in that area from immigrants from regions with different isotope values.

Underlying the enamel layer is the tooth dentin, which makes up the largest proportion of the tooth. Dentin has an organic matrix of collagenous proteins surrounded by apatite crystals. Dentin is less mineralized, more organic and softer than enamel, but harder than bone (LeGeros, 1981; Choo-Smith, et al., 2008).

2.5.3 Pb and Sr in bones and teeth

Both Sr^{2+} and Pb^{2+} can substitute for Ca^{2+} in the food web, and are deposited in the hydroxyapatite crystal lattice of bones and teeth (Comar, et al., 1957). Sr and Pb are both incorporated into body tissues from ingested water and food, as well as through inhalation of airborne particles. Different $^{87}Sr/^{86}Sr$ values in enamel and bone from a single individual may indicate dietary changes over time, and hence residence change (Ericson, 1985).

Pb follows the same pathways as Ca, and easily accumulates in bones and teeth due to the low solubility of lead phosphate (Aberg, et al., 1998). In South Africa, the first studies on Pb concentrations in teeth (Van Wyk & Grobler, 1983) were done during the 1980s, when leaded petrol was still in general use. The Pb levels in teeth of children from two selected urban regions in the Cape Peninsula were compared (Van Wyk & Grobler, 1983). Children living near large industrial plants exhibited average Pb concentrations of 20 ppm in whole teeth, 10.9 ppm in enamel and 23 ppm in dentin (Van Wyk & Grobler, 1983). The Pb concentrations in the teeth of children living near light industries were significantly lower: 16.6 ppm for whole teeth, 2.92 ppm for enamel, and 19.9 ppm for dentin (Van Wyk & Grobler, 1983). About 15 years later, when leaded petrol was no longer in use, Grobler et al. (2000) studied the Pb concentrations of teeth from individuals of a

remote rural town in the Northern Cape region of South African. Their results showed mean Pb concentrations of 2.04 ppm in dentin and 0.25 ppm in enamel (Grobler, et al., 2000). Comparing these two sets of data, it is evident that Pb concentrations of teeth were much higher during the leaded petrol era, when Van Wyk & Grobler (1983) first analysed the Pb isotopic values of children's teeth in Cape Peninsula. Both studies showed that Pb concentrations were significantly higher in dentin than enamel.

Montgomery (2002) compared the Sr and Pb concentrations of different tissues in modern teeth. Enamel showed higher Sr concentrations than dentin (Montgomery, 2002), whereas the opposite was true for Pb (Van Wyk & Grobler, 1983; Grobler, et al., 2000; Montgomery, 2002). Sr is significantly more abundant in modern teeth, compared with Pb, and concentrations typically range between 50– 300 ppm (Montgomery, 2002). Areas of high-Sr geology and drinking water may lead to even higher Sr concentrations in teeth, of up to 3000 ppm (Dudás, et al., 2016).

2.6 Previous archaeological studies using Sr and Pb isotopes

The first application of Pb isotopes in archaeology was sourcing of metals used to make metal artefacts (Brill & Wampler, 1967). This idea originated when scientists found that the Pb isotopic compositions of galena ores vary in different mining areas. Brill and Wampler (1967) found that three important ancient mining areas (Laurion, Southern Spain, and Roman Britain) had different Pb isotopic compositions. Therefore, by measuring the isotopic compositions of artefacts made of Pb, researchers could trace the regions from which the Pb originated (Brill & Wampler, 1967).

Since then, a large number of archaeological studies have used Pb isotopes as provenance markers of artefacts (Joel, et al., 1988; Costaglia, et al., 2001; Durali-Mueller, et al., 2007; Iñañez, et al., 2010; Thibodeau, et al., 2012). Applications include the study of Roman artefacts from archaeological sites in Germany and comparing them with the Pb isotope ratio of potential ore sources (Durali-Mueller, et al., 2007). In addition, Pb isotopes were useful in studying the provenance of Romita pottery from the Colonial period in Mexico City (Iñañez, et al., 2010). Romita pottery is traditionally covered with a transparent Pb glaze, which is visually similar to tin-glazed Spanish majolica and other contemporary European glazed ceramics (Iñañez, et al., 2010). Studies were able to determine that Pb-based ceramic glazes were manufactured in Mexico during the 16th and 17th centuries, because the Pb isotope compositions differ significantly from those of glazes on products known to have been manufactured in Spain (Joel, et al., 1988; Iñañez, et al., 2010). Pb isotopes were also valuable for identifying material culture belonging to the Coronado expedition, which took place through

northern Mexico and the southwestern United States from 1540 to 1542 (Thibodeau, et al., 2012). The Pb isotopic ratios of metallic Pb-based artefacts from two sites associated with the Coronado expedition were very similar and it was established that these artefacts were of Mexican origin (Thibodeau, et al., 2012). The major issue in using Pb isotope analysis of artefacts in provenance studies is the melting and mixing of Pb from various sources for reworking and reuse (Stos-Gale, 1992). This results in homogenisation of the isotope ratios, and limits the ability of Pb isotopes to trace metallic artefacts to their ore sources (Baron, et al., 2009).

Sr and Pb isotopes also find valuable application in forensic studies (Bilström, 2008). For instance, Pb isotope ratios in bullets can be used to trace their sources, since bullets are generally made of Pb alloys (Bilström, 2008). Even if the bullet was not found on the crime scene, the bullet residues may remain in a victim's body. Considerable differences among Pb isotope signatures of ammunition do indeed exist (Zeichner, et al., 2006).

2.6.1 Pb and Sr isotopes as palaeodietary tracers

Sr isotopes of archaeological skeletal tissues have been used to study past migration patterns since the 1980s (Ericson, 1985). Since then, more and more archaeological studies have used Sr isotopes to differentiate between local and non-local individuals, and to determine the origin of migrants and slaves (Sealy, et al., 1995; Montgomery, et al., 2003; Montgomery, et al., 2005; Pellegrini, et al., 2008; Schroeder, et al., 2009; Montgomery, 2010; Lamb, et al., 2014; Copeland, et al., 2016; Kootker, et al., 2016; Parker Pearson, et al., 2016). Most of these studies have used Sr isotopes along with other isotope systems to answer archaeological questions about migration and mobility. A combination of Sr, C, N, and O isotopes have been used for reconstructing palaeodiets and migratory patterns of individuals, where Sr gives information on their geological environment (Ericson, 1985), C and N isotopes reflect their diet (DeNiro & Epstein, 1978; Ambrose & Norr, 1993) and O isotopes reflect the isotopic composition of ingested water, and is thus related to climate (Longinelli, 1984; Budd, et al., 2004; Evans, et al., 2012). This isotope combination was used to detect variation in diet of King Richard III, indicating relocation from eastern to western England during his early childhood years (Lamb, et al., 2014). In Britain, Sr isotopes can clearly differentiate between individuals living on younger marine carbonate rocks and those living on older volcanic rocks (Montgomery, et al., 2003), but cannot differentiate between individuals local to Great Britain and those from other parts of northern Europe where the geology is similar to Britain (Evans, et al., 2010; Evans, et al., 2012). In a study of mobility in late-glacial central Italy, Sr isotopes were used to test the hypothesis that wild horses and red deer were moving between the coastal plain and the Apennine uplands (Pellegrini, et

al., 2008). Although there was no clear evidence for transhumance, the ranging behaviour of the two species was different (Pellegrini, et al., 2008).

A number of archaeological and palaeontological studies have analysed Pb isotopes in bones and teeth for examining past mobility and geographical origins of archaeological individuals (Ghazi, 1994; Aberg, et al., 1998; Montgomery, 2002; Shaw, et al., 2016; Dudás, et al., 2016). Progressively more studies are comparing Pb with Sr isotopes, to assess whether Pb can extend the interpretations made from Sr isotopic data (Montgomery, 2002; Shaw, et al., 2016; Dudás, et al., 2016). Sr and Pb isotopes have been used to identify people from the Roman period, due to the increased use of anthropogenic Pb during this period (Montgomery, 2002; Shaw, et al., 2016). By combining Pb and Sr isotopic ratios of individuals' bones and teeth, scientists were able to differentiate between locals and non-locals in Great Britain (Shaw, et al., 2016), which was previously difficult to determine with Sr isotopes alone (Evans, et al., 2010; Evans, et al., 2012). Pb isotopic data could efficiently distinguish between different sources varying at the 1st or even 2nd decimal places from each other (Sharpe, et al., 2016; Shaw, et al., 2016). Figure 2 below shows that Shaw et al. (2016) were able to separate the $^{207}Pb/^{206}Pb$ vs $^{208}Pb/^{206}Pb$ ranges of the London enamel samples from those of Rome enamel samples, Mendips ore (which indicates a Welsh/English signature) and Roman coins, all varying at the 2nd decimal place from one another (see Figure 2).

Studies have found that, whilst the use of Pb and Sr isotopic systems alone can provide valuable information, a combination of the two techniques is a very powerful tool in archaeological research (Aberg, et al., 1998; Montgomery, 2002; Shaw, et al., 2016; Dudás, et al., 2016).

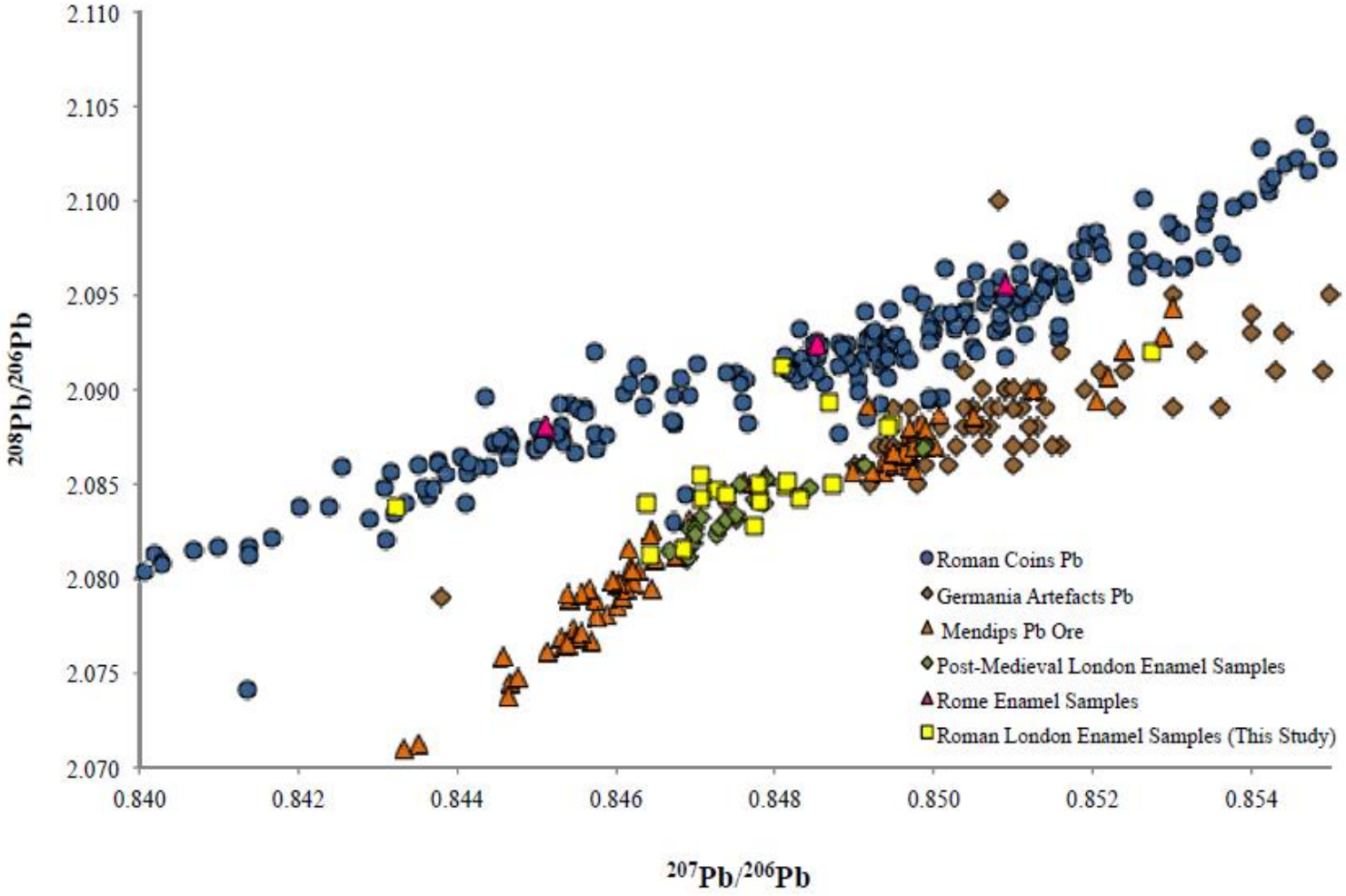

Figure 2: Comparing the $^{207}Pb/^{206}Pb$ vs $^{208}Pb/^{206}Pb$ data for London enamel samples (Shaw et al. 2016), German artefacts (Bode et al. 2009), Roman coins (Butcher and Ponting 2014), Mendips Pb Ore (Haggerty et al. 1996), Post-Medieval London enamel samples (Millard et al. 2014), and Rome enamel samples (Montgomery et al. 2010). Source of illustration: (Shaw, et al., 2016)

2.6.2 Pb and Sr isotopes as palaeodietary tracers in southwestern South Africa

Extensive research has been done on the bioavailable and whole-rock $^{87}Sr/^{86}Sr$ on the geological substrates of southwestern South Africa (see Table 4). The bioavailable Sr ranges for the Cape Granite and Malmesbury shale substrates, reported in Copeland et al. (2016) and Lehman et al. (2018), are significantly larger than the ranges of geological Sr values reported in Allsopp and Kolbe (1965) (see Table 4). This phenomenon may be due in part to differences in weathering rates of different components of rocks with different $^{87}Sr/^{86}Sr$ values (Sillen, et al., 1998). Near the coast, it is also due to blanketing by recent sands of marine origin.

Radloff et al. (2010) reported bioavailable $^{87}Sr/^{86}Sr$ values of different geological substrates in the De Hoop Nature Reserve (DHNR) in southwestern South Africa, measured on rodent teeth. There is a clear distinction between the bioavailable $^{87}Sr/^{86}Sr$ values of shales and those of the coastal sands and limestones (Radloff, et al., 2010). However, the bioavailable $^{87}Sr/^{86}Sr$ values could not differentiate between all the different geologies of the De Hoop Nature Reserve region (Figure 3). An important limitation of the Sr isotope system world-wide is the tendency of coastal terrestrial areas (covered by marine sands) to have $^{87}Sr/^{86}Sr$ values reflecting the composition of present-day seawater at 0.709241 ± 32 (Veizer, 1989). This is due to the presence of marine-derived calcareous sediments at coastal terrestrial environments, such as beach deposits and dunes with high fractions of shell, aeolianites, and calcarenites (Radloff, et al., 2010; Copeland, et al., 2016).

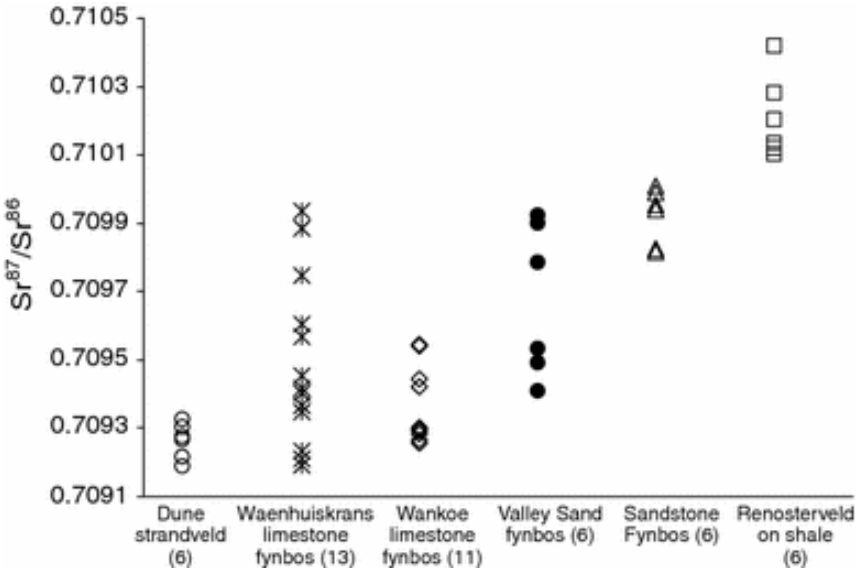

Figure 3: Bioavailable $^{87}Sr/^{86}Sr$ ratios of the different vegetation types (on different geological substrates) of De Hoop Nature Reserve, illustrating the overlapping $^{87}Sr/^{86}Sr$ ratios of most of the substrates (Radloff, et al., 2010)

Lehmann et al. (2018) and Copeland et al. (2016) analysed the $^{87}Sr/^{86}Sr$ values of fossil teeth recovered from the Elandsfontein and Pinnacle Point archaeological sites respectively, to find out whether the animals lived on local vegetation, which is today relatively nutrient poor, or migrated to nutrient rich areas to obtain food. Both studies found that the $^{87}Sr/^{86}Sr$ values of the fossil teeth fell within the local ranges, indicating that the animals did not migrate to areas of different geology (Copeland, et al., 2016; Lehmann, et al., 2018). The vegetation in the past environment must have had sufficient nutrients for these animals' needs (Copeland, et al., 2016; Lehmann, et al., 2018). Figure 4 below is an isoscape of bioavailable $^{87}Sr/^{86}Sr$ of southernmost South Africa, which illustrates an increase in bioavailable $^{87}Sr/^{86}Sr$ away from the south coast (Copeland, et al., 2016). These studies have found that although $^{87}Sr/^{86}Sr$ may vary naturally in rocks of different compositions and ages, strengthening its utility to differentiate between certain substrates (Ericson, 1985; Copeland, et al., 2016), Sr isotopes are inadequate when one wants to differentiate between the distinctive substrates of near-coastal environments.

Limited research is available for the bioavailable or whole-rock Pb isotopic ratios of southwestern South Africa. Soderberg & Compton (2007) analysed $^{206}Pb/^{207}Pb$ (1.141 ±0.008) and $^{208}Pb/^{207}Pb$ (2.404 ±0.017) of a protea sample derived from the Table Mountain substrate of the Cape Floristic Region. The purpose of their study was to determine how the fynbos ecosystem supports abundant and diverse vegetation on soils derived from nutrient-poor bedrock. The Pb and Sr isotope composition of the soil and vegetation determined that dust deposition is a significant source of nutrients to fynbos ecosystems (Soderberg & Compton, 2007).

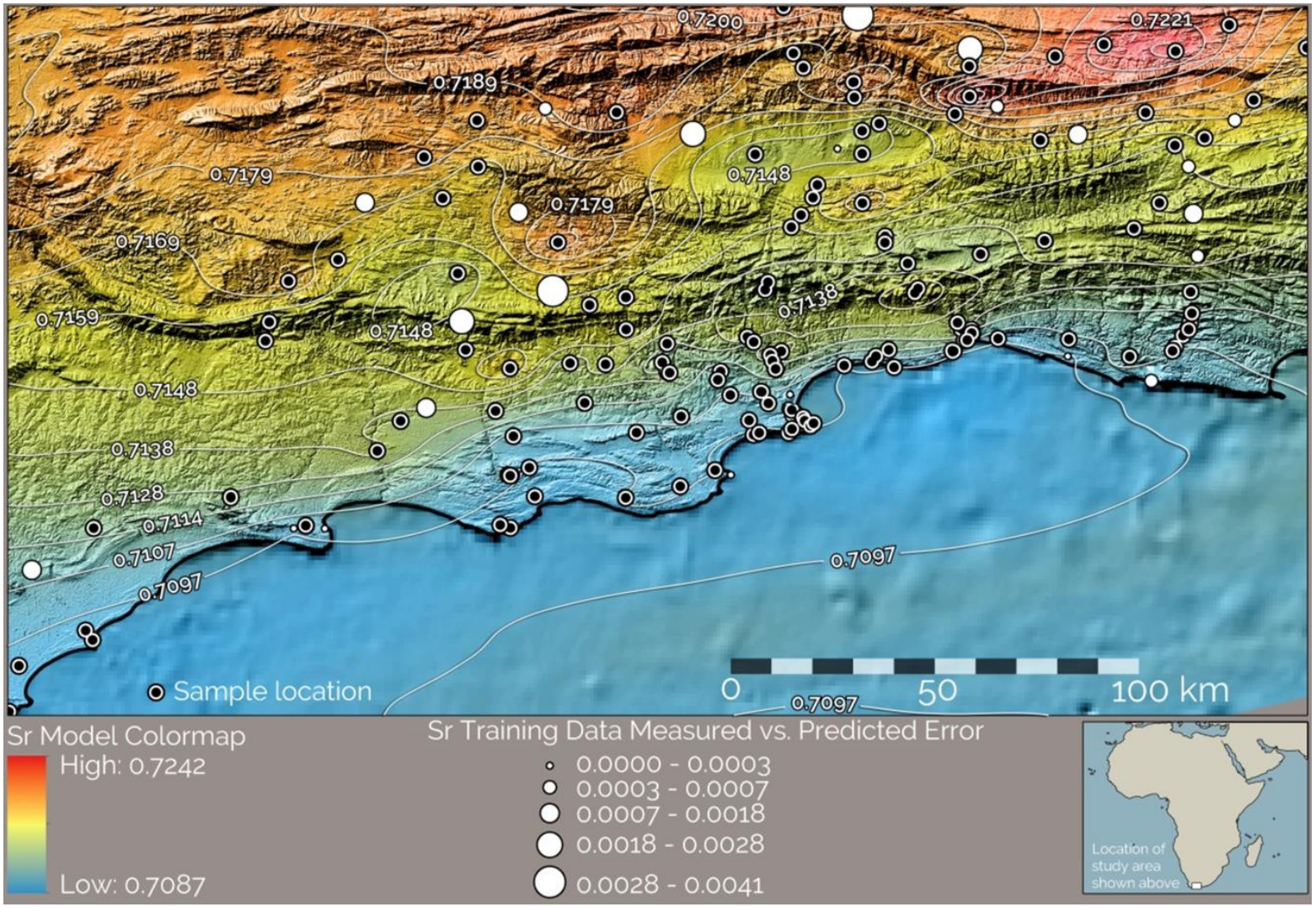

Figure 4: A plot of bioavailable $^{87}Sr/^{86}Sr$ vs. distance from the ocean for the different geological substrates of the South Coast of South Africa (Copeland, et al., 2016).

Table 4: Previously published results of $^{87}Sr/^{86}Sr$ in biological and geological samples from southwestern South Africa.

Reference	Sample Type & Location	Geological substrates of southwestern South Africa								
		Malmesbury shales	Cape Granite Suite	Cape Supergroup			Karoo sediments		Bredasdorp Group	Quaternary coastal sands
				Table Mountain	Bokkeveld	Witteberg	Little Karoo	Great Karoo		
(Allsop & Kolbe, 1965)	Rocks (Cape Peninsula)	0.7208 – 0.7873	0.7701 – 1.1602							
(Sealy, et al., 1991)	Modern bone of mammals (southwestern South Africa)	0.71777 – 0.71794		0.71543 – 0.71746						0.70938 – 0.71169
(Soderberg & Compton, 2007)	Plant & soil (The Cape Floristic Region)			Plants: 0.722 ± 0.005, 0.724 ± 0.005 Soil: 0.735 ± 0.005						
(Radloff, et al., 2010)	Modern teeth of rodents (south coast – De Hoop Nature Reserve)	Shale Renosterveld: 0.71009 – 0.71042		0.70982 – 0.71001					0.70906 – 0.70988	Dune strandveld: 0.70919 – 0.70933
(Copeland, et al., 2016)	Plants (south coast – Pinnacle Point)	0.7095 – 0.7157	0.7095 – 0.7177	0.7092 – 0.7169	0.7093 – 0.7209	0.7164 – 0.7237	0.7124-0.7202	0.7168-0.7237	0.7092 – 0.7101	
(Lehmann, et al., 2018)	Modern bone and teeth, and plants (west coast – Vredenburg Peninsula)	0.714092 – 0.720390	0.711421 – 0.723563	0.714092 – 0.720390						0.709380 – 0.711690

2.7 Measuring Sr and Pb isotopes

To obtain high precision Sr and Pb isotope ratios in bones and teeth, scientists have made use of two isotope analytical techniques: 1) Thermal Ionisation Mass Spectrometry (TIMS) and 2) Multi-collector Inductively Coupled Plasma Mass Spectrometry (MC-ICP-MS). The first TIMS instruments were single-collector systems, which limited the accuracy and precision in isotope ratio measurements due to ion-beam fluctuations (Bürger, et al., 2015). Multi-collector TIMS instruments were introduced in the 1980s to overcome these limitations and to measure several isotopes at the same time (Bürger, et al., 2015). The major disadvantage of TIMS is that it is a rather time-consuming procedure, whereas MC-ICP-MS has a simple sample preparation process and provides fast analyses. Therefore, although TIMS data is very precise, it is not able to generate big data sets easily, whereas MC-ICP-MS can measure substantially more samples in a given time. The MC-ICP-MS instrument allows the analysis of samples introduced either as solutions or as solid materials. In the case of solution analysis, a multi-collector (e.g. NU Plasma II) ICP-MS instrument is used to obtain isotopic ratios (Shaw, et al., 2016; Sharpe, et al., 2016; Copeland, et al., 2016). The elements of interest, Sr and Pb, must be chemically separated from the sample matrix prior to isotopic composition analysis by solution-MC-ICP-MS (Pin, et al., 1994). The direct analysis of solid samples can be done through a technique known as laser ablation (LA-MC-ICP-MS).

Isotope fractionation is a common occurrence for isotopic analysis with TIMS and MC-ICP-MS. Fractionation of natural (un-spiked) elements can be corrected by normalizing to an isotopic ratio whose value is constant in nature. $^{87}Sr/^{86}Sr$ values can be corrected for mass fractionation using the invariant Sr isotope ratio, $^{86}Sr/^{88}Sr = 0.1194$ (Sealy, et al., 1995; Pin, et al., 2014). However, Pb has no constant isotope ratio available for correction of mass fractionation by internal normalization (Rehkämper & Halliday, 1998), due to ^{204}Pb being its only non-radiogenic isotope. This limits the precision and accuracy of isotopic analysis with TIMS (Rehkämper & Halliday, 1998). Fortunately, MC-ICP-MS analysis can overcome this limitation by using a combination of external reference and internal isotope pairs with mass numbers similar to that of Pb (Rehkämper & Halliday, 1998; Pin, et al., 2014). The addition of thallium, with the isotopes ^{203}Tl and ^{205}Tl, is commonly used to correct the measured Pb isotope ratios (Rehkämper & Halliday, 1998; Pin, et al., 2014).

The international standard used for $^{87}Sr/^{86}Sr$ analysis is a strontium carbonate isotopic standard, known as NIST SRM 987 (Pin, et al., 1994). This enables determination of the long-term precision of the instrument as well as comparison of datasets between laboratories (Slovak & Paytan, 2011). Earlier multi-collector TIMS instruments produced external reproducibility of ± 0.00004 for

VG Micromass 30 (Sealy, et al., 1991) and ± 0.00002 to 0.00003 for VG Sector mass spectrometer (Sealy, et al., 1995; Oslick, et al., 1994) at 2σ standard deviation for the SRM (NBS) 987 Sr standard. More recent multi-collector TIMS instruments, such as the Thermo Trition, have measured the $^{87}Sr/^{86}Sr$ value of SRM 987 as 0.71025 ± 0.00001 (Shaw, et al., 2016). Solution-MC-ICP-MS can obtain internal errors of ± 0.00001 to 0.00003 (Copeland, et al., 2008) and external reproducibility of ± 0.00002 – 0.00003 (2σ) for SRM 987 Sr standard (Copeland, et al., 2016). $^{87}Sr/^{86}Sr$ measurements through solution-MC-ICP-MS is generally more accurate and precise than that of laser ablation, due to potential isobaric interferences during laser ablation analysis (Slovak & Paytan, 2011). Laser ablation techniques can produce internal precisions between ± 0.00001 to 0.0001 for $^{87}Sr/^{86}Sr$ ratios and external reproducibility of ± 0.0002 – 0.0003 for Sr carbonate standard (Copeland, et al., 2008).

NIST SRM 981 is the most widely used reference material for Pb isotope analysis (Thirlwall, 2002). The external precision and accuracy of Pb isotopic ratios by means of mass spectrometry is assessed through repeat analysis of the SRM 981 Pb standard, of which the values are then compared to the known SRM 981 standard values (Thirlwall, 2002). Shaw et al. (2016) found that solution-MC-ICP-MS can obtain the following external precisions on Pb isotopic ratios: $^{206}Pb/^{204}Pb$ ±0.010; $^{207}Pb/^{204}Pb$ ±0.017; $^{208}Pb/^{204}Pb$ ±0.020; $^{207}Pb/^{206}Pb$ ±0.010; $^{208}Pb/^{206}Pb$ ±0.012. Sharpe et al. (2016) found that the values for the SRM 981 standard, analysed along with the samples by Nu Plasma solution-MC-ICP-MS, are as follows: $^{206}Pb/^{204}Pb$ = 16.937 (±0.004, 2σ), $^{207}Pb/^{204}Pb$ = 15.490 (±0.003, 2σ), and $^{208}Pb/^{204}Pb$ = 36.695 (±0.009, 2σ). It is unclear why there is such a great difference in precision between these two studies.

2.8 Potential limitations of Sr and Pb isotopes as palaeodietary indicators

When studying Sr and Pb isotopes, we must be aware of the constraints that might occur with these isotope systems. The well-recognized problem with isotopic data from archaeological materials is possible post-depositional alteration of Pb and Sr in bones and teeth (Dudás, et al., 2016). Diagenesis may alter both the concentrations and isotopic compositions of buried samples (Hoppe, et al., 2003). Another main concern with Pb isotopes is anthropogenic Pb pollution of the earth's surface, which may alter the Pb isotopic compositions of the geological/ biological environment.

2.8.1 Diagenesis

The degree and rate of diagenetic processes in skeletal material is variable and depends on various factors such as the burial length, the burial environment, the climate, hydrology, pH, temperature, the type of material (e.g. tooth enamel/ bone) as well as the chemical element (Sr / Pb) of interest (Price, et al., 1992; Schoeninger, 1995; Slovak & Paytan, 2011).

Bone is more prone to diagenetic alteration, because of its high organic matter content and high porosity, while tooth enamel is largely resistant to diagenesis due to its low organic matter content and low porosity (Koch, et al., 1997; LeGeros, 1981). Dentin is somewhat softer and more organic than enamel and is more likely to undergo post-depositional isotopic change like bone (LeGeros, 1981). However, the lower porosity of dentin (compared to bone) reduces its susceptibility to diagenetic alteration (LeGeros, 1981). In addition, the apatite in tooth enamel is hydroxylated, which makes for greater stability, whereas bone apatite is not (Pasteris, et al., 2004). Diagenesis is not a problem with samples collected as fresh bone.

2.8.2 Anthropogenic Pb pollution

The Romans knew that Pb was harmful to their health and the first known written record of the symptoms of Pb poisoning was made by Nicander in the mid-2nd century BC (Montgomery, et al., 2010). However, the Romans still continued to use Pb in their water pipes, kitchenware, Pb glazing, paint, and for medical purposes (Aberg, et al., 1998; Montgomery, et al., 2010). This resulted in an increase in Pb concentrations in human bones from low prehistoric levels to values 10 to 100 times higher (Aberg, et al., 1998). During the 20th century, the use of Pb in most of the above-mentioned applications was withdrawn, followed by a decrease in Pb concentrations in bones to nearly prehistoric levels (Aberg, et al., 1998). However, the introduction in the 1920s of alkyl-lead, used primarily as an anti-knock agent in petrol, raised atmospheric Pb levels world-wide (Bollhöfer & Rosman, 2000). The world's largest alkyl-Pb producer was Associated Octel (based in the U.K.) and its products mainly controlled the isotopic composition of Pb emitted by the burning of leaded petrol (Bollhöfer & Rosman, 2000). In South Africa, leaded petrol reached its peak between the 1970s and 1990s (Aberg, et al., 1998). Since 1996, unleaded petrol has been available to motorists and its use gradually increased until 2006, when all leaded petrol was phased out and only Pb-free petrol was available in South Africa.

Bollhöfer & Rosman (2000) measured the Pb concentrations and $^{206}Pb/^{207}Pb$, $^{208}Pb/^{207}Pb$ and $^{206}Pb/^{204}Pb$ ratios of aerosols collected at various sites in the Southern Hemisphere between the years 1994 and 1999. The aerosols sampled in the southern parts of the world, especially South Africa, had lower $^{206}Pb/^{207}Pb$ and $^{208}Pb/^{207}Pb$ ratios compared to the Northern Hemisphere (Bollhöfer & Rosman, 2000), probably due to the supply of alkyl-Pb from a common supplier such as Associated Octel. In 1994 – 1995, the $^{206}Pb/^{207}Pb$ of alkyl-Pb in the U.K. was 1.055, while $^{208}Pb/^{207}Pb$ was 2.335 (Bollhöfer & Rosman, 2000). The aerosols collected by Bollhöfer & Rosman (2000) were primarily from cities where much of the atmospheric Pb derived from motor vehicle emissions. In 1998, the measured Pb isotopic composition in Cape Town aerosols ranged between 1.085 – 1.090 for $^{206}Pb/^{207}Pb$, 2.353 – 2.358 for $^{208}Pb/^{207}Pb$, and 16.87 – 16.99 for $^{206}Pb/^{204}Pb$ (Bollhöfer & Rosman, 2000), which were slightly higher than those of leaded petrol. This may be due to a change in the isotopic composition of the alkyl-Pb used, or a decrease in the contribution of leaded petrol to aerosols due to the introduction of unleaded petrol in South Africa in 1996 (Bollhöfer & Rosman, 2000).

Chapter 3: Materials and Methodology

The samples analysed for this thesis comprise a variety of animal bone and tooth samples, as well as some plants, mainly from the Western Cape region of South Africa. Samples from three different geological substrates of the Northern Cape region of South Africa were also included. Most samples were collected in the last few years, and therefore are from the present-day unleaded petrol era, but there are a few samples from the 1980s, when leaded petrol was still in used in South Africa. These are all from remote areas where there is likely to be little influence from motor vehicle emissions. The bones and teeth collected for this study were all from animals that had died recently. Small mammals from De Hoop were trapped and euthanased for a previous study (Radloff, 2008; Radloff et al., 2010). The isotope ratios are therefore unlikely to have been altered by diagenesis.

Table 5: List of samples obtained from different locations within southwestern South Africa. The numbering for the species is as follow: 1: *Procavia capensis* (rock hyrax), 2: *Damaliscus pygargus pygargus* (bontebok), 3: *Raphicerus melanotis* (Cape grysbok) 4: *Raphicerus campestris* (steenbok), 5: *Pelea capreolus* (grey rhebok); 6: *Antidorcas marsupialis* (springbok), 7: *Hystrix africae-australis* (porcupine), 8: *Chersina angulata* (angulate tortoise).

Sample	UCT ID	Collection year	Sample Type	Species	Location	Underlying Geology
1MS	UCT 719	1982	Quill	7	Doornbosch	Karoo Supergroup
2MS	UCT 722	1982	Bone	4	Doringrivier	Karoo Supergroup
3MS	UCT 821	1982	Bone	6	Churchhaven	Coastal marine sands
4MS	UCT 2102	1986	Bone	2	Bontebok National Park	Cape Supergroup
5MS	UCT 2105	1986	Bone	3	Bontebok National Park	Cape Supergroup
6MS	UCT 4290	1991	Tooth	3	Botterkloof	Karoo Supergroup
7MS	UCT 3923	1990	Tooth	1	Gifberg	Cape Supergroup
8MS	UCT 3924	1990	Tooth	1	Gifberg	Cape Supergroup
9MS	UCT 3925	1990	Tooth	1	Gifberg	Cape Supergroup
10MS	UCT15472	2013	Tooth	1	Kransgat River	Karoo Supergroup
11MS	UCT14347	2013	Tooth	1	Mertenhof	Karoo Supergroup
12MS	UCT 15489	2013	Tooth	1	Mertenhof	Karoo Supergroup

Sample	UCT ID	Collection year	Sample Type	Species	Location	Underlying Geology
13MS	UCT 15492	2013	Tooth	1	Mertenhof	Karoo Supergroup
14MS		2014	Tooth	1	Bushmanskloof	Karoo Supergroup
15MS	UCT 15528	2014	Tooth	1	Namaqua National Park	Namaqua Metamorphic Complex
16MS	UCT 15536	2014	Tooth	1	Namaqua National Park	Namaqua Metamorphic Complex
17MS	UCT 15548	2014	Teeth	1	Richtersveld National Park	Richtersveld
18MS	UCT 776	1982	Tortoise carapace	8	Koeberg	Coastal marine sands
19MSa		2015	Bone	1	Dabidas, Namaqua land	Granites
19MSb		2015	Teeth	1	Dabidas, Namaqua land	Granites
20MS		2016	Bone	5	Bontebok National Park	Cape Supergroup
21MS		2016	Dentin (from 20MS)	5	Bontebok National Park	Cape Supergroup
22MS		2016	Enamel (from 20MS)	5	Bontebok National Park	Cape Supergroup
23MS		2016	Bone	2	Bontebok National Park	Cape Supergroup
24MS		2016	Dentin (from 23MS)	2	Bontebok National Park	Cape Supergroup
25MS		2016	Enamel (from 23MS)	2	Bontebok National Park	Cape Supergroup

In addition, 16 rodent tooth samples were selected from a previous study by Radloff et al. (2010). Samples were chosen to represent each of the distinct geological substrates of the De Hoop Nature Reserve, as listed in Table 6. Also, see geological map below (Figure 5).

Table 6: List of rodent teeth samples from the De Hoop Nature Reserve. All *Rhabodomys pumilio* (four-striped grass mouse) except 7A O, which is *Otomys irroratus* (vlei rat).

Sample	Underlying Geology
1A R	Strandveld Formation of the Bredasdorp Group
2A R	Strandveld Formation of the Bredasdorp Group
3A R	Limestones of the Bredasdorp Group
4A R	Limestones of the Bredasdorp Group
5A R	Limestones of the Bredasdorp Group
7A O	Strandveld Formation of the Bredasdorp Group
8A R	Table Mountain Sandstone of Cape Supergroup
9A R	Table Mountain Sandstone of Cape Supergroup
10A R	Table Mountain Sandstone of Cape Supergroup
12A R	Limestones of the Bredasdorp Group
13A R	Limestones of the Bredasdorp Group
14A R	Limestones of the Bredasdorp Group
19A R	Limestones of the Bredasdorp Group
20A R	Strandveld Formation of the Bredasdorp Group
21A R	Table Mountain Sandstone of Cape Supergroup
22A R	Limestones of the Bredasdorp Group

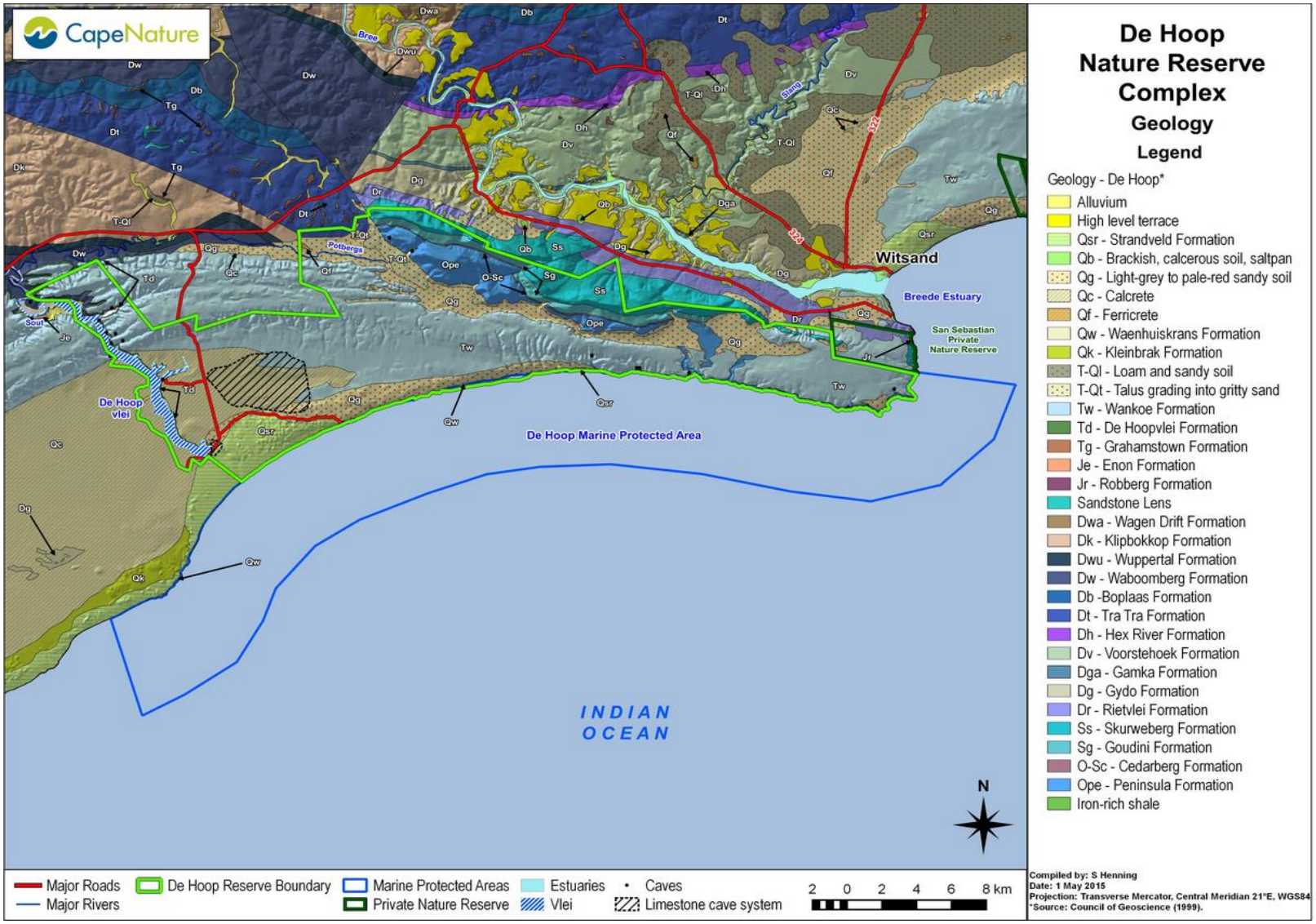

Figure 5: A geological map of the De Hoop Nature Reserve, from Cape Nature (Henning, 2015). Source of base map: Council of Geoscience (1999).

The choice of samples for analysis was constrained by what was available. Consequently, the samples above represented most of the geological substrates of southwestern South Africa, however, these samples did not adequately represent granite substrates. Therefore, on 30th January 2017, multiple plant samples were collected from granite substrates on Rooiheuwel farm, Vredenburg Peninsula (see Table 7 below). Plant samples were labelled according to their location (given by way points), starting at WP 1 at the lowest elevation on the farm, furthest away from the sea, moving in a westerly direction towards WP 5, situated at the highest hill on the farm, looking out to the sea. Only plants growing on granite-derived soils were sampled, avoiding areas with archaeological remains such as marine shells that may have influenced soil $^{87}Sr/^{86}Sr$.

Table 7: Description of the plant samples collected on the Cape granite bedrock geology of Rooiheuwel farm, Vredenburg Peninsula (the location of the archaeological site of Kasteelberg)

Sample	Elevation (m.a.s.l.)	Latitude (South)	Longitude (East)	Distance from the coast (km)
WP 1	81	32° 49' 28.4"	17° 57' 39.3"	6
WP 2	106	32° 48' 48.1"	17° 57' 13.6"	5
WP 3	126	32° 48' 50.0"	17° 57' 08.3"	4.8
WP 4	130	32° 48' 50.1"	17° 57' 05.2"	4.8
WP 5	173	32° 48' 53.5"	17° 56' 52.2"	4.5

Pre-treatment of the various types of samples was carried out as explained below:

3.1 Bone and tooth samples

Bones and teeth were surfaced-cleaned with a Dremel tool fitted with a rotating emery disc to remove superficial contamination. Samples weighing approximately 50 mg were cut and placed in labelled micro-centrifuge tubes. Two of the larger tooth samples were separated into enamel and dentin using a diamond powder coated dental drill-bit. Enamel was collected either as powder or small fragments. After the enamel had been removed the underlying yellowish dentin was exposed and could be sampled as a small fragment. The samples were placed in beakers filled with MQ-water in an ultrasonic bath for about 10 minutes, then left to dry on a watch glass in an oven at 40°C overnight.

Figure 6: Bones and teeth were surfaced-cleaned with a Dremel tool (left) and placed in beakers filled with MQ-water in an ultrasonic bath for about 10 minutes (right) to remove superficial contamination.

The samples were weighed (masses were recorded to the second decimal place) and placed into labelled 7ml teflon beakers. Each batch comprised 8 samples, along with a blank (marked as TPB, for Total Procedure Blank) and 50 mg of an in-house carbonate standard (NM 95). 4ml of 65% HNO_3 was added to each beaker, then placed on a hotplate at 140°C with a lid on and left to dissolve overnight. The lids were then removed and placed next to the beakers on the hotplate and the samples left to dry down. The beakers were removed from the hotplate and left for a few minutes to cool. 2ml of 65% HNO_3 was added to the residue in each beaker and the beakers again placed on the hotplate (without lids) and left to dry down. After the samples had dried and cooled down, the beakers were removed from the hotplate and 2.5 ml of 1M HNO_3 were added to each beaker and allowed to settle overnight, with their lids on.

Samples were split (1:4) between the ICP-MS facility, where Sr and Pb concentrations were measured, and the Radiogenic Isotope Facility (RIF) laboratories, for measurement of isotope ratios. Splitting of the samples took place in the RIF lab, where 0.5ml sub-samples of the 1M HNO_3 solutions were weighed out, dried down, and sent to the ICP-MS lab for measurement of the elemental concentrations of strontium (Sr) and lead (Pb). The remaining 2ml fractions were used for Pb and Sr separation (column) chemistry in preparation for the analysis of the isotope ratios of these samples.

3.2 Plant samples

Plant samples were thermally decomposed to ash. First, plants were cut into small pieces with garden scissors, so they would fit into quartz crucibles. The scissors were cleaned before and after each sample was cut, by wiping with a paper towel. The crucibles were placed (uncovered) in a muffle furnace at an initial temperature of 300°C and the temperature increased by 100°C every hour until a temperature of 650°C was reached, then left overnight. The next day, the muffle furnace was switched off and opened to cool down, before removing the crucibles. If necessary, the crucibles were stored in a desiccator. The ashed samples were ground to a fine powder, using a mortar and pestle. Approximately 50 mg of each sample was weighed out (masses were recorded) and placed in a Teflon beaker. One batch comprised five plant samples, along with a reference material and a blank (empty beaker). The basalt in-house reference material, ALR33G, was processed as an unknown along with plant samples. 4ml of 4:1 concentrated HF:HNO_3 was added to each beaker, then placed on a hotplate at 140°C with a lid on and left for 48 hours for the sample to dissolve. The lids were then removed and placed next to the beakers on the hotplate and the samples left to dry down. The beakers were removed from the hotplate and left for a few minutes to cool. 2ml of 65% HNO_3 was added to the residue in each beaker and the beakers again placed on the hotplate (without lids) and left to dry down. This step was then repeated for the second nitric conversion. After the samples had dried and cooled down, the beakers were removed from the hotplate and 2 ml of 1M HNO_3 were added to each beaker and allowed to settle overnight, with their lids on. The solutions were then put through ion exchange columns to isolate Pb and Sr.

3.3 Measurement of Sr and Pb concentrations by ICP-MS

Samples were diluted with 5% HNO_3 to about 25g (masses were recorded to the 4th decimal place) into 50mL clean centrifuge tubes and then tilted to mix. The 5% HNO_3 solution contains 10ppb Re, Rh, In and Bi, which was used as internal standards. For analysis of Sr concentration, 100µL of this 25g sample solution was pipetted into 15mL cleaned centrifuge tubes marked "Sample name – Sr" (and aliquot masses recorded) followed by an addition of 9.9mL of 5% HNO_3 to these Sr-marked centrifuge tubes for further dilution (diluted masses recorded). For analysis of Pb concentration, 500µL of the original 25g sample solution was pipetted into another set of 15mL centrifuge tubes marked "Sample name – Pb" (and aliquot masses recorded) followed by an addition of 9.5 mL of 5% HNO3 to these Pb-marked centrifuge tubes for further dilution (diluted masses recorded).

Figure 7: Dilution of samples with 5% HNO_3 to 25g (masses were recorded to the 4th decimal place). Next, 100µL of this 25g sample solution was pipetted into 15mL centrifuge tubes (and aliquot masses were recorded) and marked "Sample name – Sr".

Elemental concentrations of Sr and Pb were determined on a Thermo X-series II quadrupole ICP-MS, to assess the quantity of sample required for isotopic analysis. Since there are no published Sr or Pb concentration data for NM95, the in-house standard solutions were run as unknowns to assess accuracy. Calibration curves were obtained using artificial multi-element standards, from which standard solutions were made.

3.4 Combined Sr-Pb separation scheme

The method used for the combined Sr-Pb separation chemistry was based primarily on Pin et al. (2014) with a few adjustments. This crucial step involves the pre-concentration of Sr and Pb, present in only trace amounts, and removal of the matrix elements from the bulk digested sample (Pin, et al., 2014), prior to isotope ratio determination by high-precision MC-ICP-MS.

This combined Sr-Pb separation scheme required new Savillex Teflon columns, which first had to go through an extensive cleaning process. The cleaning procedure consisted of soaking for one night in "2% decon" (decontamination process), followed by one night in 1:1 HCl, two nights in 1:1 HNO_3, one night in Milli-Q water, and lastly, one night in a drying box. After cleaning, the columns were cut to 2cm lengths and fitted with frits with a porosity of about 30µm and thickness of about 2.5mm. These frits were wetted with methanol to optimise flow, which was done by filling the columns three times with methanol and letting it flow through. Columns were then filled with 0.05M HNO_3 and left to drip through before filling the bed of the column with Sr.Spec resin (Eichrom), slurried in a few ml of 0.05M HNO_3. The columns were cleaned and conditioned using three cycles of 10ml 6M HCl, followed by 10ml 0.05M HNO_3.

Each 2mL sample fraction in 1 M HNO_3 was centrifuged at 4000rpm for 20min to ensure that any solid residues settled out. The sample solution was then loaded in 2 x 0.9ml aliquots onto the columns with a waste beaker beneath each column. After complete draining of the sample solution, the columns were washed twice with 0.5mL 1M HNO_3, then 2 x 1mL of 7M HNO_3 to elute unwanted elements, especially barium. The Sr fraction was then collected with 2mL of 0.05M HNO_3 into a clean, labelled teflon beaker. Finally, the Pb fraction was collected with 4mL of 6M HCl into another clean, labelled teflon beaker. The Sr and Pb fractions were placed on a hotplate at 140°C to dry down. Once the Sr fractions had dried and cooled down, 2ml of 0.2% HNO_3 were added and ultrasonicated for 30min. The Pb fractions were dried and cooled down, then underwent two nitric conversions. A few drops of concentrated HNO_3 were added, just enough to cover the bottom of the beaker, then dried down on the hotplate (and this step repeated). Next, 1ml of 2% HNO_3 was added and ultrasonicated for 30min. These Pb and Sr fractions were then taken to the MC-ICP-MS laboratory for analysis. Table 8 summarises the method used for the combined Sr-Pb separation chemistry.

Table 8: Procedure for combined Sr-Pb Separation Chemistry

Column	1	2	3	4	5	6	7	8	9	10
Sample name										
Mass (mg) of sample										
Sr concentration (ppm)										
Pb concentration										
1. Weigh ±50mg of sample into 7ml teflon beakers.										
2. Add 4ml of 65% HNO_3 to each sample; close the beaker and digest on a hotplate overnight at 140°C.										
3. Open beakers carefully and dry down the sampes at 140°C.										
4. Once dried, cool the samples and add 2ml 65% HNO_3. Dry down immediately.										
5. Add 2ml 1M HNO_3 and allow to settle overnight.										
6. Pipette out 2 x 1ml sample into centrifuge tubes and spin at 4000rpm for 20mins.										
Column chemistry and elution of Sr, Pb										
Sample Loading: (waste beaker)		2 x 0.9ml of sample			0.9	0.9				
Wash:		2 x 0.5ml of 1M HNO_3			0.5	0.5				
Elution of Ba (waste beaker)		2ml of 7M HNO_3			2					
Collecting:										
Elution of Sr (place clean, labelled, 7ml beaker beneath each column)		2ml of 0.05M HNO_3			2					
Elution of Pb (place clean, labelled, 7ml beaker beneath each column)		4ml of 6M HCl			0.5	3	0.5			
For **Sr**: Dry down all samples on hotplate at 140°C. Cool and pipette in 2ml of 0.2% HNO_3. Ultrasonicate for 30mins.										
For **Pb**: Dry down all samples on hotplate at 140°C. Convert to nitrate by adding few drops of concentrated HNO_3 and dry down again (repeat this step). Cool and pipette in 1ml of 2% HNO_3. Ultrasonicate for 30mins.										
Column cleaning:	**1**	**2**	**3**	**4**	**5**	**6**	**7**	**8**	**9**	**10**
10ml of 6M HCl										
10ml of 0.05M HNO_3										
10ml of 6M HCl										
10ml of 0.05M HNO_3										
10ml of 6M HCl										
10ml of 0.05M HNO_3										

3.5 Measurement of Sr and Pb isotope composition using high resolution multi-collector inductively-coupled-plasma mass spectrometry (HR-MC-ICP-MS)

Multi-collector ICP-MS offers greatly increased resolution and precision with the combined advantages of both TIMS and ICP-MS. Although the low abundance ^{204}Pb isotope is associated with a larger measurement error than ^{206}Pb, ^{207}Pb, and ^{208}Pb, this instrument can analyse ^{204}Pb with good internal precision (see Table 9).

Sr and Pb isotope analyses were performed on a NuPlasma HR MC-ICP-MS from Nu Instruments. For this study, samples were introduced into the MC-ICP-MS as solutions, using the Nu Instruments DSN-100 desolvating nebuliser. Solution analysis typically requires at least 50ng of the element of interest, achieved through the combined Sr-Pb separation chemistry as described earlier.

The separated Sr fraction for each sample, dissolved in 2 ml 0.2% HNO_3, was diluted to 200 ppb Sr for isotope analysis. Analyses were referenced to bracketing analyses of NIST SRM987, using an $^{87}Sr/^{86}Sr$ reference value of 0.710255. All Sr isotope data were corrected for Rb interference using the measured signal for ^{85}Rb and the natural $^{85}Rb/^{87}Rb$ ratio. Instrumental mass fractionation was corrected using the measured $^{86}Sr/^{88}Sr$ ratio and the exponential law, and a true $^{86}Sr/^{88}Sr$ value of 0.1194. Analytical error associated with measurements by solution is ±0.00002 (2σ). The long-term external reproducibility on the $^{87}Sr/^{86}Sr$ ratio measurements on the in-house carbonate standard NM95, is 0.00002 at the 2-sigma level, based on repeat analysis at the MC-ICP-MS facility at UCT.

The separated Pb fraction, dissolved in 1 ml 2% HNO_3, was diluted to 50 ppb for isotope analysis. NIST SRM9997 Tl (Thallium) was added to all standards and samples to give a Pb:Tl ratio of approximately 10:1. NIST SRM981 was used as the reference standard, with $^{208}Pb/^{204}Pb$, $^{207}Pb/^{204}Pb$, $^{206}Pb/^{204}Pb$ normalizing values of 36.7219, 15.4963, 16.9405, respectively (Galer & Abouchami, 1998). All Pb isotope data was corrected for Hg isobaric interference by subtraction of on-peak background measurements. Instrumental mass fractionation was corrected using the exponential law, and a $^{205}Tl/^{203}Tl$ value of 2.3889. The reproducibility of the measurements is reported below.

Chapter 4: Results

This chapter presents the Sr and Pb concentrations and isotopic ratios for all samples analysed. However, prior to presenting the data, of primary importance in this study is the feasibility of the method and consequently, the integrity of the data. Therefore, method evaluation will form part of this results section.

4.1 Method evaluation

The isotopic ratios measured for the NM95 in-house carbonate standard of each batch were compared with one another, to determine if the results were consistent. Table 9 and Figure 8 shows that the NM95 in-house carbonate standard was relatively consistent for each analysis, with only a slight offset in Pb isotope ratios in the September 2016 analysis (for batch 2). This batch comprises samples 10ms to 17ms.

Table 9: The Sr and Pb isotopic ratios for NM95 (in-house carbonate reference standard) of each batch, with the respective 2-sigma internal as well as the 2-sigma external errors from the mean. A different standard (ALR33G) was used for the plant samples (WP 1 – 5), therefore, we cannot compare its $^{87}Sr/^{86}Sr$ value with that of NM95.

Batch #	1	2	3	4	5		
Samples	2–9ms	10–17ms	18–25ms	1AR–9AR	10AR–22AR		
Date of analysis	Aug-16	Sep-16	Oct-16	Nov-16	Dec-16	Mean	±2sigma external
$^{87}Sr/^{86}Sr$	0.708931	0.708923	0.708942	0.708947	0.708949	0.708938	0.00002
±2s internal	0.00001	0.00001	0.00001	0.00001	0.00001		
$^{208}Pb/^{204}Pb$	38.2319	37.9804	38.2466	38.2131	38.2765	38.1897	0.239
±2s internal	0.0026	0.0023	0.0028	0.0030	0.0026		
$^{207}Pb/^{204}Pb$	15.7985	15.7614	15.7959	15.7987	15.7944	15.7898	0.032
±2s internal	0.0010	0.0008	0.0011	0.0011	0.0009		
$^{206}Pb/^{204}Pb$	20.7234	20.1203	20.7174	20.6919	20.5234	20.5553	0.513
±2s internal	0.0013	0.0009	0.0015	0.0012	0.0009		
$^{208}Pb/^{206}Pb$	1.8449	1.8877	1.8463	1.8468	1.8650	1.8581	0.0369
±2s internal	0.00006	0.00005	0.00004	0.00006	0.00006		
$^{207}Pb/^{206}Pb$	0.7624	0.7834	0.7625	0.7635	0.7696	0.7683	0.0179
±2s internal	0.00002	0.00001	0.00002	0.00001	0.00002		
$^{208}Pb/^{207}Pb$	2.4200	2.4097	2.4213	2.4188	2.4234	2.4186	0.0105

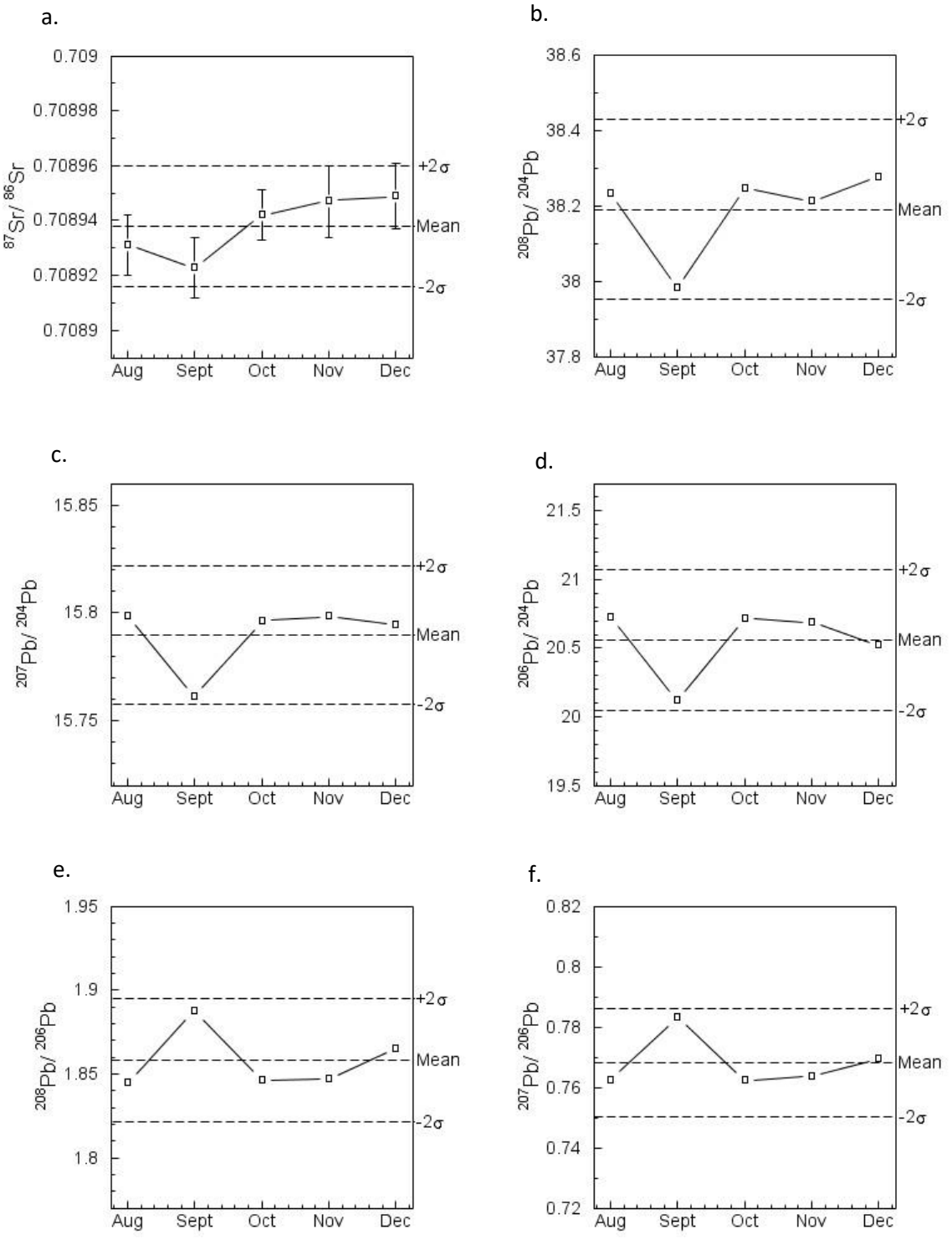

Figure 8: Sr and Pb isotopic ratios of NM95 in-house carbonate standard analysed for each batch (or date of analysis). The internal 2-sigma errors are shown for each Sr isotope analysis. The internal errors for the Pb isotopic ratios were so small that they are included within the size of the points as plotted above. The dotted lines indicate the means and the external 2-sigma errors.

A further evaluation of the method consisted of comparing the Sr isotopic ratios of the rodent teeth measured by laser ablation by Radloff et al. (2010) with the solution values obtained on the same samples for this study. The Sr isotopic ratios of the solution technique exhibited a lower external 2-sigma error (±0.00002) than those of the laser ablation technique (±0.0003).

Table 10: Comparison of $^{87}Sr/^{86}Sr$ values obtained by the solution technique with those obtained by laser ablation, with 2-sigma errors. All samples from De Hoop Nature reserve.

Sample nr.	Geological Substrate	Solution Technique ($^{87}Sr/^{86}Sr$)	±2s internal	±2s external	Laser Ablation ($^{87}Sr/^{86}Sr$)	±2s internal	±2s external
1A R	Dune Strandveld	0.709260	0.00001	0.00002	0.709330	0.00005	0.0003
2A R	Dune Strandveld	0.709256	0.00001	0.00002	0.709190	0.00003	0.0003
3A R	Waenhuiskrans Limestone	0.709267	0.00001	0.00002	0.709400	0.00008	0.0003
4A R	Waenhuiskrans Limestone	0.709431	0.00002	0.00002	0.709370	0.00001	0.0003
5A R	Wankoe Limestone	0.709225	0.00002	0.00002	0.709260	0.00001	0.0003
7A O	Valley Sand (Strandveld)	0.709942	0.00001	0.00002	0.709780	0.00004	0.0003
8A R	Table Mountain Sandstone	0.710280	0.00001	0.00002	0.710010	0.00001	0.0003
9A R	Table Mountain Sandstone	0.710063	0.00001	0.00002	0.709960	0.00001	0.0003
10A R	Table Mountain Sandstone	0.709925	0.00002	0.00002	0.709820	0.00001	0.0003
12A R	Waenhuiskrans Limestone	0.709388	0.00001	0.00002	0.709880	0.00007	0.0003
13A R	Waenhuiskrans Limestone	0.709270	0.00001	0.00002	0.709570	0.00005	0.0003
14A R	Waenhuiskrans Limestone	0.709160	0.00001	0.00002	0.709230	0.00001	0.0003
19A R	Wankoe Limestone	0.709141	0.00001	0.00002	0.709290	0.00009	0.0003
20A R	Valley Sand (Strandveld)	0.709681	0.00001	0.00002	0.709530	0.00006	0.0003
21A R	Table Mountain Sandstone	0.710083	0.00001	0.00002	0.709940	0.00001	0.0003
22A R	Wankoe Limestone	0.709196	0.00001	0.00002	0.709280	0.00001	0.0003

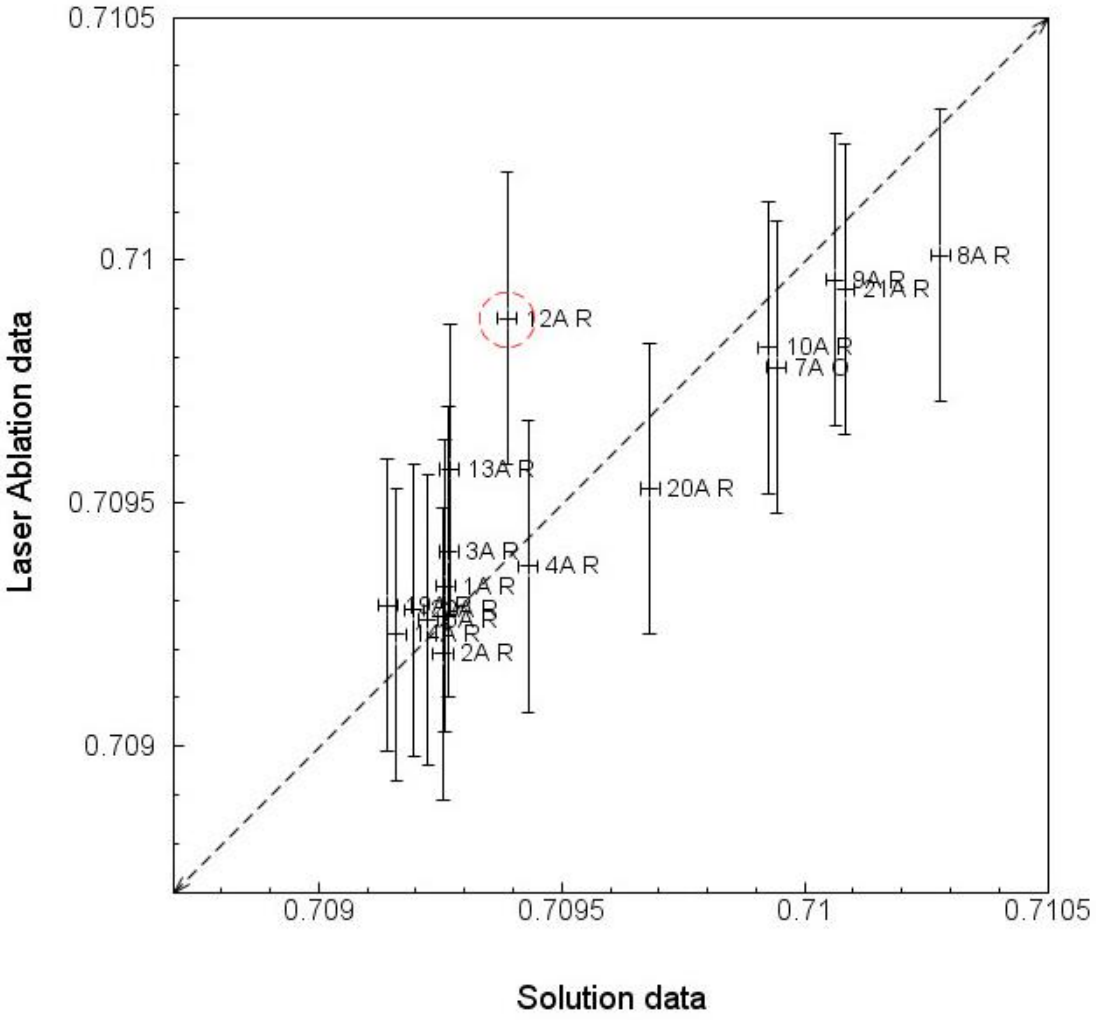

Figure 9: $^{87}Sr/^{86}Sr$ values obtained by laser ablation vs. solution MC-ICP-MS for the same samples from the De Hoop Nature Reserve. The vertical error bars represent the external 2-sigma error for laser ablation at ±0.0003. The smaller horizontal error bars represent the external 2-sigma error for solution data at ±0.00002. Red circle indicates the single sample for which the two results are notably different.

The majority of $^{87}Sr/^{86}Sr$ values from the solution technique plotted within the error bars of the laser ablation measurements (Figure 9), indicating that the results of this master's study are consistent with those of Radloff et al. (2010). Only one sample (12A R) from the Waenhuiskrans limestone substrate yielded significantly different $^{87}Sr/^{86}Sr$ results by the two techniques: 0.709880 by laser ablation compared with 0.709388 by solution. A deviation from the 1:1 trend occurs in Figure 9, where it appears as if the curve is flattening off towards higher $^{87}Sr/^{86}Sr$ values for solution data compared to laser ablation data. The reason for this is unknown, seeing as this occurred in different samples and were analysed at 2 different time periods (2 different batches).

4.2 Concentration data

Table 11 presents the Sr and Pb concentration data for all the bone and tooth samples of this study. The Sr concentrations ranged between 111 ppm and 1862 ppm, whereas the Pb concentrations ranged between 0.012 ppm and 2.30 ppm. As shown in Figure 10, all the bone samples had Sr concentrations below 900 ppm and Pb concentrations below 1 ppm, while the whole-tooth samples had Sr concentrations up to about 1900 ppm with Pb concentrations below 0.8 ppm. The concentration data reported here match the observations made by Montgomery (2002), showing higher Sr concentrations in teeth, compared to Pb. Interestingly, all the samples with high Pb concentrations had low Sr concentrations and those with very high Sr concentrations had low Pb concentrations. All of the samples having Sr concentrations in excess of 1000ppm were rock hyrax (dassie) whole-tooth samples and the one vlei rat tooth sample. Out of the entire sample set, only 7 samples had Pb concentrations above 0.5ppm. All of the bontebok samples (n=4) had Pb concentrations above 0.5ppm with Sr concentrations below 500ppm. Most of the concentration data represents bone and whole tooth samples, with only two cases where the dentin and enamel of an individual was separated. In both these cases, the Pb concentrations were higher in the dentin than the enamel, as seen in previous studies (Van Wyk & Grobler, 1983; Grobler, et al., 2000; Montgomery, 2002). In addition, the Pb concentrations were also higher in the dentin compared to the individual's bone.

Figure 10 also shows the concentration data distinguished by geological substrate. All the samples from the Karoo sediments had Pb concentrations below 0.4 ppm, with Sr concentrations ranging from 111 ppm for the bone samples up to 1862 ppm for the tooth samples. The samples from the limestone, dunes strandveld, and coastal substrates had relatively low Pb and mid Sr concentrations, compared to the rest of the sample set, which concentrations below 0.7 ppm for Pb and below 700 ppm for Sr. Out of the entire sample set, the sample with the highest Pb concentration was a bontebok dentin sample from the Cape Supergroup, while the highest Sr concentration was measured in a dassie tooth from the Cape Supergroup.

Table 11: Elemental concentrations of Sr and Pb in the samples. The numbering for the species is as follow: 1: *Procavia capensis* (rock hyrax), 2: *Damaliscus pygargus pygargus* (bontebok), 3: *Raphicerus melanotis* (Cape grysbok) 4: *Raphicerus campestris* (steenbok), 5: *Pelea capreolus* (grey rhebok); 6: *Antidorcas marsupialis* (springbok), 7: *Hystrix africae-australis* (porcupine), 8: *Chersina angulata* (angulate tortoise), 9: *Rhabodomys pumilio* (four-striped grass mouse), 10: *Otomys irroratus* (vlei rat).

Sample	Sample type	Species	Geological substrate	Sr (ppm)	%RSD	Pb (ppm)	%RSD
2 ms	Bone	4	Karoo Sediments	111	0.292	0.316	3.06
3 ms	Bone	6	Coastal-marine sands	146	0.395	0.297	0.606
4 ms	Bone	2	Cape System	299	0.315	1.02	1.81
5 ms	Bone	3	Cape System	454	0.095	0.153	3.09
6 ms	Tooth	3	Karoo Sediments	211	0.580	0.327	0.885
7 ms	Tooth	1	Cape System	1830	0.698	0.139	0.075
8 ms	Tooth	1	Cape System	1552	0.724	0.396	0.336
9 ms	Tooth	1	Cape System	1600	0.751	0.050	1.64
10 ms	Tooth	1	Karoo Sediments	1390	1.12	0.024	5.67
11 ms	Tooth	1	Karoo Sediments	1445	1.12	< d.l.	
12 ms	Tooth	1	Karoo Sediments	1862	0.191	0.122	5.27
13 ms	Tooth	1	Karoo Sediments	1051	0.065	0.193	1.59
14 ms	Tooth	1	Karoo Sediments	1860	0.144	0.020	16.0
15 ms	Tooth	1	Metamorphic Complex	1378	0.680	0.051	3.42
16 ms	Tooth	1	Metamorphic Complex	1150	0.054	0.213	3.14
17 ms	Teeth	1	Richtersveld Suite	891	0.203	0.028	7.00
18 ms	Tortoise carapace	8	Coastal-marine sands	774	0.312	0.758	1.62
19 ms A	Bone	1	Granite rocks	771	0.381	0.248	2.06
19 ms B	Tooth	1	Granite rocks	752	0.578	0.115	0.267
20 ms	Bone	5	Cape System	288	0.376	0.328	1.18
21 ms	Dentin (20MS)	5	Cape System	394	1.60	0.411	0.227
22 ms	Enamel (20MS)	5	Cape System	485	0.343	0.138	0.228
23 ms	Bone	2	Cape System	330	1.52	0.755	0.801
24 ms	Dentin (23MS)	2	Cape System	403	0.178	2.30	0.799
25 ms	Enamel (23MS)	2	Cape System	347	1.62	1.69	1.52
1A R	Bone	9	Dune Strandveld	524	0.325	0.684	7.45
2A R	Bone	9	Dune Strandveld	882	0.495	0.143	11.4
3A R	Bone	9	Waenhuiskrans Limestone	374	0.250	0.399	2.07
4A R	Bone	9	Waenhuiskrans Limestone	206	0.584	0.246	7.76
5A R	Tooth	9	Wankoe Limestone	493	0.497	0.025	2.98
7A O	Tooth	10	Valley Sand (Strandveld)	1114	0.291	0.265	2.25

Sample	Sample type	Species	Geological substrate	Sr (ppm)	%RSD	Pb (ppm)	%RSD
8A R	Tooth	9	Table Mountain Sandstone	511	0.291	0.737	3.41
9A R	Tooth	9	Table Mountain Sandstone	277	0.579	0.276	2.25
10A R	Tooth	9	Table Mountain Sandstone	367	0.314	0.379	0.182
12A R	Tooth	9	Waenhuiskrans Limestone	195	0.103	0.117	13.7
13A R	Tooth	9	Waenhuiskrans Limestone	291	0.914	0.225	2.67
14A R	Tooth	9	Waenhuiskrans Limestone	778	0.754	0.039	3.81
19A R	Tooth	9	Wankoe Limestone	337	0.397	0.012	122
20A R	Tooth	9	Valley Sand (Strandveld)	316	0.640	0.269	1.51
21A R	Tooth	9	Table Mountain Sandstone	223	0.378	0.163	2.79
22A R	Tooth	9	Wankoe Limestone	138	0.627	0.186	9.89

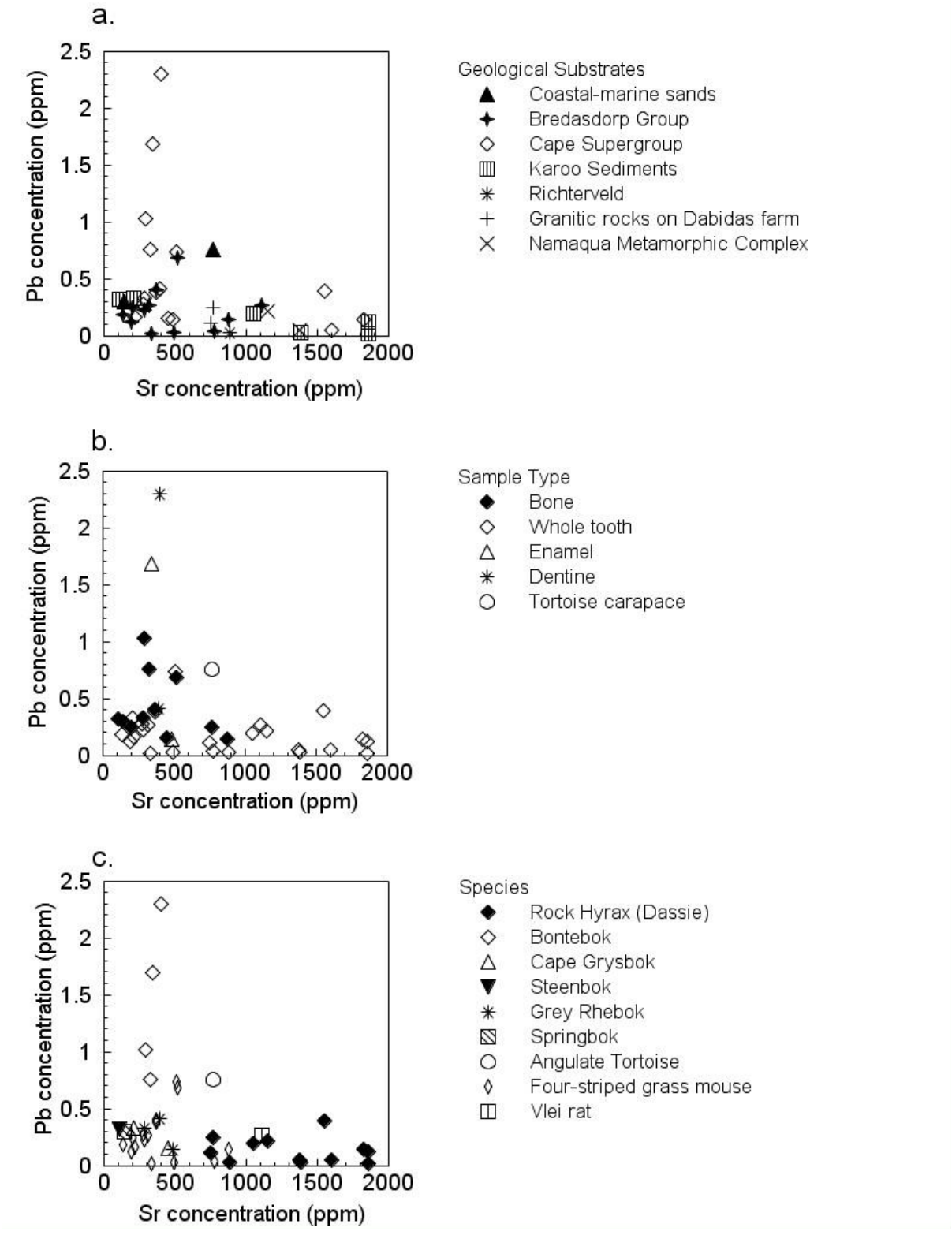

Figure 10a, b and c: Sr vs. Pb concentrations (ppm), grouped according to the geological substrate (Fig.10a), sample type (Fig.10b) and species (Fig.10c).

4.3 Isotopic composition data

4.3.1 Sr isotopic ratios

The isotopic ranges for the bioavailable Sr of each geological substrate are given in Table 12 and illustrated in Figure 11. $^{87}Sr/^{86}Sr$ for the samples from southwestern South Africa ranged between 0.709 for the coastal-marine sands to 0.719 for the Karoo sediments. As shown in Figure 11b, $^{87}Sr/^{86}Sr$ was distinctly higher in the geological substrates of the Northern Cape region of South Africa, compared to the Western Cape region. The samples from Namaqua National Park had $^{87}Sr/^{86}Sr$ of up to 0.755, followed by the sample from Dabidas farm, ranging between 0.734 – 0.739, and the sample from Richtersveld National Park, with an $^{87}Sr/^{86}Sr$ ratio of 0.726. These three areas within the Northern Cape Province comprise older and very different bedrock geology compared to the Western Cape samples in this study.

The $^{87}Sr/^{86}Sr$ ratios of all the samples from the Karoo Supergroup ranged between 0.715–0.719, while the samples from the Cape Supergroup had a slightly lower $^{87}Sr/^{86}Sr$ range between 0.712–0.713. These ratios were somewhat higher than the marine $^{86}Sr/^{87}Sr$ value of 0.7092 (Veizer, 1989). The plant samples collected from the Cape Granites on Kasteelberg, located at Rooiheuwel farm, had $^{87}Sr/^{86}Sr$ ratios between 0.712–0.715, slightly above the marine signal and similar to the samples from the Cape Supergroup. These values are lower than one would expect for granites (Allsop & Kolbe, 1965), probably due to a contribution from marine-derived Sr. The two waypoints with the lowest $^{87}Sr/^{86}Sr$ values were WP 5 (0.7117), which was situated on the highest hill on Kasteelberg and more exposed to possible sea spray, and WP 4 (0.7115), which was situated just behind the highest hill and more sheltered from possible sea spray.

The rodent tooth samples from De Hoop Nature Reserve had $^{87}Sr/^{86}Sr$ values ranging from 0.709 for the Bredasdorp Group (corresponding to the marine signal) to about 0.710 for the samples from the Table Mountain Sandstones, which is slightly below the other Cape Supergroup samples. The Sr isotopic ratios for this study were lowest in the samples from coastal marine sands, ranging between 0.709 – 0.7095, which is consistent with the marine signal. This is expected, seeing as the plants in this area grow on Holocene shell-rich coastal sands which are exposed to sea-spray, influencing the Sr value of the nearby soil and plants.

Table 12: The Sr isotopic ratios of all the samples from this study.

Sample	Location	Geological substrate	$^{87}Sr/^{86}Sr$	±2s internal
1ms	Doornbosch	Karoo Sediments	0.716505	0.00003
2ms	Doringriver	Karoo Sediments	0.718790	0.00001
3ms	Churchhaven	Quaternary coastal-marine sands	0.709483	0.00001
4ms	Bontebok National Park	Cape Supergroup	0.712552	0.00001
5ms	Bontebok National Park	Cape Supergroup	0.712491	0.00001
6ms	Botterkloof	Karoo Sediments	0.716740	0.00001
7ms	Gifberg	Cape Supergroup	0.712384	0.00001
8ms	Gifberg	Cape Supergroup	0.712719	0.00001
9ms	Gifberg	Cape Supergroup	0.712713	0.00001
10ms	Kransgat River	Karoo Sediments	0.715720	0.00001
11ms	Mertenhof	Karoo Sediments	0.718972	0.00001
12ms	Mertenhof	Karoo Sediments	0.718927	0.00001
13ms	Mertenhof	Karoo Sediments	0.718601	0.00001
14ms	Bushmanskloof	Karoo Sediments	0.715184	0.00001
15ms	Namaqua National Park	Metamorphic Complex	0.755445	0.00001
16ms	Namaqua National Park	Metamorphic Complex	0.746843	0.00001
17ms	Richtersveld National Park	Richtersveld Suite	0.726132	0.00001
18ms	Koeberg	Quaternary coastal-marine sands	0.709282	0.00001
19ms A	Dabidas farm	Granitic gneisses	0.734004	0.00001
19ms B	Dabidas farm	Granite gneisses	0.739244	0.00001
20ms	Bontebok National Park	Cape Supergroup	0.712673	0.00001
21ms	Bontebok National Park	Cape Supergroup	0.712978	0.00001
22ms	Bontebok National Park	Cape Supergroup	0.713088	0.00002
23ms	Bontebok National Park	Cape Supergroup	0.712947	0.00001
24ms	Bontebok National Park	Cape Supergroup	0.712802	0.00001
25ms	Bontebok National Park	Cape Supergroup	0.712370	0.00001
1A R	De Hoop Nature Reserve	Bredasdorp Group	0.709260	0.00001
2A R	De Hoop Nature Reserve	Bredasdorp Group	0.709256	0.00001
3A R	De Hoop Nature Reserve	Bredasdorp Group	0.709267	0.00001
4A R	De Hoop Nature Reserve	Bredasdorp Group	0.709431	0.00002
5A R	De Hoop Nature Reserve	Bredasdorp Group	0.709225	0.00002
7A O	De Hoop Nature Reserve	Bredasdorp Group	0.709942	0.00001
8A R	De Hoop Nature Reserve	Cape Supergroup	0.710280	0.00001
9A R	De Hoop Nature Reserve	Cape Supergroup	0.710063	0.00001
10A R	De Hoop Nature Reserve	Cape Supergroup	0.709925	0.00002
12A R	De Hoop Nature Reserve	Bredasdorp Group	0.709388	0.00001
13A R	De Hoop Nature Reserve	Bredasdorp Group	0.709270	0.00001
14A R	De Hoop Nature Reserve	Bredasdorp Group	0.709160	0.00001
19A R	De Hoop Nature Reserve	Bredasdorp Group	0.709141	0.00001

Sample	Location	Geological substrate	$^{87}Sr/^{86}Sr$	±2s internal
20A R	De Hoop Nature Reserve	Bredasdorp Group	0.709681	0.00001
21A R	De Hoop Nature Reserve	Cape Supergroup	0.710083	0.00001
22A R	De Hoop Nature Reserve	Bredasdorp Group (limestones)	0.709196	0.00001
WP 1	Kasteelberg, Rooiheuwel farm	Cape Granites	0.712497	0.00001
WP 2	Kasteelberg, Rooiheuwel farm	Cape Granites	0.712900	0.00001
WP 3	Kasteelberg, Rooiheuwel farm	Cape Granites	0.714618	0.00001
WP 4	Kasteelberg, Rooiheuwel farm	Cape Granites	0.711469	0.00001
WP 5	Kasteelberg, Rooiheuwel farm	Cape Granites	0.711661	0.00001

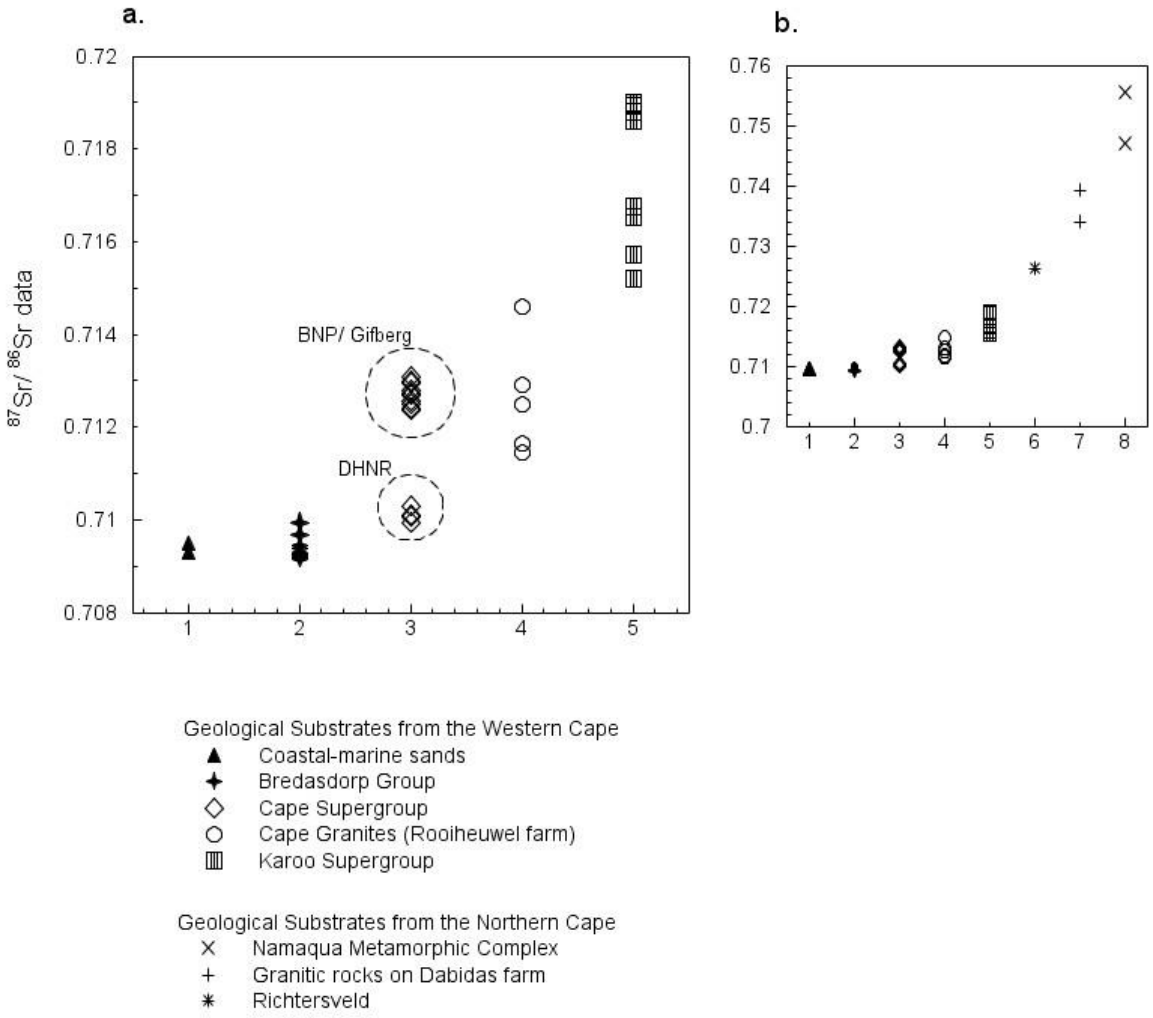

Figure 11a and b: Fig. 11a (on the left) illustrates $^{87}Sr/^{86}Sr$ of samples collected from various geological substrates of the Western Cape Province. Fig. 11b (on the right) includes the samples from Northern Cape Province of South Africa. Errors are included within the sizes of the points as plotted.

4.3.2 Pb isotopic ratios

The Pb isotopic ratios for all the Western Cape samples define relatively small variations: $^{208}Pb/^{204}Pb$= 36.9902–38.4602, $^{207}Pb/^{204}Pb$ = 15.5344–15.6573, $^{206}Pb/^{204}Pb$ = 17.1713–18.5140, $^{208}Pb/^{206}Pb$ = 2.0774–2.1543, $^{207}Pb/^{206}Pb$ = 0.8451–0.9047 and $^{208}Pb/^{207}Pb$ = 2.3812–2.4484.

The two samples from the coastal-marine sands had the lowest isotopic ratios for $^{208}Pb/^{204}Pb$ (36.9902 and 37.1605), $^{207}Pb/^{204}Pb$ (15.5344 and 15.5504), $^{206}Pb/^{204}Pb$ (17.1713 and 17.4064) and $^{208}Pb/^{207}Pb$ (2.3812 and 2.3897) but also the highest ratios for $^{207}Pb/^{206}Pb$ (0.8934–0.9047) and $^{208}Pb/^{206}Pb$ (2.1349–2.1543) compared to the rest of the samples in this study. The samples derived from the Karoo and Cape Supergroup substrates had overlapping ranges: $^{208}Pb/^{204}Pb$ = 37.1027–38.2528; $^{207}Pb/^{204}Pb$ = 15.480–15.6361; $^{206}Pb/^{204}Pb$ = 17.2768–18.3912; $^{208}Pb/^{206}Pb$ = 2.0793–2.1475; $^{207}Pb/^{206}Pb$ = 0.8502–0.8999; and $^{208}Pb/^{207}Pb$ = 2.3863–2.4484. The rodent tooth samples from the Bredasdorp Group had Pb isotopic ratios that ranged slightly higher (varying in the 1st decimal place) than those of the Karoo and Cape samples: $^{208}Pb/^{204}Pb$ = 37.3821–38.4602, $^{207}Pb/^{204}Pb$ = 15.5645–15.6465, $^{206}Pb/^{204}Pb$ = 17.4866–18.5140 and $^{208}Pb/^{207}Pb$ = 2.4017–2.4581. The $^{208}Pb/^{206}Pb$ and $^{207}Pb/^{206}Pb$ ranges were slightly lower (varying in the 2nd decimal place) than those of the Karoo and Cape samples: 2.0774–2.1378 and 0.8451–0.8901.

The plant samples from the Cape Granites at Rooiheuwel farm had somewhat narrower Pb isotopic ranges compared the Karoo and Cape samples: $^{208}Pb/^{204}Pb$ = 37.3190–38.1071, $^{207}Pb/^{204}Pb$ = 15.6073–15.6573, $^{206}Pb/^{204}Pb$ = 17.3714–18.0632, and $^{208}Pb/^{207}Pb$ = 2.3911– 2.4338. For these ranges, the lowest ratio was analysed at waypoint (WP 5), located on the highest hill overlooking the sea, while the highest ratio was analysed at WP 4. The inverse was true for the $^{208}Pb/^{206}Pb$ and $^{207}Pb/^{206}Pb$ ratios, ranging between 2.3911–2.4338 and 0.8668–0.8880, respectively. For these ranges, the lowest ratio was analysed at WP 4 and the highest ratio was analysed at WP 5.

The samples from the granites on Dabidas and the volcanic rocks from the Richtersveld Suite, in the Northern Cape region, had similar Pb isotopic ratios to each other, as well as some similarity to the Pb ranges of the Karoo and Cape Supergroups: $^{208}Pb/^{204}Pb$ (38.0220–38.1186), $^{207}Pb/^{204}Pb$ (15.6206–15.461), $^{206}Pb/^{204}Pb$ (18.0293–18.1758), $^{208}Pb/^{207}Pb$ (2.4336–2.4365), $^{208}Pb/^{206}Pb$ (2.0952–2.1143) and $^{207}Pb/^{206}Pb$ (0.8634–0.8678). The two samples from the ultrametamorphic rocks of Namaqua National Park had very different Pb isotopic ratios than the rest, with the highest $^{208}Pb/^{204}Pb$ (39.9670 and 40.2761), $^{207}Pb/^{204}Pb$ (15.7453 and 15.7518), $^{206}Pb/^{204}Pb$ (19.7667 and 19.9811), and $^{208}Pb/^{207}Pb$ (2.5383 and 2.5569). These two samples also had the lowest $^{207}Pb/^{206}Pb$ (0.7880 and 0.7968) and $^{208}Pb/^{206}Pb$ (2.0002 and 2.0375) values compared to the rest of the sample collection.

Table 13: The Pb isotopic ratios of all the samples in this study, with the internal 2-sigma errors on each analysis. Acronyms: BNP = Bontebok National Park, NNP = Namaqua National Park, NMC = Namaqua Metamorphic Complex, RNP = Richtersveld National Park, DHNR = De Hoop Nature Reserve.

Sample nr.	Sampling Location	Geological substrate	$^{208}Pb/^{204}Pb$	±2s	$^{207}Pb/^{204}Pb$	±2s	$^{206}Pb/^{204}Pb$	±2s	$^{208}Pb/^{206}Pb$	±2s	$^{207}Pb/^{206}Pb$	±2s	$^{208}Pb/^{207}Pb$	$^{206}Pb/^{207}Pb$
1ms	Doorn-bosch	Karoo Supergroup	37.2249	0.002	15.5647	0.0007	17.3892	0.0007	2.1407	0.0001	0.8951	0.00001	2.3916	1.1172
2ms	Doringriver	Karoo Supergroup	38.2406	0.002	15.6361	0.0008	18.3912	0.0010	2.0793	0.00003	0.8502	0.00001	2.4457	1.1762
3ms	Church-haven	Coastal-marine sands	37.1605	0.003	15.5504	0.0010	17.4064	0.0010	2.1349	0.0001	0.8934	0.00002	2.3897	1.1194
4ms	BNP	Cape Supergroup	37.6454	0.002	15.5803	0.0007	17.8072	0.0007	2.1140	0.0001	0.8749	0.00001	2.4162	1.1429
5ms	BNP	Cape Supergroup	37.1027	0.003	15.5480	0.0013	17.2768	0.0014	2.1475	0.0001	0.8999	0.00002	2.3863	1.1112
6ms	Botterkloof	Karoo Supergroup	38.0267	0.005	15.6203	0.0020	18.1308	0.0021	2.0973	0.0001	0.8615	0.00002	2.4344	1.1607
7ms	Gifberg	Cape Supergroup	37.3051	0.004	15.5561	0.0016	17.4229	0.0017	2.1411	0.0001	0.8928	0.00003	2.3981	1.1200
8ms	Gifberg	Cape Supergroup	37.7052	0.007	15.6001	0.0029	17.7332	0.0033	2.1262	0.0001	0.8797	0.00003	2.4170	1.1367
9ms	Gifberg	Cape Supergroup	37.8232	0.016	15.5926	0.0054	17.8215	0.0090	2.1219	0.0002	0.8745	0.00015	2.4257	1.1429
10ms	Kransgat	Karoo Supergroup	37.7091	0.008	15.5884	0.0032	17.7634	0.0039	2.1229	0.0001	0.8775	0.00003	2.4190	1.1395
11ms	Mertenhof	Karoo Supergroup	37.8827	0.014	15.6228	0.0049	17.8470	0.0055	2.1225	0.0001	0.8754	0.00006	2.4248	1.1424
12ms	Mertenhof	Karoo Supergroup	37.8726	0.012	15.6085	0.0047	17.8965	0.0052	2.1161	0.0001	0.8721	0.00003	2.4264	1.1466
13ms	Mertenhof	Karoo Supergroup	38.0558	0.006	15.6165	0.0024	18.0626	0.0028	2.1069	0.0001	0.8646	0.00003	2.4369	1.1566
14ms	Bushmans-kloof	Karoo Supergroup	37.5814	0.007	15.5923	0.0028	17.6841	0.0031	2.1250	0.0001	0.8817	0.00003	2.4103	1.1342
15ms	NNP	NMC	40.2761	0.006	15.7518	0.0025	19.7667	0.0026	2.0375	0.0001	0.7968	0.00004	2.5569	1.2549
16ms	NNP	NMC	39.9670	0.010	15.7453	0.0004	19.9811	0.0005	2.0002	0.0001	0.7880	0.00004	2.5383	1.2690

Sample nr.	Sampling Location	Geological substrate	$^{208}Pb/^{204}Pb$	±2s	$^{207}Pb/^{204}Pb$	±2s	$^{206}Pb/^{204}Pb$	±2s	$^{208}Pb/^{206}Pb$	±2s	$^{207}Pb/^{206}Pb$	±2s	$^{208}Pb/^{207}Pb$	$^{206}Pb/^{207}Pb$
17ms	RNP	Richtersveld Suite	38.0220	0.008	15.6206	0.0035	18.0927	0.0039	2.1017	0.0001	0.8634	0.00003	2.4341	1.1583
18ms	Koeberg	Coastal-marine sands	36.9902	0.002	15.5344	0.0008	17.1713	0.0007	2.1543	0.0001	0.9047	0.00002	2.3812	1.1054
19ms A	Dabidas	Granite rocks	38.1186	0.004	15.6451	0.0014	18.0293	0.0019	2.1143	0.0001	0.8678	0.00005	2.4365	1.1524
19ms B	Dabidas	Granite rocks	38.0767	0.008	15.6461	0.0030	18.1758	0.0032	2.0952	0.0001	0.8609	0.00003	2.4336	1.1617
20ms	BNP	Cape Supergroup	38.2456	0.002	15.6219	0.0009	18.2872	0.0009	2.0914	0.0001	0.8542	0.00001	2.4482	1.1706
21ms	BNP	Cape Supergroup	38.2528	0.002	15.6236	0.0008	18.2901	0.0008	2.0915	0.0001	0.8542	0.00001	2.4484	1.1707
22ms	BNP	Cape Supergroup	38.1191	0.004	15.6158	0.0013	18.1413	0.0016	2.1013	0.0001	0.8608	0.00002	2.4411	1.1617
23ms	BNP	Cape Supergroup	38.0897	0.002	15.6130	0.0008	18.1131	0.0007	2.1029	0.0001	0.8620	0.00002	2.4396	1.1601
24ms	BNP	Cape Supergroup	37.8012	0.005	15.5955	0.0009	17.8977	0.0068	2.1121	0.0001	0.8714	0.00030	2.4239	1.1476
25ms	BNP	Cape Supergroup	37.8348	0.002	15.5894	0.0008	17.8480	0.0008	2.1199	0.0001	0.8735	0.00001	2.4270	1.1449
1A R	DHNR	Bredasdorp Group	37.6182	0.004	15.5824	0.0016	17.6855	0.0016	2.1270	0.0001	0.8810	0.00002	2.4141	1.1350
2A R	DHNR	Bredasdorp Group	37.6068	0.004	15.5798	0.0019	17.6879	0.0019	2.1261	0.0001	0.8808	0.00002	2.4138	1.1353
3A R	DHNR	Bredasdorp Group	37.8440	0.004	15.6045	0.0017	17.9411	0.0020	2.1093	0.0001	0.8697	0.00003	2.4252	1.1497
4A R	DHNR	Bredasdorp Group	37.8314	0.006	15.6004	0.0024	17.9098	0.0025	2.1123	0.0001	0.8710	0.00003	2.4250	1.1480
5A R	DHNR	Bredasdorp Group	37.6333	0.007	15.5851	0.0029	17.7049	0.0033	2.1258	0.0001	0.8804	0.00003	2.4147	1.1360
7A O	DHNR	Bredasdorp Group	38.1729	0.003	15.6243	0.0013	18.1993	0.0014	2.0974	0.0001	0.8585	0.00002	2.4432	1.1648

Sample nr.	Sampling Location	Geological substrate	$^{208}Pb/^{204}Pb$	±2s	$^{207}Pb/^{204}Pb$	±2s	$^{206}Pb/^{204}Pb$	±2s	$^{208}Pb/^{206}Pb$	±2s	$^{207}Pb/^{206}Pb$	±2s	$^{208}Pb/^{207}Pb$	$^{206}Pb/^{207}Pb$
8A R	DHNR	Cape Supergroup	38.0225	0.003	15.6104	0.0009	18.0666	0.0008	2.1046	0.0001	0.8640	0.00001	2.4357	1.1573
9A R	DHNR	Cape Supergroup	37.7274	0.015	15.6010	0.0061	17.7103	0.0066	2.1300	0.0001	0.8808	0.00005	2.4183	1.1352
10A R	DHNR	Cape Supergroup	38.0316	0.003	15.6266	0.0011	18.0811	0.0011	2.1033	0.0001	0.8642	0.00002	2.4338	1.1571
12A R	DHNR	Bredasdorp Group	37.7830	0.006	15.5933	0.0022	17.8424	0.0024	2.1176	0.0001	0.8739	0.00003	2.4230	1.1442
13A R	DHNR	Bredasdorp Group	38.4602	0.004	15.6465	0.0012	18.5140	0.0012	2.0774	0.0001	0.8451	0.00002	2.4581	1.1833
14A R	DHNR	Bredasdorp Group	37.3821	0.008	15.5645	0.0032	17.4866	0.0036	2.1378	0.0001	0.8901	0.00003	2.4017	1.1235
19A R	DHNR	Bredasdorp Group	37.7210	0.012	15.5886	0.0050	17.8184	0.0055	2.1170	0.0001	0.8749	0.00004	2.4198	1.1430
20A R	DHNR	Bredasdorp Group	37.9489	0.004	15.6118	0.0018	17.9940	0.0019	2.1090	0.0001	0.8676	0.00002	2.4308	1.1526
21A R	DHNR	Cape Supergroup	37.9668	0.004	15.6244	0.0017	17.9292	0.0020	2.1175	0.0001	0.8714	0.00002	2.4300	1.1475
22A R	DHNR	Bredasdorp Group	37.4257	0.010	15.5678	0.0042	17.5065	0.0044	2.1378	0.0001	0.8892	0.00003	2.4040	1.1245
WP 1	Kasteelberg	Cape Granites	37.8860	0.003	15.6477	0.0010	17.8617	0.0009	2.1211	0.0001	0.8761	0.00002	2.4212	1.1415
WP 2	Kasteelberg	Cape Granites	37.5709	0.003	15.6258	0.0011	17.5965	0.0010	2.1351	0.0001	0.8880	0.00002	2.4044	1.1261
WP 3	Kasteelberg	Cape Granites	37.7582	0.003	15.6318	0.0009	17.7868	0.0008	2.1228	0.0001	0.8788	0.00002	2.4155	1.1379
WP 4	Kasteelberg	Cape Granites	38.1071	0.002	15.6573	0.0007	18.0632	0.0006	2.1096	0.0001	0.8668	0.00001	2.4338	1.1537
WP 5	Kasteelberg	Cape Granites	37.3190	0.003	15.6073	0.0008	17.3714	0.0008	2.1483	0.0001	0.8985	0.00001	2.3911	1.1130

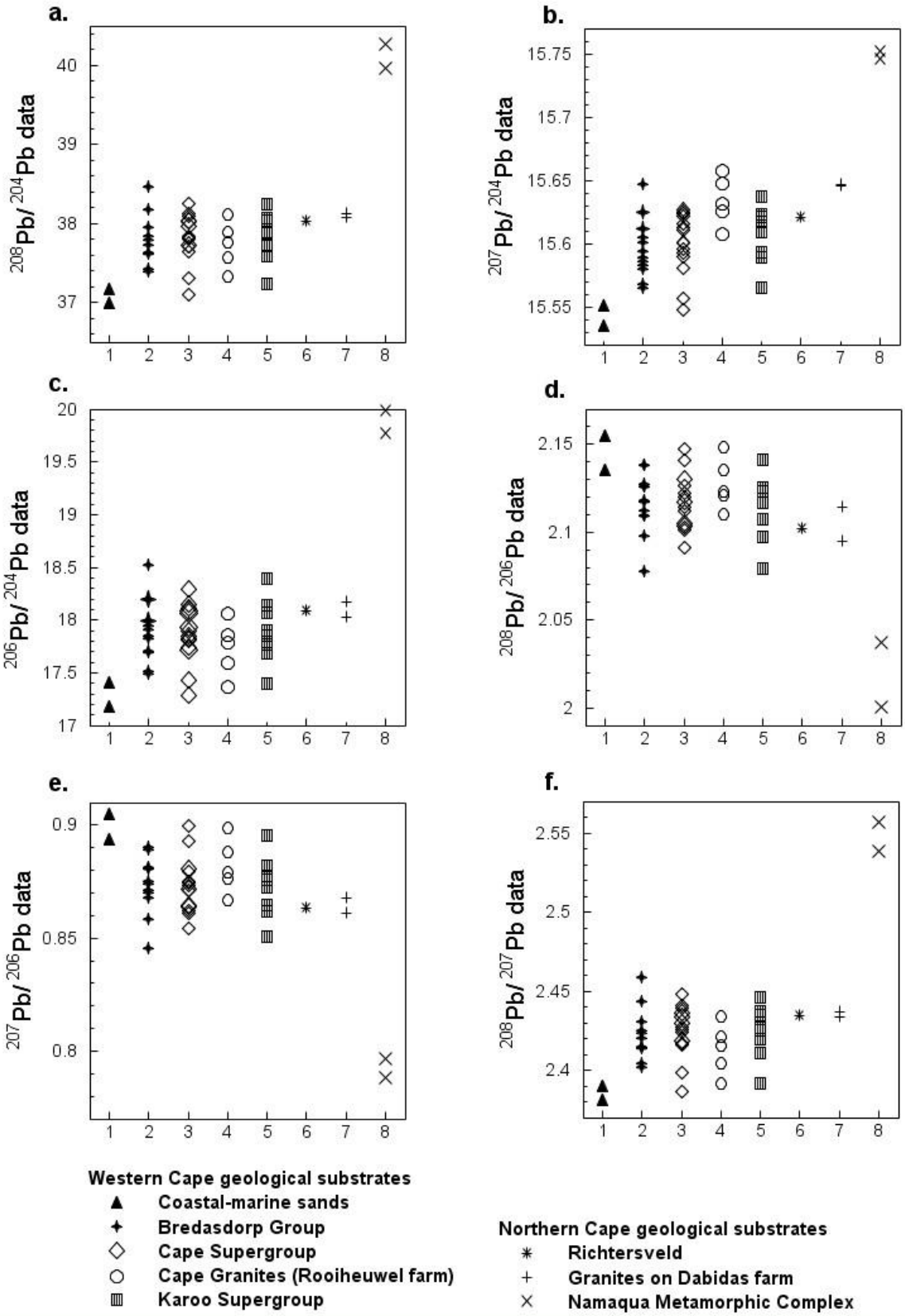

Figure 12: Plot illustrating the Pb isotopic ranges for (a.) $^{208}Pb/^{204}Pb$, (b.) $^{207}Pb/^{204}Pb$, (c.) $^{206}Pb/^{204}Pb$, (d.) $^{208}Pb/^{206}Pb$, (e.) $^{207}Pb/^{206}Pb$ and (f.) $^{208}Pb/^{207}Pb$ for all samples collected from the various geological substrates in this study. Errors are included within the sizes of the points as plotted.

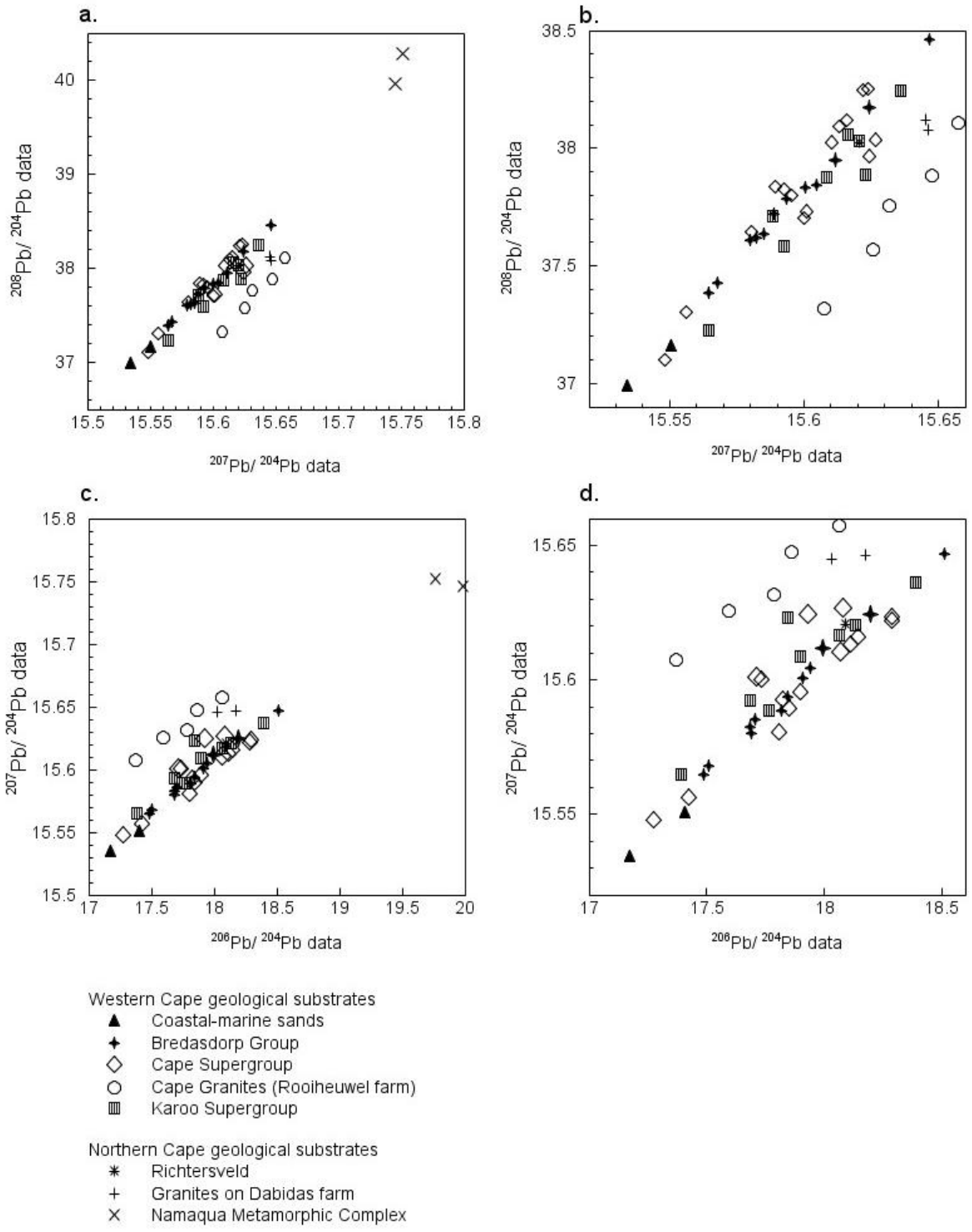

Figure 13: Fig. 13a (on the top left) illustrates ^{208}Pb/^{204}Pb vs ^{207}Pb/^{204}Pb and Fig. 13c (bottom right) illustrates ^{207}Pb/^{204}Pb vs ^{206}Pb/^{204}Pb of samples collected from various geological substrates of the Western- and Northern Cape Provinces. Fig. 13b and d (on the top and bottom right, respectively) excludes the samples from Namaqua National Park. Errors are included within the sizes of the points as plotted.

From Figure 12, the individual Pb isotope ratios seem not to discriminate clearly between the different geologies. Figure 13 plots the Pb isotope pairs against one another, showing two parallel trends which clearly separate the Cape Granite samples from the rest. Evidently from Figure 13, the bioavailable Pb ratios of two samples derived from granite rocks on Dabidas farm (in the Northern Cape) plot closely to those from the Cape Granites (Western Cape). Based on $^{87}Sr/^{86}Sr$, the Cape Granites did not group with the Dabidas granites. Pb were able to distinguish the Cape Granites from the other substrates. Although the variations are quite small (in the 1st or 2nd decimal place), previous studies were also able to distinguish between different sources that had Pb isotopic ratios varying at the 2nd decimal place.

Table 14: Pb and Sr concentrations (ppm) and isotopic ratios for all samples

Sample	Geological substrate	Species	Sr (ppm)	Pb (ppm)	87Sr/ 86Sr	208Pb/ 204Pb	207Pb/ 204Pb	206Pb/ 204Pb	208Pb/ 206Pb	207Pb/ 206Pb	208Pb/ 207Pb	206Pb/ 207Pb
1ms	Karoo Sediments				0.7165	37.2249	15.5647	17.3892	2.1407	0.8951	2.3916	1.1172
2ms	Karoo Sediments	4	110.6	0.3156	0.7188	38.2406	15.6361	18.3912	2.0793	0.8502	2.4457	1.1762
3ms	Coastal-marine sands	6	146.4	0.2971	0.7095	37.1605	15.5504	17.4064	2.1349	0.8934	2.3897	1.1194
4ms	Cape System	2	298.9	1.0230	0.7126	37.6454	15.5803	17.8072	2.1140	0.8749	2.4162	1.1429
5ms	Cape System	3	454.0	0.1529	0.7125	37.1027	15.5480	17.2768	2.1475	0.8999	2.3863	1.1112
6ms	Karoo Sediments	3	211.0	0.3265	0.7167	38.0267	15.6203	18.1308	2.0973	0.8615	2.4344	1.1607
7ms	Cape System	1	1830.0	0.1385	0.7124	37.3051	15.5561	17.4229	2.1411	0.8928	2.3981	1.1200
8ms	Cape System	1	1552.0	0.3960	0.7127	37.7052	15.6001	17.7332	2.1262	0.8797	2.4170	1.1367
9ms	Cape System	1	1600.0	0.0498	0.7127	37.8232	15.5926	17.8215	2.1219	0.8745	2.4257	1.1429
10ms	Karoo Sediments	1	1390.0	0.0240	0.7157	37.7091	15.5884	17.7634	2.1229	0.8775	2.4190	1.1395
11ms	Karoo Sediments	1	1445.0	< d.l.	0.7190	37.8827	15.6228	17.8470	2.1225	0.8754	2.4248	1.1424
12ms	Karoo Sediments	1	1862.0	0.1219	0.7189	37.8726	15.6085	17.8965	2.1161	0.8721	2.4264	1.1466
13ms	Karoo Sediments	1	1051.0	0.1931	0.7186	38.0558	15.6165	18.0626	2.1069	0.8646	2.4369	1.1566
14ms	Karoo Sediments	1	1860.0	0.0201	0.7152	37.5814	15.5923	17.6841	2.1250	0.8817	2.4103	1.1342
15ms	Namaqua Metamorphic Complex (NMC)	1	1378.0	0.0510	0.7554	40.2761	15.7518	19.7667	2.0375	0.7968	2.5569	1.2549
16ms	NMC	1	1150.0	0.2133	0.7468	39.9670	15.7453	19.9811	2.0002	0.7880	2.5383	1.2690
17ms	Richtersveld Suite	1	890.8	0.0277	0.7261	38.0220	15.6206	18.0927	2.1017	0.8634	2.4341	1.1583
18ms	Coastal-marine sands	8	773.6	0.7580	0.7093	36.9902	15.5344	17.1713	2.1543	0.9047	2.3812	1.1054
19ms A	Granite rocks	1	771.2	0.248	0.7340	38.1186	15.6451	18.0293	2.1143	0.8678	2.4365	1.1524

Sample	Geological substrate	Species	Sr (ppm)	Pb (ppm)	87Sr/ 86Sr	208Pb/ 204Pb	207Pb/ 204Pb	206Pb/ 204Pb	208Pb/ 206Pb	207Pb/ 206Pb	208Pb/ 207Pb	206Pb/ 207Pb
19ms B	Granite rocks	1	752.2	0.115	0.7392	38.0767	15.6461	18.1758	2.0952	0.8609	2.4336	1.1617
20ms	Cape System	5	287.7	0.328	0.7127	38.2456	15.6219	18.2872	2.0914	0.8542	2.4482	1.1706
21ms	Cape System	5	394.3	0.411	0.7130	38.2528	15.6236	18.2901	2.0915	0.8542	2.4484	1.1707
22ms	Cape System	5	484.7	0.138	0.7131	38.1191	15.6158	18.1413	2.1013	0.8608	2.4411	1.1617
23ms	Cape System	2	329.9	0.755	0.7129	38.0897	15.6130	18.1131	2.1029	0.8620	2.4396	1.1601
24ms	Cape System	2	402.6	2.302	0.7128	37.8012	15.5955	17.8977	2.1121	0.8714	2.4239	1.1476
25ms	Cape System	2	347.3	1.686	0.7124	37.8348	15.5894	17.8480	2.1199	0.8735	2.4270	1.1449
1A R	Dune Strandveld	9	524.2	0.684	0.7093	37.6182	15.5824	17.6855	2.1270	0.8810	2.4141	1.1350
2A R	Dune Strandveld	9	881.8	0.143	0.7093	37.6068	15.5798	17.6879	2.1261	0.8808	2.4138	1.1353
3A R	Waenhuiskrans Limestone	9	374.4	0.399	0.7093	37.8440	15.6045	17.9411	2.1093	0.8697	2.4252	1.1497
4A R	Waenhuiskrans Limestone	9	206.1	0.246	0.7094	37.8314	15.6004	17.9098	2.1123	0.8710	2.4250	1.1480
5A R	Wankoe Limestone	9	492.5	0.025	0.7092	37.6333	15.5851	17.7049	2.1258	0.8804	2.4147	1.1360
7A O	Valley Sand (Strandveld)	10	1114	0.265	0.7099	38.1729	15.6243	18.1993	2.0974	0.8585	2.4432	1.1648
8A R	Table Mountain Sandstone	9	511.1	0.737	0.7103	38.0225	15.6104	18.0666	2.1046	0.8640	2.4357	1.1573
9A R	Table Mountain Sandstone	9	276.7	0.276	0.7101	37.7274	15.6010	17.7103	2.1300	0.8808	2.4183	1.1352
10A R	Table Mountain Sandstone	9	367.1	0.379	0.7099	38.0316	15.6266	18.0811	2.1033	0.8642	2.4338	1.1571
12A R	Waenhuiskrans Limestone	9	194.8	0.117	0.7094	37.7830	15.5933	17.8424	2.1176	0.8739	2.4230	1.1442
13A R	Waenhuiskrans Limestone	9	290.7	0.225	0.7093	38.4602	15.6465	18.5140	2.0774	0.8451	2.4581	1.1833
14A R	Waenhuiskrans Limestone	9	777.5	0.039	0.7092	37.3821	15.5645	17.4866	2.1378	0.8901	2.4017	1.1235
19A R	Wankoe Limestone	9	336.6	0.012	0.7091	37.7210	15.5886	17.8184	2.1170	0.8749	2.4198	1.1430
20A R	Valley Sand (Strandveld)	9	316.3	0.269	0.7097	37.9489	15.6118	17.9940	2.1090	0.8676	2.4308	1.1526

Sample	Geological substrate	Species	Sr (ppm)	Pb (ppm)	87Sr/ 86Sr	208Pb/ 204Pb	207Pb/ 204Pb	206Pb/ 204Pb	208Pb/ 206Pb	207Pb/ 206Pb	208Pb/ 207Pb	206Pb/ 207Pb
21A R	Table Mountain Sandstone	9	223.2	0.163	0.7101	37.9668	15.6244	17.9292	2.1175	0.8714	2.4300	1.1475
22A R	Wankoe Limestone	9	137.8	0.186	0.7092	37.4257	15.5678	17.5065	2.1378	0.8892	2.4040	1.1245
WP 1	Cape Suite Granites				0.7125	37.8860	15.6477	17.8617	2.1211	0.8761	2.4212	1.1415
WP 2	Cape Suite Granites				0.7129	37.5709	15.6258	17.5965	2.1351	0.8880	2.4044	1.1261
WP 3	Cape Suite Granites				0.7146	37.7582	15.6318	17.7868	2.1228	0.8788	2.4155	1.1379
WP 4	Cape Suite Granites				0.7115	38.1071	15.6573	18.0632	2.1096	0.8668	2.4338	1.1537
WP 5	Cape Suite Granites				0.7117	37.3190	15.6073	17.3714	2.1483	0.8985	2.3911	1.1130

Chapter 5: Discussion and Conclusions

This chapter will compare the results obtained in this study with relevant data from previous studies, to investigate whether Pb isotopes can be used to distinguish between different geological substrates in this region, especially those with similar $^{87}Sr/^{86}Sr$. A secondary goal is to investigate whether samples collected during the leaded petrol era can be used for this purpose. Ultimately, the goal is to find out whether using the Pb isotope system in addition to Sr is of significant value in studying the mobility and paleodietary habits of animals and humans from the southwestern region of South Africa.

Table 15: Comparison of $^{87}Sr/^{86}Sr$ ranges for different geologies found in this study with those in previous studies

	Malmesbury shales	Cape Granite Suite	Cape System (TM Sandstone)	Karoo Sediments	Bredasdorp Group	Quaternary sands
This study	N/A	0.7115 – 0.7146	0.7099 – 0.7131	0.7152 – 0.7190	0.7091 – 0.7099	0.7093 – 0.7095
Sealy et al. (1991)	0.7178 – 0.7179	N/A	0.7154 – 0.7175	N/A	N/A	0.7094 – 0.7117
Radloff et al. (2010)	0.7101 – 0.7104	N/A	0.7098 – 0.7100	N/A	0.7092 – 0.7099	0.7099
Copeland et al. (2016)	0.7095 – 0.7157	0.7095 – 0.7177	0.7092 – 0.7209	0.7124 – 0.7237	0.7092 – 0.7101	0.7104 – 0.7162
Lehman et al. (2018)	0.7141 – 0.7204	0.7114 – 0.7236	0.7141 – 0.7204	N/A	N/A	0.7094 – 0.7117

As Table 15 and Figure 14 show, $^{87}Sr/^{86}Sr$ values measured for the different geologies in this study fall within those of previous studies, except for a slight expansion of the range (to lower values) for the Bredasdorp group. This may be taken to mean that we have now adequately characterised bioavailable $^{87}Sr/^{86}Sr$ ranges for the major geological substrates of southwestern South Africa. However, many of the geologies had overlapping $^{87}Sr/^{86}Sr$ ranges, for instance the bioavailable $^{87}Sr/^{86}Sr$ ranges of the Malmesbury shales and Cape Granite Suite are similar, as well as the Cape and Karoo geologies (Copeland, et al., 2016; Lehmann, et al., 2018). The older substrates (granites, TMS, Malmesbury) show higher $^{87}Sr/^{86}Sr$ than the Quaternary sands and Bredasdorp formation, which have values closer to seawater. However, this study has found that some samples from older substrates close to the coast (e.g. Cape Granites at Vredenburg Peninsula), had very low Sr values, indicating marine input. Consequently, another way of distinguishing between these geologies was investigated, namely the analysis of their Pb isotopic ranges.

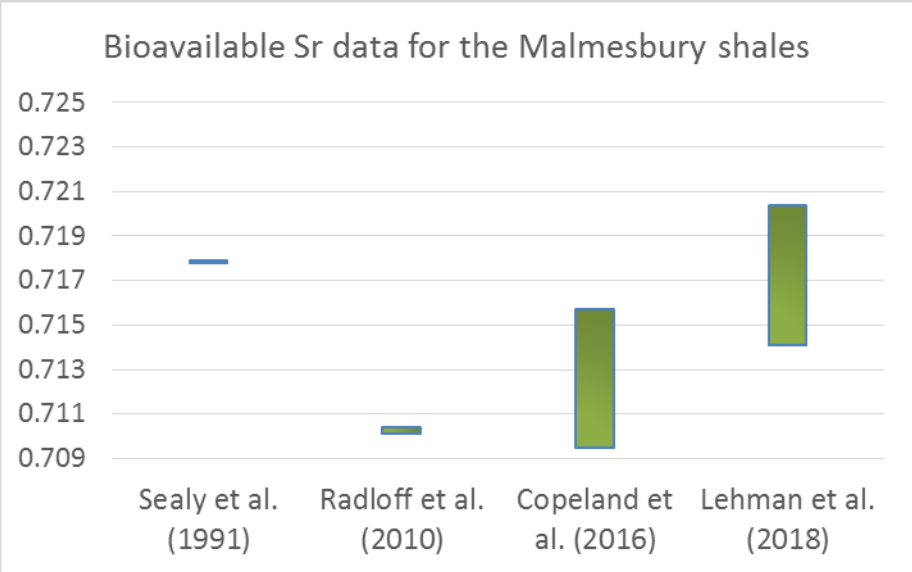
Bioavailable Sr data for the Malmesbury shales
0.725
0.723
0.721
0.719
0.717
0.715
0.713
0.711
0.709
Sealy et al. (1991)
Radloff et al. (2010)
Copeland et al. (2016)
Lehman et al. (2018)

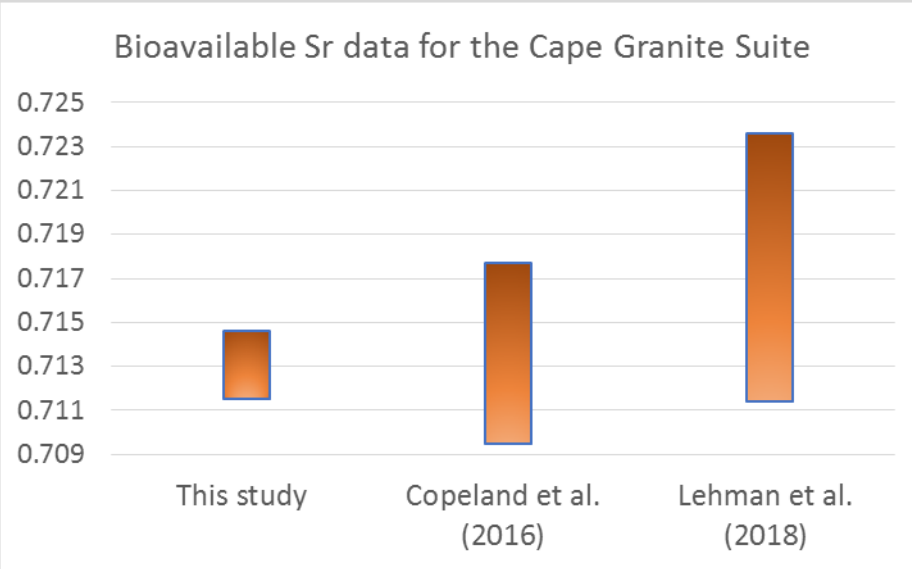
Bioavailable Sr data for the Cape Granite Suite
0.725
0.723
0.721
0.719
0.717
0.715
0.713
0.711
0.709
This study
Copeland et al. (2016)
Lehman et al. (2018)

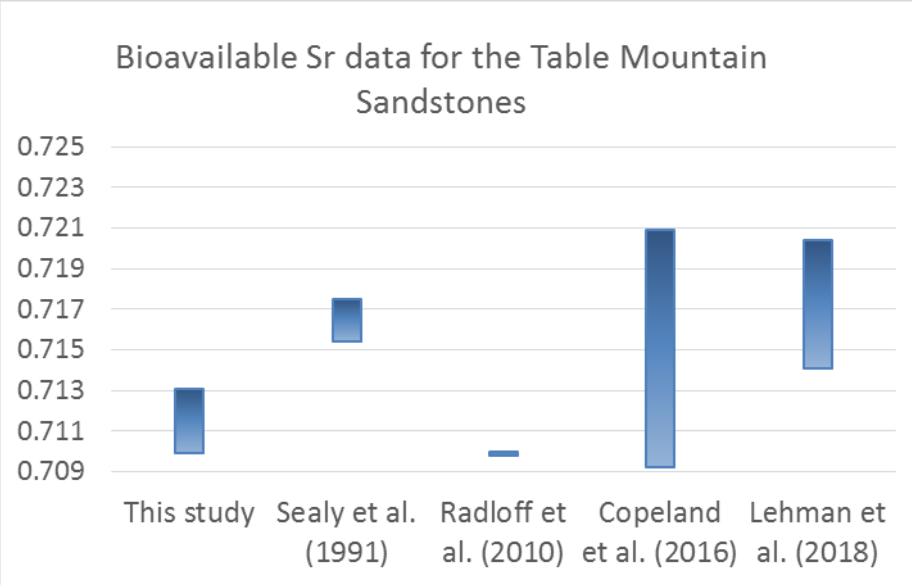
Bioavailable Sr data for the Table Mountain Sandstones
0.725
0.723
0.721
0.719
0.717
0.715
0.713
0.711
0.709
This study
Sealy et al. (1991)
Radloff et al. (2010)
Copeland et al. (2016)
Lehman et al. (2018)

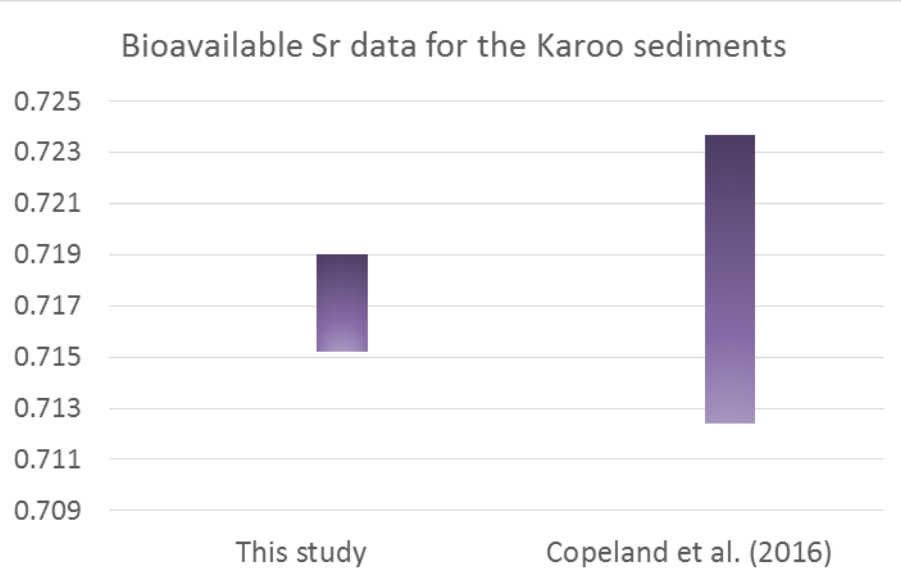
Bioavailable Sr data for the Karoo sediments
0.725
0.723
0.721
0.719
0.717
0.715
0.713
0.711
0.709
This study
Copeland et al. (2016)

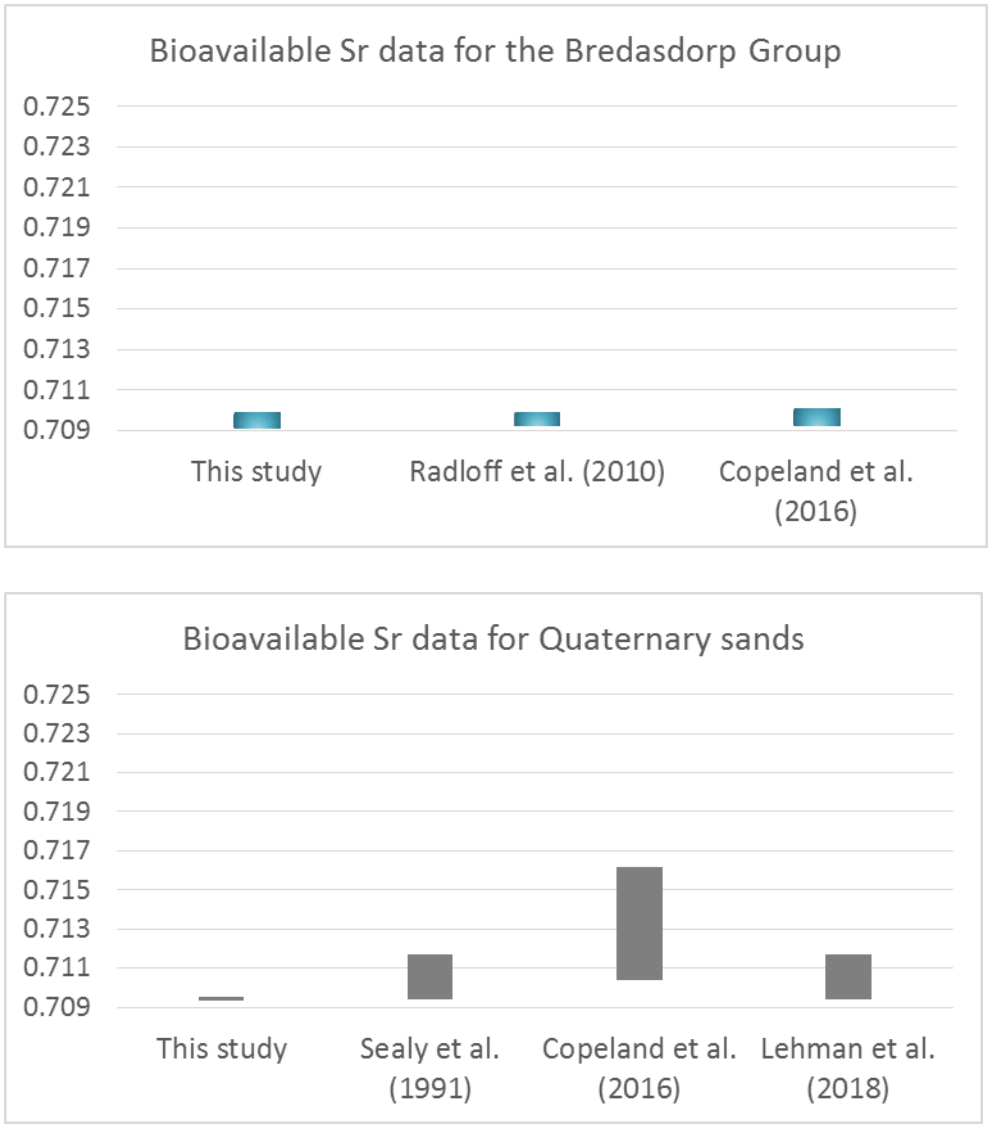

Figure 14: Comparison of the bioavailable $^{87}Sr/^{86}Sr$ ranges found in this study for different geologies with those in previous studies

This study reports much narrower Sr isotopic ranges for each substrate compared to Copeland et al. (2016) and Lehman et al. (2018), although the same analytical methods were applied. In addition, a clear distinction in Sr isotope ranges between the Karoo and Cape substrates exist in this study, while Copeland et al. (2016) measured very broad and overlapping $^{87}Sr/^{86}Sr$ ranges for these two substrates. When comparing the samples sizes, Copeland et al. (2016) had greater sample sizes for the Karoo (n = 50) and Cape Supergroups (n = 35), compared to this study (n = 8 and 15, respectively). This might explain the narrower Sr ranges for this study, however, the sample sizes for the granite substrates of these two studies were the same (n = 7). It must, however, be noted that this study avoided sampling from areas overlain by recent marine-derived sands. This could also have led to the narrower Sr ranges reported in this study.

5.1 Utility of Sr and Pb isotopes at coastal marine environments

As previously stated, the majority of former studies have shown Sr isotopes to be of limited value at coastal marine environments. The bioavailable $^{87}Sr/^{86}Sr$ values of granitic substrates are significantly higher further away from the coast, while lower closer to the coast (see Figure 15). This study measured a bioavailable Sr range of 0.712 – 0.715 for the Cape Granite substrate at Vredenburg Peninsula. Copeland et al. (2016) measured Sr isotopic values below 0.71 for plant samples from the Cape Granite Suite collected within 5km from the coastline. The samples from the granitic rocks on Dabidas farm was 115km from the nearest coast, resulting in much higher Sr values up to 0.74.

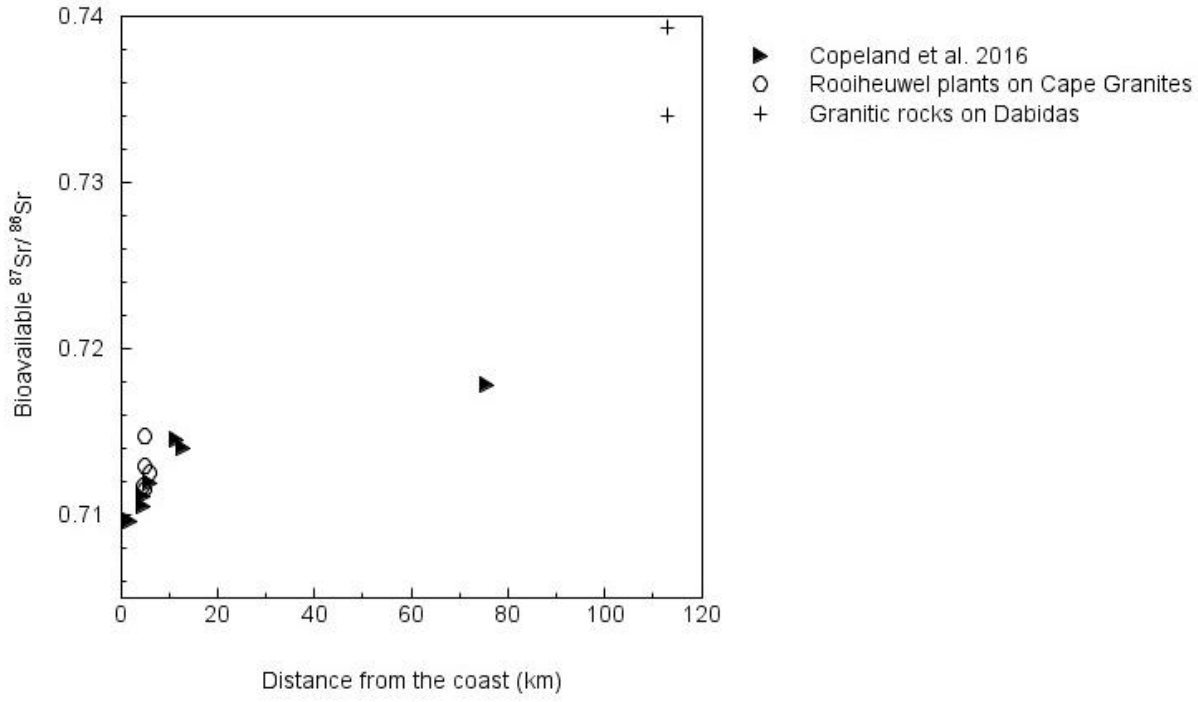

Figure 15: Bioavailable $^{87}Sr/^{86}Sr$ values of granitic substrates compared to the distance from the coast

Since many of the samples are from near-coastal areas, it is important to assess whether marine-derived aerosols influence the Sr and Pb isotopic compositions of these samples. The $^{87}Sr/^{86}Sr$ of seawater is well constrained at 0.7092 (Veizer, 1989). The Pb isotopic compositions of seawater analysed by Paul et al. (2015) will be used as a comparison as it characterises the Pb isotopic compositions of seawater from different depths in the south eastern Atlantic Ocean. Since sea spray in near-coastal environments derives from surface water, only the values for surface seawater are applicable in this study: $^{207}Pb/^{206}Pb = 0.8643$; $^{208}Pb/^{206}Pb = 2.1040$; $^{206}Pb/^{204}Pb = 18.0730$; $^{207}Pb/^{204}Pb = 15.6200$; and $^{208}Pb/^{204}Pb = 38.0300$ (Paul, et al., 2015). These marine Pb ratios will be compared with the isotopic ratios of the terrestrial samples analysed here. These samples will also be compared to the Pb isotopic compositions of the South Atlantic surface water sampled during the 1990s and analysed by Alleman et al. (2001). This is necessary seeing as samples 1ms to 9ms, as well as 18ms, were collected between 1982 and 1990 when leaded petrol was still in use. Of these samples, only 3ms and 18ms derives from coastal marine substrates.

Figure 16 compares the bioavailable Sr and Pb isotopic ratios of all the Western Cape samples in this study with the marine values, while Figure 17 presents only the bioavailable Pb isotopic ratios of the coastal marine sands, Cape Granite and Bredasdorp substrates compared to the Pb marine signal. Although the coastal marine sands and Bredasdorp Group substrates exhibited strong Sr marine signals, their Pb isotopic ratios were quite unlike the marine Pb signal. Among the plant samples collected from the Cape Granites on Kasteelberg, only WP 4 had a $^{207}Pb/^{206}Pb$ value (0.8668) closest to the marine signal (0.8643), varying at the 3rd decimal place. Also, samples 8AR and 10AR from the Bredasdorp Group substrates had similar $^{208}Pb/^{206}Pb$ (2.1046 and 2.1033, respectively) and $^{207}Pb/^{206}Pb$ ratios (0.8640 and 0.8642, respectively) to the marine signal ($^{208}Pb/^{206}Pb = 2.1040$ and $^{207}Pb/^{206}Pb = 0.8643$), varying in the 4th decimal place. The remaining samples had very different values. The marine contribution to bioavailable Sr in the terrestrial environment is much greater than the contribution to bioavailable Pb. This is most probably due to the concentrations of Sr and Pb in seawater, with Sr having a relatively high concentration of 7.62 ppm (Capo, et al., 1998) compared to Pb (5.22×10^{-6} ppm) (Paul, et al., 2015) . In addition, coastal soils contain not only aerosol-derived marine Sr, but frequently also include fragments of shells and other marine carbonates, so their $^{87}Sr/^{86}Sr$ values are like those of seawater.

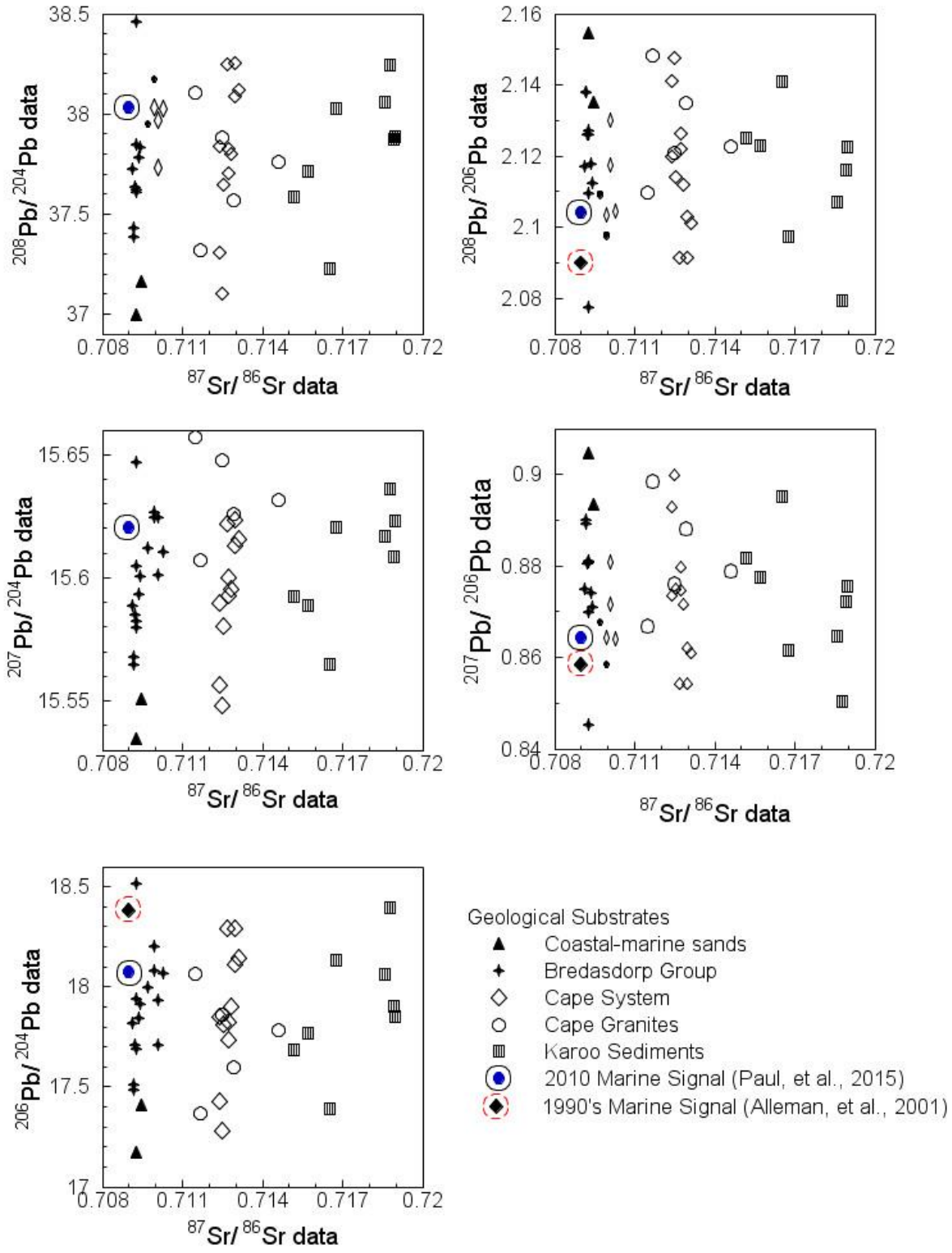

Figure 16: Pb vs. Sr isotopic data of all the samples from southwestern South Africa, compared to the marine Pb and Sr isotopic compositions of seawater in 2010 (Paul, et al., 2015) as well as 1993 (Alleman, et al., 2001).

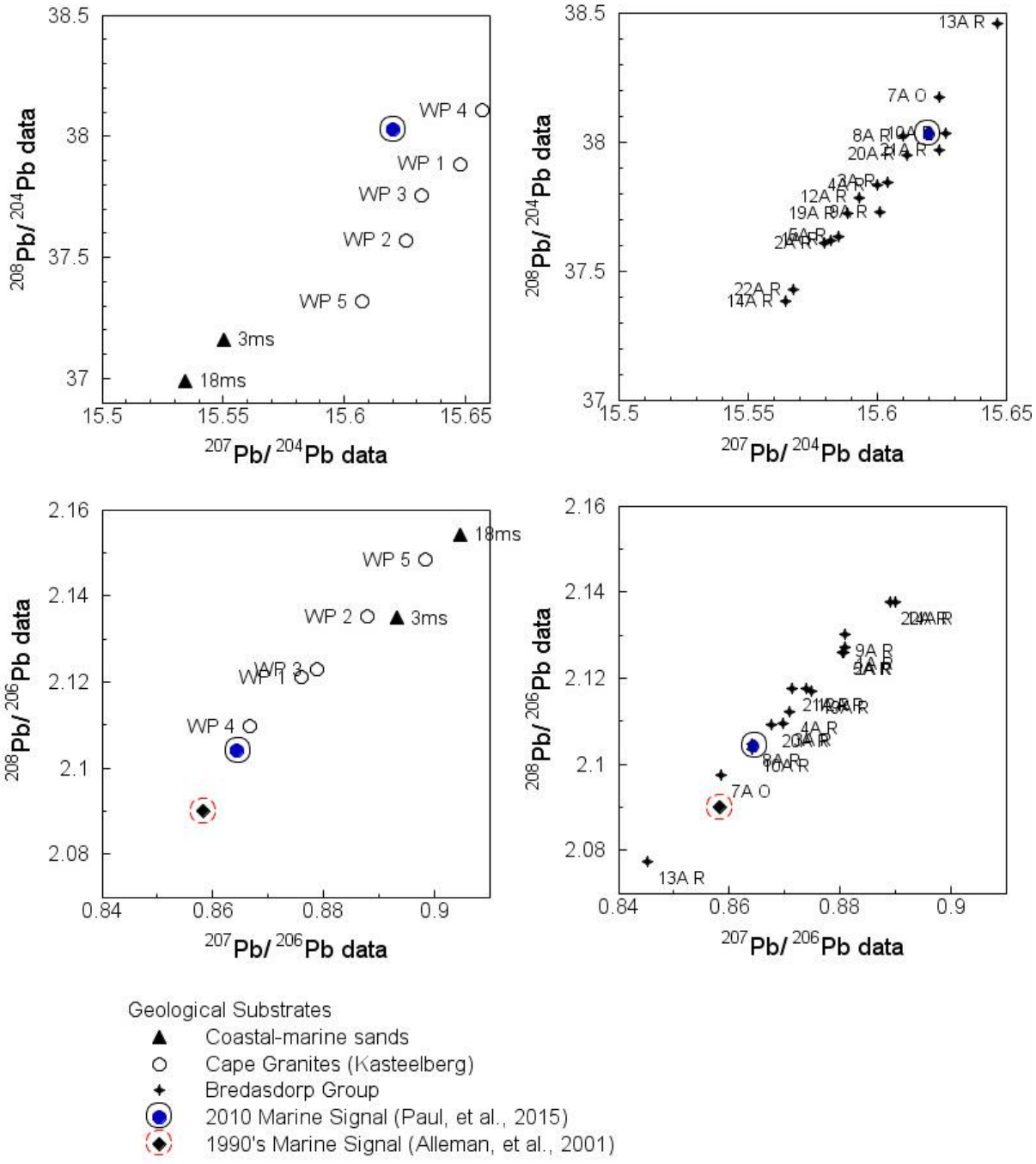

Figure 17: Bioavailable Pb isotopic ratios of the Cape Granite, coastal-marine sands and Bredasdorp limestone substrates compared to the marine Pb isotopic compositions of seawater in 2010 (Paul, et al., 2015) as well as 1993 (Alleman, et al., 2001).

5.2 Utility of samples derived from leaded-petrol era

As previously mentioned, alkyl-Pb was globally introduced as an anti-knock agent in petrol during the 1970s (Bollhöfer & Rosman, 2000). From 1996, unleaded petrol was made available to South African motorists and from 2006 leaded petrol was no longer available in South Africa. A few of the samples from this study were collected during the 1980s, when leaded petrol was still in use. This section will compare the Pb isotopic ratios of these samples with those collected after 2006. The samples from the 1980s will also be compared with the values measured in 1994-1995 for alkyl-Pb in leaded petrol from Associated Octel (U.K.), the world's largest alkyl-Pb producer (Bollhöfer & Rosman, 2000). Values for these 1980s samples will also be compared with measurements of the Pb isotopic composition of Cape Town's aerosols, studied in 1998 after unleaded petrol had been introduced; however, leaded petrol was still available (Bollhöfer & Rosman, 2000).

The $^{208}Pb/^{207}Pb$ and $^{206}Pb/^{207}Pb$ ratios of Cape Town aerosols in 1998 were somewhat higher than the leaded petrol signature (Figure 18). The 1980s samples had Pb isotope ratios distinctly higher than Cape Town's aerosols in 1998 and even higher than the common leaded petrol signature. From Figure 18, the red circled points (samples from the 1980s leaded petrol era) cover the same range as the non-circled points, so it does not seem as if there is clear evidence of a petrol influence. Another argument to keep in mind is that these 1980s samples were collected either from National Parks in the Western Cape, or at coastal areas, where Pb emissions from motor vehicles are much less than in urban areas.

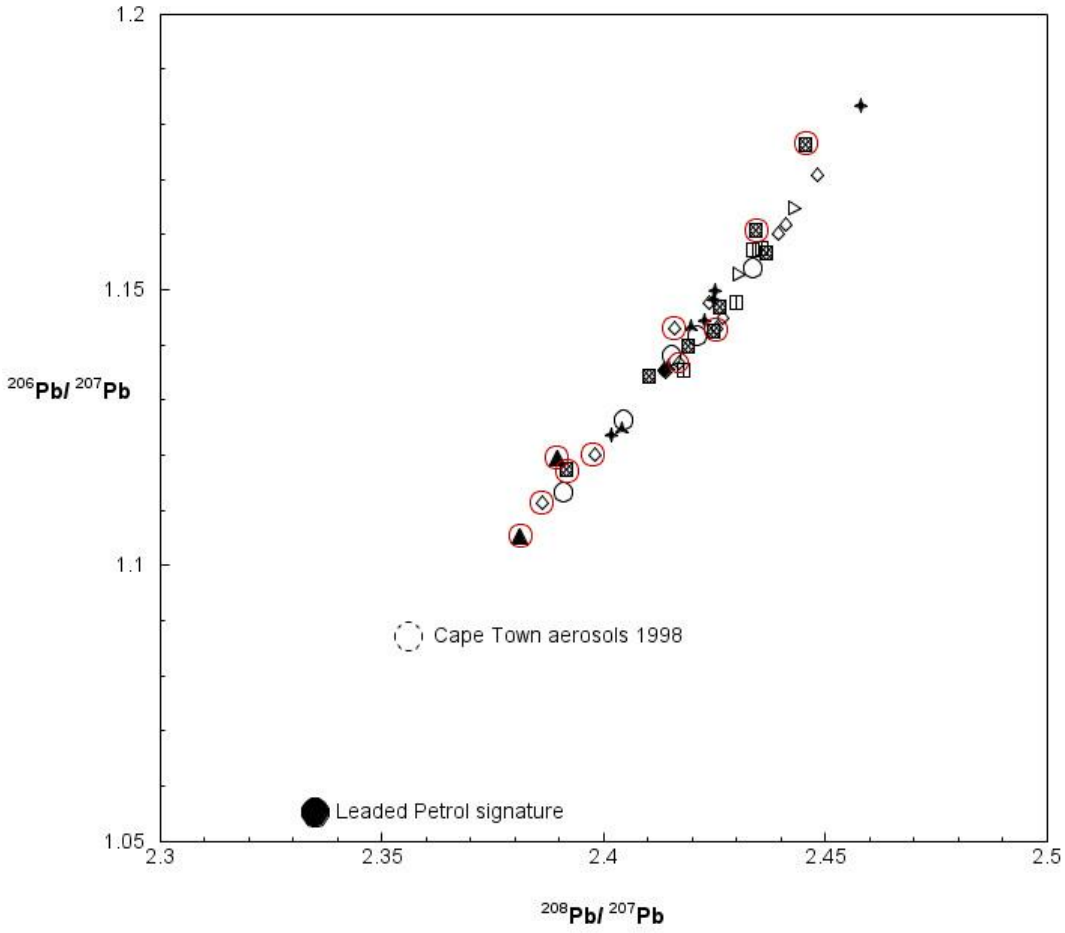

Geological localities
- Quaternary Limestones and Coastal-Marine sands
- Wankoe Limestone Fynbos (DHNR)
- Waenhuiskrans Limestone Fynbos (DHNR)
- Dune Strandveld (DHNR)
- Valley Sand Fynbos on Strandveld Formation (DHNR)
- Table Mountain Sandstone Fynbos (DHNR)
- Karoo sediments
- Cape Supergroup (Table Mountain Sandstones and Bokkeveld Shales)
- Cape Granite plants on Kasteelberg (Rooiheuwel farm)

Figure 18: Pb isotopic ratios of all the samples collected within the various geological substrates of the Western Cape region of South Africa, compared with the values for leaded petrol and for aerosols in Cape Town in 1998. Samples collected in the 1980s (leaded-petrol era) are circled in red.

5.3 Conclusion

The column chemistry protocol used for the combined Sr-Pb separation chemistry successfully provided rapid separation of the elements of interest, and produced fractions suitable for high precision isotope ratio measurements by MC-ICP-MS. The results demonstrate that Sr and Pb isotopic ratios can be determined with good internal precision, as well as a high degree of long-term reproducibility, based on repeat analyses of the reference materials at the MC-ICP-MS facility in UCT. In addition, this study achieved an order of a magnitude more precise results by solution analysis compared to the laser ablation technique.

Isotopic analyses of organisms' tissues allow important insights into the palaeo-diets and palaeo-landscape usage of these individuals. $^{87}Sr/^{86}Sr$ can efficiently discriminate between individuals living in coastal-marine environments and those living further inland. However, Sr was not able to sufficiently separate the samples from the Cape Granite Suite and those from the Cape System (Table Mountain sandstones), while Pb isotopes could. Furthermore, the bioavailable Pb isotopic ratios of plants and animals' tissues along the coast were not altered by the marine environment, as their Pb ratios were distinct from the maritime Pb signature. Pb isotope data can give potentially valuable information on palaeo-landscape usage, and can be used as an additional isotope system to extend interpretations based on Sr isotopes.

Another important conclusion of this study is that the samples from the 1980s were shown to be useful, since their Pb isotope ratios were distinct from that of leaded petrol in 1994 and instead were similar to the rest of the more recent samples. However, we should bear in mind that these historical samples were collected at National Parks and rural areas of the Western Cape, where Pb emissions from motor vehicles were very low. Therefore, when using older samples from the leaded petrol era, it would be best if these samples were collected from remote areas, where Pb pollution is not likely to have been important.

In conclusion, this study demonstrated the value of using a combination of both Sr and Pb isotope systems in this region, to retrieve valuable information from archaeological and palaeontological tissues, and reliable records of where humans and animals lived on the landscape.

References

Aberg, G., Fosse, G. & Stray, H., 1998. Man, nutrition and mobility: A comparison of teeth and bone from the Medieval era and the present from Pb and Sr isotopes. *The Science of the Total Environment,* Volume 224, pp. 109-119.

Adriano, D., 1986. *Trace elements in the terrestrial environment.* Berlin: Springer-Verlag.

Alleman, L. et al., 1999. Invasion of the abyssal North Atlantic by modern anthropogenic lead. *Geophysical Research Letters,* Volume 26, p. 1477–1480.

Alleman, L. Y. et al., 2001. Isotopic evidence of contaminant lead in the South Atlantic troposphere and surface waters. *Deep-Sea Research ,* II(48), p. 2811–2827.

Allsop, H. & Kolbe, P., 1965. Isotopic Age Determinations on the Cape Granite and Intruded Malmesbury Sediments, Cape Peninsula, South Africa. *Geochimica et Cosmochimica Acta ,* Volume 29, pp. 1115-1130.

Ambrose, S. H. & Norr, L., 1993. Experimental Evidence for the Relationship of the Carbon Isotope Ratios of Whole Diet and Dietary Protein to Those of Bone Collagen and Carbonate. In: J. B. Lambert & G. Grupe, eds. *Prehistoric Human Bone - Archaeology at the Molecular Level.* Urbana, Illinois, USA: Springer Berlin Heidelberg, pp. 1-37.

Arora, M. et al., 2006. Spatial distribution of lead in human primary teeth as a biomarker of pre- and neonatal lead exposure. *Science of The Total Environment,* 371(1-3), pp. 55-62.

Bacon, J. & Bain, D., 1995. Characterization of environmental water samples using strontium and lead stable-isotope compositions. *Environmental Geochemistry and Health,* Volume 17, pp. 39-49.

Balcaen, L., De Schrijver, I., Moens, L. & Vanhaecke, F., 2005. Determination of the 87Sr/86Sr isotope ratio in USGS silicate reference materials by multi-collector ICP–mass spectrometry. *International Journal of Mass Spectrometry,* 242(2-3), pp. 251-255.

Baron, S., Le-Carlier, C., Carignan, J. & Ploquin, A., 2009. Archaeological reconstruction of medieval lead production: Implications for ancient metal provenance studies and paleopollution tracing by Pb isotopes. *Applied Geochemistry,* 24(11), pp. 2093-2101.

Baron, S., Tamas, C., Cauuet, B. & Munoz, M., 2011. Lead isotope analyses of goldesilver ores from Rosia Montana (Romania): a first step of a metal provenance study of Roman mining activity in Alburnus Maior (Roman Dacia). *Journal of Archaeological Science ,* Volume 38 , pp. 1090-1100.

Baskaran, M., 2011. "Environmental Isotope Geochemistry": Past, Present and Future. In: M. Baskaran, ed. *Handbook of Environmental Isotope Geochemistry.* s.l.:Springer-Verslag Berlin Heidelberg, pp. 3-10.

Bender, M. M., Rouhani, I., Vines, H. M. & Black, C. C., 1973. 13C/12C Ratio Changes in Crassulacean Acid Metabolism Plants. *Plant Physiology,* Volume 52, pp. 427-430.

Bentley, R. A., 2006. Strontium Isotopes from the Earth to the Archaeological Skeleton: A Review. *Journal of Archaeological Method and Theory,* 13(3), pp. 135-187.

Bilström, K., 2008. Radiogenic isotopes and their applications within a range of scientific fields. In: I. Subías & B. Bauluz, eds. *Instrumental Techniques Applied to Mineralogy and Geochemistry.* Stockholm, Sweden: Sociedad Española de Mineralogía, pp. 111-131.

Bocherens, H. & Drucker, D., 2003. Trophic Level Isotopic Enrichment of Carbon and Nitrogen in Bone Collagen. *International Journal of Osteoarchaeology,* Volume 13, pp. 46-53.

Bollhöfer, A. & Rosman, K. J. R., 2000. Isotopic source signatures for atmospheric lead: The Southern Hemisphere. *Geochimica et Cosmochimica Acta,* 64(19), pp. 3251-3262.

Boskey, A. L., 2007. Mineralization of bones and teeth. *Element,* Volume 3, pp. 387-393.

Boyle, E. A., Chapnick, S. D., Shen, G. T. & Bacon, M. P., 1986. Temporal variability of lead in the western North Atlantic. *Journal of Geophysical Research ,* 91(C7), p. 8573–8593.

Boyle, E. A. et al., 2014. Anthropogenic Lead Emissions in the Ocean: The Evolving Global Experiment. *Oceanography,* 27(1), pp. 69-75.

Brill, R. H. & Wampler, J. M., 1967. Isotope Studies of Ancient Lead. *American Journal of Archaeology,* 71(1), pp. 63-77.

Budd, P. et al., 2004. Investigating population movement by stable isotope analysis: a report from Britain. *Antiquity,* 78(299), pp. 127-141.

Bürger, S. et al., 2015. Thermal ionization mass spectrometry. In: T. Prohaska, J. Irrgeher, A. Zitek & N. Jakubowski, eds. *Sector Field Mass Spectometry for Elemental and Isotopic Analysis.* Cambridge: Royal Society of Chemistry, pp. 318-428.

Capo, R. C., Steward, B. W. & Chadwick, O. A., 1998. Strontium isotopes as tracers of ecosystem processes: theory and methods. *Geoderma,* Volume 82, pp. 197-225.

Charalampides, G. & Manoliadis, O., 2002. Sr and Pb isotopes as environmental indicators in environmental studies. *Environment International ,* Volume 28 , pp. 147-151.

Choo-Smith, L.-P.et al., 2008. Investigating dental and other mineralized tissues. In: P. Lasch & J. Kneipp, eds. *Biomedical Vibrational Spectroscopy.* Canada: John Wiley & Sons, Inc., pp. 263-286.

Chrisholm, B. S., Nelson, D. E. & Schwarcz, H. P., 1982. Stable-Carbon Isotope Ratios as a Measure of Marine Versus Terrestrial Protein in Ancient Diets. *Science,* 216(4550), pp. 1131-1132.

CN Reserve, 2012. *Cederberg Nature Reserve Complex Management Plan 2013-2018,* s.l.: Cape Nature.

Comar, C., Russell, R. & Wasserman, R., 1957. Strontium-calcium movement from soil to man. *Science ,* Volume 126, p. 485–492.

Copeland, S. R. et al., 2016. Strontium isotope investigation of ungulate movement patterns on the Pleistocene Paleo-Agulhas Plain of the Greater Cape Floristic Region, South Africa. *Quaternary Science Reviews ,* Volume 141 , pp. 65-84.

Copeland, S. R. et al., 2011. Strontium isotope evidence for landscape use by early hominins. *Nature,* Volume 474, pp. 76-79.

Copeland, S. R. et al., 2008. Strontium isotope ratios (87Sr/86Sr) of tooth enamel: a comparison of solution and laser ablation multicollector inductively coupled plasma mass spectrometry methods. *Rapid Communications in Mass Spectrometry,* 22(20), p. 3187–3194.

Copeland, S. R. et al., 2010. Strontium isotope ratios in fossil teeth from South Africa: assessing laser ablation MC-ICP-MS analysis and the extent of diagenesis. *Journal of Archaeological Science,* Volume 37, p. 1437–1446.

Cornell, D. H. et al., 2006. The Namaqua-Natal Province. In: M. R. Johnson, C. R. Anhaeusser & R. J. Thomas, eds. *The Geology of South Africa.* s.l.:Counsil of Geoscience, pp. 325-379.

Costaglia, P. et al., 2001. Pb-isotope signatures of Italian alabasters: possible application to provenance studies of works of art. *European Journal of Mineralogy,* Volume 13, pp. 421-428.

Cox, G. & Sealy, J., 1997. Investigating Identity and Life Histories: Isotopic Analysis and Historical Documentation of Slave Skeletons Found on the Cape Town Foreshore, South Africa. *International Journal of Historical Archaeology,* 1(3), pp. 207-224.

De Sanctis, E., Monti, S. & Ripani, M., 2016. Radioactivity and Penetrating Power of Nuclear Radiation. In: *Energy from Nuclear Fission, An Introduction.* Switzerland: Springer, pp. 39-87.

DeNiro, M. J., 1985. Postmortem preservation and alteration of in vivo bone collagen isotope ratios in relation to palaeodietary reconstruction. *Nature,* Volume 319, pp. 806-809.

DeNiro, M. J. & Epstein, S., 1978. Influence of diet on the distribution of carbon isotopes in animals. *Geochimica et Cosmochimica Acta,* 42(5), pp. 495-506.

DeNiro, M. J. & Epstein, S., 1981. Influence of diet on the distribution of nitrogen isotopes in animals. *Geochimica et Cosmochimica Acta,* Volume 45, pp. 341-351.

Desfenant, F., Veron, A., Camoin, G. & Nyberg, J., 2006. Reconstruction of pollutant lead invasion into the tropical North Atlantic during the twentieth century. *Coral Reefs ,* Volume 25, p. 473–484.

Dickin, A., 1995. *Radiogenic Isotope Geochemistry.* Cambridge : Cambridge University Press.

Dickin, A. P., 2005. *Radiogenic Isotope Geology.* 2nd ed. United States of America: Cambridge University Press.

Dudás, F., LeBlanc, S., Carter, S. & Bowring, S., 2016. Pb and Sr concentrations and isotopic compositions in prehistoric North American teeth: A methodological study. *Chemical Geology,* Volume 429, pp. 21-32.

Durali-Mueller, S., Brey, G. P., Wigg-Wolf, D. & Lahaye, Y., 2007. Roman lead mining in Germany: its origin and development through time deduced from lead isotope provenance studies. *Journal of Archaeological Science,* Volume 34, pp. 1555-1567.

Edwards, L. E. & Pojeta, J., 1993. *Fossils, Rocks, and Time.* s.l.:U.S. Geological Survey.

Ehleringer, J. R., 1991. 13C/12C Fractionation and its Utility in Terrestrial Plant Studies. In: D. Coleman & B. Fry, eds. *Carbon Isotope Techniques.* San Diego, California: Academic Press, Inc., pp. 187-200.

Erel, Y., Harlavan, Y. & Blum, J. D., 1994. Lead isotope systematics of granitoid weathering. *Geochimica et Cosmochimica Acta,* 58(23), pp. 5299-5306.

Ericson, J. E., 1985. Strontium Isotope Characterization in the Study of Prehistoric Human Ecology. *Journal of Human Evolution,* Volume 14, pp. 503-514.

Evans, J. A., Chenery, C. A. & Montgomery, J., 2012. A summary of strontium and oxygen isotope variation in archaeological human tooth enamel excavated from Britain. *Journal of Analytical Atomic Spectrometry,* Volume 27, pp. 754-764.

Evans, J., Montgomery, J., Wildman, G. & Boulton, N., 2010. Spatial variations in biosphere 87Sr/86Sr in Britain. *Journal of the Geological Society,* Volume 167, pp. 1-4.

Faure, G., 1986. *Principles of Isotope Geology.* 2nd ed. New York: John Wiley & Sons Inc..

Fölling, P., Zartman, R. & Frimmel, H., 2000. A novel approach to double-spike Pb–Pb dating of carbonate rocks: examples from Neoproterozoic sequences in southern Africa. *Chemical Geology,* Volume 171, p. 97–122.

Gage, J. P., Francis, M. J. O. & Triffitt, J. T., 1989. *Collagen and Dental Matrices.* London: Butterworth-Heinemann.

Galer, S. & Abouchami, W., 1998. Practical application of lead triple spiking for correction of instrumental mass discrimination. *Mineralogical Magazine,* Volume 62A (1), p. 491–492.

Ghazi, A. M., 1994. Lead in archaeological samples: an isotopic study by ICP-MS. *Applied Geochemistry,* Volume 9, pp. 627--636.

Ghazi, M. A. & Millette, J. R., 2006. Chapter 4: Lead. In: R. D. Morrison & B. L. Murphy, eds. *Environmental Forensics: Contaminant Specific Guide.* s.l.:Academic Press, pp. 56-74.

Gresse, P. G., von Veh, M. W. & Frimmel, H. E., 2006. Namibian (Neoproterozoic) to Early Cambrian Successions. In: M. R. Johnson, C. R. Anhaeusser & R. J. Thomas, eds. *The Geology of South Africa.* Johannesburg & Pretoria: Geological Society of South Africa & Council for Geoscience, pp. 395-420.

Grobler, S., Theunissen, F. & Kotze, T., 2000. The relation between lead concentrations in human dental tissues and in blood. *Archives of Oral Biology ,* Volume 45, pp. 607-609.

Gutiérrez-Salazar, M. d. P. & Reyes-Gasga, J., 2003. Microhardness and chemical composition of human tooth. *Materials Research,* 6(3), pp. 367-373.

Hamelin, B., Ferrand, J., Alleman, L. & Nicolas, E., 1997. Isotopic evidence of pollutant lead transport from North America to the subtropical North Atlantic gyre. *Geochimica et Cosmochimica Acta,* Volume 61, p. 4423–4228.

Hedges, R., Clement, J. & Thomas, C., 2007. Collagen turnover in the adult femoral mid-shaft: Modeled from anthropogenic radiocarbon tracer measurements.. *American Journal of Physical Anthropology ,* Volume 133, p. 808–816.

Helmers, E., Mart, L. & Schrems, O., 1991. Lead in Atlantic surface waters as a tracer for atmospheric input. *Fresenius Journal of Analytical Chemistry,* Volume 340, p. 580–584.

Helmers, E., Mart, L., Schulz-Baldes, M. & Ernst, W., 1990. Temporal and spatial variations of lead concentrations in Atlantic surface waters. *Marine Pollution Bulletin,* 21(11), pp. 515-518.

Helmers, E. & van der Loeff, M., 1993. Lead and aluminum in Atlantic surface waters (50°N to 50°S) reflecting anthropogenic and natural sources in the eolian transport. *Journal of Geophysical Research,* Volume 98, p. 20261–20273.

Henning, S., 2015. *Projection: Traverse Mercator, Central Meridian 21 degrees E, WGS 84.* [Art] (Council of Geoscience).

Hoefs, J., 2010. *Stable Isotope Geochemistry.* 6th ed. Göttingen, Germany: Springer.

Hoppe, K. A., Koch, P. L. & Furutani, T. T., 2003. Assessing the preservation of biogenic strontium in fossil bone and tooth enamel. *Osteoarchaeology,* Volume 13, pp. 20-28.

Iñañez, J. G. et al., 2010. Romita pottery revisited: a reassessment of the provenance of ceramics from Colonial Mexico by LA-MC-ICP-MS. *Journal of Archaeological Science ,* Volume 37, pp. 2698-2704.

Joel, E., Olin, J., Blackman, M. & Barnes, I., 1988. Lead isotope studies of Spanish, Spanish-Colonial, and Mexican majolica. In: R. Farquhar & R. Hancock, eds. *Proceedings of the 26th International Archaeometry Symposium.* Toronto: University of Toronto Archaeometry Laboratory, pp. 185-188.

Johnson, M. R., Anhaeusser, C. R. & Thomas, R. J., 2006. *The Geology of South Africa.* 1st ed. Johannesburg & Pretoria: Geological Society of South Africa & Council for Geoscience.

Johnson, M. R. et al., 2006. Sedimentary Rocks of the Karoo Supergroup. In: M. R. Johnson, C. R. Anhaeusser & R. J. Thomas, eds. *The Geology of South Africa.* s.l.:Council of Geoscience, pp. 461-499.

Johnston, K. A., 2010. *Methodological Developments in the Use of Stable Isotope Analysis for Reconstructing Paleodiets,* United States: Southern Illinois University Carbondale .

Jowsey, J., Kelley, P. & Riggs, D., 1965. Quantitative microradiographic radiographic studies of normal and osteoporotic bone. *The Journal of Bone and Joint Surgery,* 47(4), p. 785–806.

Khan, F. M., 2010. *The Physics of Radiation Therapy.* 4th ed. Philadelphia, Pennsylvania, United States: Lippincott Williams & Wilkins, Wolters Kluwer.

Koch, P. L., Tuross, N. & Fogel, M. L., 1997. The Effects of Sample Treatment and Diagenesis on the Isotopic Integrity of Carbonate in Biogenic Hydroxylapatite. *Journal of Archaeological Science,* Volume 24, pp. 417-429.

Kohn, M. J., Rakovan, M. J. & Hughes, J. M., 2002. Stable Isotope Compositions of Biological Apatite. *Geochemical, Geobiological, and Materials Importance. Reviews in Mineralogy and Geochemistry,* Volume 48, pp. 455-488.

Komárek, M., Ettler, V., Chrastný, V. & Mihaljevic, M., 2008 . Lead isotopes in environmental sciences: a review.. *Environment International ,* 34(4), pp. 562-77.

Kootker, L. M., Mbeki, L., Morris, A. G. & Davies, G. R., 2016. Dynamics of Indian Ocean Slavery Revealed through Isotopic Data from the Colonial Era Cobern Street Burial Site, Cape Town, South Africa (1750-1827). *PLoS One,* 11(6), pp. 1-20.

Kovda, I. V. et al., 2016. Carbon isotope composition in landscape components and its changes under different ecological conditions. *Biology Bulletin,* 43(2), pp. 177-184.

Lamb, A. L., Evans, J. E., Buckley, R. & Appleby, J., 2014. Multi-isotope analysis demonstrates significant lifestyle changes in King Richard III. *Journal of Archaeological Science,* Volume 50, pp. 559-565.

LeGeros, R., 1991. Calcium Phosphates in Oral Biology and Medicine. *Monographs in Oral Science,* Volume 15, pp. 108-129.

LeGeros, R. Z., 1981. Apatites in biological systems. *Progress in Crystal Growth and Characterization,* 4(1-2), pp. 1-45.

Lehmann, S. et al., 2018. Environmental and ecological implications of strontium isotope ratios in mid-Pleistocene fossil teeth from Elandsfontein, South Africa. *Palaeo3,* Volume 490, pp. 84-94.

Libes, S., 1992. *An introduction to marine biochemistry.* Chichester: John Wiley & Sons.

Li, H. & Niu, Y., 2003. Multi-collector ICP-MS Analysis of Pb Isotope Ratios in Rocks: Data, Procedure and Caution. *Acta Geologica Sinica,* 77(1), pp. 44-58.

Longinelli, A., 1984. Oxygen isotopes in mammal bone phosphate: A new tool for paleohydrological and paleoclimatological research?. *Geochlmrca d Cosmochimrca Acla ,* Volume 48, pp. 385-390.

Malainey, M. E., 2010. *A Consumer's Guide to Archaeological Science: Analytical Techniques.* Canada: Springer Science.

Martin, A., Harbison, S., Beach, K. & Cole, P., 2012. *An Introduction to Radiation Protection.* 6th ed. Florida, United States: CRC Press, Taylor & Francis Group.

Míková, J. & Denková, P., 2007. Modified chromatographic separation scheme for Sr and Nd isotope analysis in geological silicate samples. *Journal of Geosciences,* Volume 52, pp. 221-226.

Mitton, D., Roux, C. & Laugier, P., 2010. Bone Overview. In: P. Laugier & G. Haïat, eds. *Bone Quantitative Ultrasound.* s.l.:Springer, pp. 1-28.

Montgomery, J., 2002. *Lead and Strontium Isotope Compositions of Human Dental Tissues as an Indicator of Ancient Exposure and Population Dynamics,* Bradford: Department of Archaeological Sciences, University of Bradford.

Montgomery, J., 2010. Passports from the past: Investigating human dispersals using strontium isotope analysis of tooth enamel. *Annals Of Human Biology,* 37(3), pp. 325-346.

Montgomery, J. et al., 2010. 'Gleaming white and deadly' : using lead to track human exposure and geographic origins in the Roman period in Britain. *Journal of Roman Archaeology,* Issue 78, pp. 199-226.

Montgomery, J., Evans, J. & Neighbour, T., 2003. Sr isotope evidence for population movement within the Hebridean Norse community of NW Scotland. *Journal of The Geological Society ,* 160(5), pp. 649-653.

Montgomery, J., Evans, J., Powlesland, D. & Roberts, C., 2005. Continuity or colonization in Anglo-Saxon England? Isotope evidence for mobility, subsistence practice, and status at West Heslerton. *American Journal of Physical Anthropology ,* 126(2), pp. 123-138.

Nöthling, J. O., Du Toit, J. S. & Myburgh, J. G., 2014. Lead isotope ratios in bone ash of blesbok (*Damaliscus pygargus phillipsi*): A means of screening for the accumulation of contaminants from uraniferous rocks. *Journal of Environmental Science and Health, Part A,* Volume 49, pp. 1251-1257.

O'Connell , T. C. & Hedges, R. E. M., 1999. Isotopic Comparison of Hair and Bone: Archaeological Analyses. *Journal of Archaeological Science,* Volume 26, pp. 661-665.

O'Connell, T. C. & Hedges, R. E. M., 2001. Isotopic Comparison of Hair, Nail and Bone: Modern Analyses. *Journal of Archaeological Science,* Volume 28, pp. 1247-1255.

Oslick, J., Miller, K., Feigenson, M. & Wright, J., 1994. Testing Oligocene-Miocene strontium isotopic correlations: Relationships with an inferred glacioeustatic record. *Palaeoceanography,* Volume 9, pp. 427-443.

Parker Pearson, M. et al., 2016. Beaker people in Britain: migration, mobility and diet. *Antiquity,* 90(351), pp. 620-637.

Parkington, J., 1991. Approaches to Dietary Reconstruction in the Western Cape: Are You What You Have Eaten?. *Journal of' Archaeological Science,* Volume 18, pp. 331-342.

Pasteris, J. et al., 2004 . Lack of OH in nanocrystalline apatite as a function of degree of atomic order: implications for bone and biomaterials.. *Biomaterials,* 25(2), pp. 229-38.

Paul, M. et al., 2015. High-precision measurements of seawater Pb isotope compositions by double spike thermal ionization mass spectrometry. *Analytica Chimica Acta,* Volume 863, pp. 59-69.

Pellegrini, M. et al., 2008. Faunal migration in late-glacial central Italy: implications for human resource exploitation. *Rapid Communications In Mass Spectrometry ,* 22(11), pp. 1714-1726.

PerkinElmar , 2004-2011. *ICP-Mass Spectrometry Technical Note: The 30-Minute Guide to ICP-MS.* [Online]

Available at: http://www.perkinelmer.com/PDFs/Downloads/tch_icpmsthirtyminuteguide.pdf [Accessed 21 November 2016].

Pin, C., Briot, D., Bassin, C. & Poitrasson, F., 1994. Concomitant separation of strontium and samarium-neodynium for isotopic analysis in silicate samples, based on specific extraction chromatography. *Analytica Chimica Acta,* Volume 298, pp. 209-217.

Pin, C., Gannounb, A. & Duponta, A., 2014. Rapid, simultaneous separation of Sr, Pb, and Nd by extraction chromatography prior to isotope ratios determination by TIMS and MC-ICP-MS. *Analytical Spectrometry,* Volume 29, pp. 1858-1870.

Pollard, M., Batt, C., Stern, B. & Young, S. M. M., 2007. *Analytical Chemistry in Archaeology.* New York: Cambridge University Press.

Porcelli, D. & Baskaran, M., 2011. An Overview of Isotope Geochemistry in Environmental Studies. In: M. Baskaran, ed. *Handbook of Environmental Isotope Geochemistry.* s.l.:Springer-Verlag Berlin Heidelberg, pp. 11-32.

Price, T. D., Blitz, J., Burton, J. & Ezzo, J. A., 1992. Diagenesis in prehistoric bone: Problems and solutions. *Journal of Archaeological Science,* 19(5), pp. 513-529.

Price, T. D., Burton, J. H. & Bentley, R. A., 2002. The characterization of biologically available strontium isotope ratios for the study of prehistoric migration. *Archaeometry,* Volume 44, pp. 117-135.

Radloff, F. G. T., Mucina, L., Bond, W. J. & le Roux, P. J., 2010. Strontium isotope analyses of large herbivore habitat use in the Cape Fynbos region of South Africa. *Oecologia,* Volume 164, pp. 567-578.

Rankama, K., 1954. *Isotope Geology.* New York: McGraw-Hill.

Rehkämper, M. & Halliday, A. N., 1998. Accuracy and long-term reproducibility of lead isotopic measurements by multiple-collector inductively coupled plasma mass spectrometry using an external method for correction of mass discrimination. *International Journal of Mass Spectrometry,* 181(1-3), pp. 123-133.

Richards, M. P., Pettitt, P. B., Stiner, M. C. & Trinkaus, E., 2001. Stable isotope evidence for increasing dietary breadth in the European mid-Upper Paleolithic. *Proceedings of National Academy of Sciences (PNAS) of the USA,* 98(11), pp. 6528-6532.

Roberts, D. L., Botha, G. A., Maud, R. R. & Pether, J., 2006. Coastal Cenozoic Deposits. In: M. R. Johnson, C. R. Anhaeusser & R. J. Thomas, eds. *The Geology of South Africa.* s.l.:Council of Geoscience, pp. 605-628.

Rutherford, E., 1913. The Structure of the Atom. *Nature,* 92(2302), p. 423.

ScARF, 2012. *Human and Animal Sciences: Isotope Analysis.* [Online]
Available at:
http://www.scottishheritagehub.com/sites/default/files/u12/ScARF%20Science%20June%202012.p

df
[Accessed 5 January 2017].

Schifano, G., Eeden van, O. & Coertze, F., 1970. *Geological Map of the Republic of South Africa and the kingdoms of Lesotho and Swaziland. South-Western Sheet.,* s.l.: Trigonometrical Survey Office.

Schoene, B., 2014. U–Th–Pb Geochronology. *Treatise on Geochemistry,* 4(10), pp. 341-378.

Schoeninger, M., 1995. Stable isotope studies in human evolution. *Evol Anthropol,* Volume 4, p. 83–98.

Schoeninger, M. J. & DeNiro, M. J., 1984. Nitrogen and carbon isotopic composition of bone collagen from marine and terrestrial animals. *Geochimica et Cosmochimica Acta,* 48(4), pp. 625-639.

Schroeder, H. et al., 2009. Trans-Atlantic Slavery: Isotopic Evidence for Forced Migration to Barbados. *American Journal of Physical Anthropology ,* Volume 139, p. 547–557.

Sealy, J., Armstrong, R. & Schrire, C., 1995. Beyond lifetime averages: Tracing life histories through isotopic analysis of different calcified tissues from archaeological human skeletons. *Antiquity,* Volume 69, pp. 290-300.

Sealy, J., Johnson, M., Richards, M. & Nehlich, O., 2014. Comparison of two methods of extracting bone collagen for stable carbon and nitrogen isotope analysis: comparing whole bone demineralization with gelatinization and ultrafiltration. *Journal of Archaeological Science,* Volume 47, pp. 64-69.

Sealy, J. et al., 1991. 87Sr/86Sr as a Dietary Indicator in Modern and Archaeological Bone. *Journal of Archaeological Science,* Volume 18, pp. 399-416.

Sharpe, A. E. et al., 2016. Lead (Pb) Isotope Baselines for Studies of Ancient Human Migration and Trade in the Maya Region. *PLoS ONE,* 11(11), pp. 1-28.

Shaw, H. et al., 2016. Identifying migrants in Roman London using lead and strontium stable isotopes. *Journal of Archaeological Science,* Volume 66, pp. 57-68.

Shen, G. & Boyle, E., 1988. Thermocline ventilation of anthropogenic lead in the western North Atlantic. *Journal of Geophysical Research,* Volume 93, p. 15715–15732.

Shen, G. T. & Boyle, E. A., 1987. Lead in corals: reconstruction of historical industrial fluxes to the surface ocean. *Earth and Planetary Science,* Volume 82, pp. 289-304.

Shin, J. Y., O'Connell, T., Black, S. & Hedges, R., 2004. Differentiating bone osteonal turnover rates by density fractionation; validation using the bomb 14C atmospheric pulse. *Radiocarbon,* 46(2), pp. 853-861.

Sillen, A., Hall, G., Richardson, S. & Armstrong, R., 1998. 87Sr/86Sr ratios in modern and fossil food-webs of the Sterkfontein Valley: implications for early hominid habitat preference. *Geochimica et Cosmochimica Acta,* 62(14), pp. 2463-2473.

Sillen, A. & Sealy, J., 1995. Diagenesis of Strontium in Fossil Bone: A Reconsideration of Nelsonet al. (1986). *Journal of Archaeological Science,* 22(2), pp. 313-320.

Simon Fraser University; Museum of Archaeology and Ethnology, 2010. *INVESTIGATING FORENSICS: Stable Isotopes.* [Online]
Available at: http://www.sfu.museum/forensics/eng/pg_media-media_pg/isotopes/
[Accessed 10 11 2016].

Slovak, N. & Paytan, A., 2011. Applications of Sr Isotopes in Archaeology. In: M. Baskaran, ed. *Handbook of Environmental Isotope Geochemistry.* Berlin Heidelberg: Springer-Verlag , pp. 743-768.

Smith, B. N. & Epstein, S., 1971. Two Categories of 1CC/12C Ratios for Higher Plants. *Plant Physiology,* Volume 47, pp. 380-384.

Snelling, A. A., 2017. Determination of the Decay Constants and Half-Lives of Uranium-238 and Uranium-235, and the Implications for U-Pb and Pb-Pb Radioisotope Dating Methodologies. *Answers Research Journal,* Volume 10, pp. 1-38.

Snyder, D., Kendall, C. & Caldwell, E., 2004. *Resources on Lead Isotopes.* [Online]
Available at: https://wwwrcamnl.wr.usgs.gov/isoig/period/pb_iig.html
[Accessed 9 11 2016].

Soderberg, K. & Compton, J. S., 2007. Dust as a Nutrient Source for Fynbos Ecosystems, South Africa. *Ecosystems,* Volume 10, pp. 550-561.

Stos-Gale, Z. A., 1992. *Application of lead isotope analysis to provenance studies in Archaeology.* England: University of Oxford.

Stos-Gale, Z. A. & Gale, N. H., 2009. Metal provenancing using isotopes and the Oxford archaeological lead isotope database (OXALID). *Archaeological and Anthropological Sciences ,* 1(3), p. 195–213.

Thamn, A. G. & Johnson, M. R., 2006. The Cape Supergroup. In: M. R. Johnson, C. R. Anhaeusser & R. J. Thomas, eds. *The Geology of South Africa.* s.l.:Council of Geoscience, pp. 334-460.

Thibodeau, A. M., Chesley, J. T. & Ruiz, J., 2012. Lead isotope analysis as a new method for identifying material culture belonging to the Vázquez de Coronado expedition. *Journal of Archaeological Science ,* Volume 39, pp. 58-66.

Thirlwall, M., 2002. Multicollector ICP-MS analysis of Pb isotopes using a 207pb-204pb double spike demonstrates up to 400 ppm/amu systematic errors in Tl-normalization. *Chemical Geology,* 184(3-4), pp. 255-279.

Tykot, R. H., 2004. Stable isotopes and diet: You are what you eat. *Physics Methods in Archaeometry,* Volume 154, pp. 433-444.

Van Wyk, C. & Grobler, S., 1983. Lead levels in deciduous teeth of children from selected urban areas in the Cape Peninsula. *S.A. Medical Journal,* Volume 63, pp. 559-562.

Vander Zanden, H. B., Soto, D. X., Bowen, G. J. & Hobson, K. A., 2016. Expanding the Isotopic Toolbox: Applications of Hydrogen and Oxygen Stable Isotope Ratios to Food Web Studies. *Ecology and Evolution,* 4(20), pp. 1-19.

Veizer, J., 1989. Strontium Isotopes in Seawater Through Time. *Annual Review of Earth and Planetary Sciences,* Volume 17, pp. 141-167.

Veron, A. et al., 1993. Response of lead cycling in the surface Sargasso Sea to changes in tropospheric input. *Journal of Geophysical Research,* Volume 98, p. 18269–18276.

Veron, A., Church, T., Patterson, C. & Flegal, A., 1994. Use of stable lead isotopes to characterize the sources of anthropogenic lead in North Atlantic surface waters. *Geochimica et Cosmochimica Acta,* Volume 58, p. 3199–3206.

Veron, A., Church, T., Rivera-Duarte, I. & Flegal, A., 1999. Stable lead isotope ratios trace thermohaline circulation in the subarctic North Atlantic. *Deep Sea Research Part II ,* Volume 46, p. 919–935.

Vervoort, J. & Mueller, P., 2007. *Integrating research and Education: Geochemical Instrumentation and Analysis.* [Online]
Available at:
http://serc.carleton.edu/research_education/geochemsheets/techniques/MCICPMS.html
[Accessed 21 November 2016].

Warembourg, F. R. & Kummerow, J., 1991. Photosynthesis/Translocation Studies in Terrestrial Ecosystems. In: D. C. Coleman & B. Fry, eds. *Carbon Isotope Techniques.* San Diego, California: Academic Press, Inc., pp. 11-36.

Weiss, D. et al., 2003. Spatial and temporal evolution of lead isotope ratios in the North Atlantic Ocean between 1981 and 1989. *Journal of Geophysical Research ,* Volume 108, p. 3306.

Whipkey, C. E., Capo, R. C., Chadwick, O. A. & Steward, B. W., 2000. The importance of sea spray to the cation budget of a coastal Hawaiian soil: a strontium isotope approach. *Chemical Geology,* Volume 168, pp. 37-48.

Wu, J. & Boyle, E., 1997. Lead in the western North Atlantic Ocean: Completed response to leaded gasoline phaseout. *Geochimica et Cosmochimica Acta ,* Volume 61, p. 3279–3283.

Zeichner, A., Ehrlich, S., Shoshani, E. & Halicz, L., 2006. Application of lead isotope analysis in shooting incident investigations. *Forensic Science International,* Volume 158, pp. 52-64.